UNIVERSITY OF BRASÍLIA
UNIVERSIDADE DE BRASÍLIA
INSTITUTE OF GEOSCIENCES
INSTITUTO DE GEOCIÊNCIAS
GRADUATE RESEARCH PROGRAM IN GEOLOGY
PROGRAMA DE PÓS-GRADUÇÃO EM GEOLOGIA
CONCENTRATION AREA – Biostratigraphy and Paleoecology
ÁREA DE CONCENTRAÇÃO – Bioestratigrafia e Paleoecologia

TAXONOMY OF ORGANIC-WALLED MICROFOSSILS FROM THE SETE LAGOAS FORMATION, BRAZIL: BIOSTRATIGRAPHY AND PALEOBIOGEOGRAPHY OF GONDWANA DURING EDIACARAN

TAXONOMIA DE MICROFÓSSEIS ORGÂNICOS DA FORMAÇÃO SETE LAGOAS, BRASIL: BIOESTRATIGRAFIA E PALEOBIOGEOGRAFIA DO GONDWANA DURANTE O EDIACARIANO

DOCTORATE THESIS

TESE DE DOUTORADO

Matheus Denezine

Doctorate Thesis Nº 196
Tese de Doutorado Nº196

Brasília, DF
2022

TAXONOMY OF ORGANIC-WALLED MICROFOSSILS FROM THE SETE LAGOAS FORMATION, BRAZIL: BIOSTRATIGRAPHY AND PALEOBIOGEOGRAPHY OF GONDWANA DURING EDIACARAN

TAXONOMIA DE MICROFÓSSEIS ORGÂNICOS DA FORMAÇÃO SETE LAGOAS, BRASIL: BIOESTRATIGRAFIA E PALEOBIOGEOGRAFIA DO GONDWANA DURANTE O EDIACARIANO

A thesis presented to the Graduate Research Program in Geology, Institute of Geosciences, University of Brasília – UnB. Requirement foresaw by the program regulation.

Tese apresentada ao Programa de Pós-Graduação em Geologia, Instituto de Geociências, Universidade de Brasília – UnB. Requisito previsto no regulamento do programa.

Supervisors - *Orientadores*:
Prof. Dermeval Aparecido do Carmo (UnB)
Prof. Shuhai Xiao (Virginia Tech)

Brasília, DF
2022

Denezine, Matheus

DD392t Taxonomia de microfósseis orgânicos da Formação Sete Lagoas, Brasil: bioestratigrafia e paleoecologia do Gondwana durante o Ediacariano / Matheus Denezine; orientador Dermeval Aparecido do Carmo; co-orientador Shuhai Xiao. -- Brasília, 2022. 140 p.

Tese(Doutorado em Geologia) -- Universidade de Brasília, 2022.

1. Formação Sete Lagoas. 2. Ediacariano. 3. Seção-tipo. 4. Bioestratigrafia. 5. Paleobiogeografia. I. Aparecido do Carmo, Dermeval, orient. II. Xiao, Shuhai, co-orient. III. Título.

ACKNOWLEDGMENTS

Initially, I want to thank all institutions that participated in the development of this research: the Coordination for the Improvement of Higher Education Personnel (CAPES), the National Council for Scientific and Technological Development (CNPq), Geological Survey of Brazil (CPRM), Brazilian Oil and Gas Company (PETROBRAS), National Agency of Petroleum, Gas, and Biofuels (ANP), the University of Brasília (UnB) and the Virginia Polytechnic Institute and State University (Virginia Tech). I also thank the Foundation for Scientific and Technological Enterprises (FINATEC) for assistance in administrative affairs supporting scientific projects in Brasília. This study was financed in part by the Coordination for the Improvement of Higher Education Personnel - Brazil (CAPES) - Finance Code 001.

I want to thank the Institute of Geosciences of the University of Brasília, and its professors, especially Professor Dermeval Aparecido do Carmo and Professor Shuhai Xiao, who have been my thesis supervisors. I'm proud of and grateful for my time working with them. Countless people supported my effort in this essay. I want to show my appreciation to Emeritus Professor Robert Hayes Giles and his daughter, my friend, Anne Giles. They had singular importance during my sandwich program in 2020 at Virginia Tech. I wish to extend my special thanks to the professors on the monitoring committee, Carlos José Souza de Alvarenga and Martino Giorgioni, for their willingness to evaluate and contribute to this work. To my family, friends, and laboratory colleagues for all their support.

AGRADECIMENTOS

Inicialmente, quero agradecer a todas as instituições que participaram do desenvolvimento desta pesquisa: à Coordenação de Aperfeiçoamento de Pessoal de Nível Superior (CAPES), ao Conselho Nacional de Desenvolvimento Científico e Tecnológico (CNPq), ao Serviço Geológico de Brasil (CPRM), à Petróleo Brasileiro S.A. (PETROBRAS), à Agência Nacional do Petróleo, Gás e Biocombustíveis (ANP), à Universidade de Brasília (UnB) e ao Instituto Politécnico e Universidade Estadual da Virgínia (Virginia Tech). Agradeço também à Fundação de Empreendimentos Científicos e Tecnológicos (FINATEC) pela assistência em assuntos administrativos apoiando projetos científicos em Brasília. O presente trabalho foi realizado com apoio da Coordenação de Aperfeiçoamento de Pessoal de Nível Superior - Brasil (CAPES) - Código de Financiamento 001.

Ao Instituto de Geociências da Universidade de Brasília, em especial ao Professor Dermeval Aparecido do Carmo e ao Professor Shuhai Xiao, que foram meus orientadores de tese. Me sinto orgulhoso e grato pelo tempo de trabalho com eles. Inúmeras pessoas apoiaram meu esforço nesse projeto. Quero mostrar meu apreço ao Professor Emérito Robert Hayes Giles, Virginia Tech e sua filha, minha amiga, Anne Giles. Eles tiveram importância singular durante meu programa sanduíche em 2020 na Virginia Tech. Gostaria de agradecer especialmente aos professores do comitê de acompanhamento de tese, professores Carlos José Souza de Alvarenga e Martino Giorgioni, pela disponibilidade em avaliar e contribuir com este trabalho. Aos meus familiares, amigos e colegas de laboratório por todo o apoio.

ABSTRACT

This thesis presents a detailed taxonomic study on organic-walled microfossils from the Sete Lagoas Formation, Ediacaran, Bambuí Group, São Francisco basin, Brazil. This formation was described from carbonate expositions in its type locality, Sete Lagoas County, Minas Gerais State. However, the stratotype section was never described. The present work presents the first description of the lectostratotype section of the Sete Lagoas Formation and the proposal of two hypostratotype sections based on the lithological description and fossil record. The studied sections are located in the Minas Gerais State and the Federal District, southeast Brazil: 1. Lectostratotype section, Sete Lagoas County; 2. Hypostratotype section from the PRF, Sete Lagoas County; 3. Hypostratotype section from the Barreiro community, Januária County; 4. Fercal section, Brasília. Nine species of organic-walled microfossils were recovered in the four studied sections from Sete Lagoas Formation: *Germinosphaera bispinosa* Mikhailova, 1986, *Leiosphaeridia crassa* (Naumova, 1949), *Leiosphaeridia jacutica* (Timofeev, 1966), *Leiosphaeridia minutissima* (Naumova, 1949), *Leiosphaeridia tenuissima* Eisenack, 1958, *Leiosphaeridia ternata* (Timofeev, 1966), *Bambuites erichsenii* Sommer, 1971, *Siphonophycus robustum* (Schopf, 1968), and *Ghoshia januarensis* new species. Additionally, an undetermined stromatolite species is also reported: *Gymnosolen* sp. Two biostratigraphic units are currently recognized in the Sete Lagoas Formation, approaching all four studied sections. Two zones are described: *Leiosphaeridia minutissima* Zone, a lowest-occurrence interval zone, lower/mid Ediacaran, and *Bambuites erichsenii* Zone, a range zone, upper Ediacaran. Stratigraphic data and organic-walled microfossil taxonomy indicate that the Sete Lagoas Formation was deposited in a neritic marine environment. The connection by a neritic zone of Amazonia with other cratons that form the western Gondwana, including the São Francisco craton, in 550 Ma is corroborated based on *Bambuites erichsenii* and *Ghoshia januarensis* occurrences. At the same time, Laurentia, Baltica, and Siberia were paleocontinents apart.

Keywords: Sete Lagoas Formation; Ediacaran; lectostratotype; biostratigraphy; paleobiogeography.

RESUMO

A presente tese apresenta um estudo taxonômico de microfósseis de parede orgânica da Formação Sete Lagoas, Ediacariano, Grupo Bambuí, bacia do São Francisco, Brasil. Essa formação foi descrita a partir de exposições de rochas carbonáticas em sua localidade-tipo, Município de Sete Lagoas, Estado de Minas Gerais. No entanto, a seção-tipo nunca foi descrita. O presente trabalho apresenta a primeira descrição da seção-tipo da Formação Sete Lagoas e a proposta de duas seções-tipo suplementares, a partir da descrição litológica e registro fossilífero. As seções estudadas estão localizadas no Estado de Minas Gerais, sudeste do Brasil: 1. Seção-tipo, Município de Sete Lagoas; 2. Seção-tipo suplementar da PRF, Município de Sete Lagoas; 3. Seção-tipo suplementar da comunidade do Barreiro, Município de Januária; bem como no Distrito Federal: 4. Seção Fercal, Brasília. Nove espécies de microfósseis de parede orgânica foram recuperadas nas quatro seções estudadas da Formação Sete Lagoas: *Germinosphaera bispinosa* Mikhailova, 1986, *Leiosphaeridia crassa* (Naumova, 1949), *Leiosphaeridia jacutica* (Timofeev, 1966), *Leiosphaeridia minutissima* (Naumova, 1949), *Leiosphaeridia tenuissima* Eisenack, 1958, *Leiosphaeridia ternata* (Timofeev, 1966), *Bambuites erichsenii* Sommer, 1971, *Siphonophycus robustum* (Schopf, 1968) e *Ghoshia januarensis* nova espécie. Adicionalmente, uma espécie indeterminada de estromatólito também é relatada: *Gymnosolen* sp. Duas unidades bioestratigráficas foram reconhecidas na Formação Sete Lagoas ao abordar as quatro seções estudadas. Duas zonas são descritas: Zona *Leiosphaeridia minutissima*, uma zona diferencial inferior, Ediacariano inferior/intermediário, e a Zona *Bambuites erichsenii*, uma zona de amplitude, Ediacariano superior. Dados estratigráficos e taxonômicos de microfósseis de parede orgânica e dos estromatólitos descritos, indicam que a Formação Sete Lagoas foi depositada em ambiente marinho nerítico. A conexão por zona nerítica da Amazônia com outros crátons que formam o Gondwana ocidental, incluindo o cráton São Francisco, em 550 Ma é corroborada com base nas ocorrências de *Bambuites erichsenii* e *Ghoshia januarensis*, enquanto os paleocontinentes Laurentia, Báltica e Sibéria estavam separados.

Palavras-chave: Formação Sete Lagoas; Ediacariano; lectostratotipo; bioestratigrafia; paleobiogeografia.

TABLE OF CONTENTS

LIST OF FIGURES

1. INTRODUCTION

The present thesis aims to characterize and assess the stratigraphic significance of the fossil assemblage from the Sete Lagoas Formation based on taxonomic, lithostratigraphic, biostratigraphic, and paleobiogeographic studies. In addition, a combined preparation for micropaleontological and sedimentological studies of samples from the Proterozoic record was developed (Appendix 1). This lithostratigraphic approach is focused on the lectostratotype section description of the Sete Lagoas Formation and the proposal of two hypostratotype sections, including an additional section. Attached to this stratigraphic framework, a taxonomic study of the fossil assemblage was conducted to evaluate its chronobiostratigraphic positioning. This approach is presented herein as a contribution to improve an updated stratigraphic framework, paleoenvironmental setting, and paleobiogeographic context of the São Francisco basin in late Ediacaran Gondwana.

The main objectives of the thesis include a taxonomy of organic-walled microfossils from the Sete Lagoas Formation, a description of its lectostratotype, the proposal of two hypostratotypes, and an additional section; a proposal of a biostratigraphic framework for the studied sections; paleoenvironmental analysis and paleobiogeographic approach. Five manuscripts resulted from part of the present thesis: 1. a combined methodological preparation for micropaleontological and sedimentological studies; 2. biostratigraphy of organic-walled microfossils from the hypostratotype Barreiro section; 3. description and implications of microbially induced sedimentary structures on the Sete Lagoas Formation; 4. Description of lectostratotype and hypostratotype of the Sete Lagoas Formation, Bambuí Group; and 5. Biostratigraphic and paleogeographic analyses of the Sete Lagoas Fm. during the Ediacaran. The five manuscripts are:

1. “METHODOLOGICAL DEVELOPMENT OF A COMBINED PREPARATION FOR MICROPALEONTOLOGICAL AND SEDIMENTOLOGICAL STUDIES OF SAMPLES FROM THE PROTEROZOIC RECORD” (Denezine et al., 2022, published on Frontiers in Earth Science – Appendix 1);
2. “ORGANIC-WALLED MICROFOSSILS FROM THE EDIACARAN SETE LAGOAS FORMATION, BAMBUÍ GROUP, SOUTHEAST BRAZIL: TAXONOMIC, STRATIGRAPHIC DISTRIBUTION, AND BIOSTRATIGRAPHIC ANALYSES” (Denezine et al., accept with revision, Journal of Paleontology);
3. “*PALAEOPHYCUS*-LIKE MICROBIAL RIDGES FROM CARBONATES OF THE EDIACARAN SETE LAGOAS FORMATION AND THEIR IMPLICATIONS FOR THE INTERPRETATION OF PUTATIVE TRACE FOSSILS” (Denezine et al., to be submitted to Sedimentology);
4. “LECTOSTRATOTYPE AND HYPOSTRATOTYPE SECTIONS OF THE SETE LAGOAS FORMATION, EDIACARAN, BAMBUÍ GROUP, BRAZIL: LITHOSTRATIGRAPHIC DESCRIPTION AND PALEONTOLOGICAL APPROACH” (In preparation);
5. “BIOSTRATIGRAPHY OF THE SETE LAGOAS FORMATION: A CHRONOSTRATIGRAPHIC AND PALEOGEOGRAPHIC APPROACH” (In preparation).

The remarkable diversity of organic-walled microfossils, particularly acanthomorphic acritarchs, in the Ediacaran Period (Huntley et al., 2006; Knoll, 1994; Vidal and Moczydłowska-Vidal, 1997) is hypothesized to be associated with the ecological rise of animals (Peterson and Butterfield, 2005). Closer to the end of Ediacaran, the advent of calcareous skeletons is evidenced by cloudinids and corumbellids (Germs, 1972; Hahn et al., 1982; Hua et al., 2005; Walde et al., 2015; Adôrno et al., 2017). Therefore, a taxonomic study of organic-walled microfossils from the Sete Lagoas Formation provides a tool for biostratigraphic correlation and offers useful data to improve the understanding of Ediacaran evolution.

2. GEOLOGICAL SETTING OF THE SETE LAGOAS FORMATION

The western portion of the São Francisco craton comprises a succession of siliciclastic and carbonate rocks dated between 1.77 Ga and 0.52 Ga (Alvarenga et al., 2012; Moreira et al., 2020; Pimentel et al., 2011) (Fig. 1). The Brasília fold belt that bounds the western margin of the São Francisco craton was deformed during the Brasiliano-Pan-African orogeny between 790 Ma and 540 Ma (Pimentel and Fuck, 1992; Pimentel et al., 1999; Caxito et al., 2021). This fold belt borders to the east with the São Francisco craton, which is covered by undeformed Neoproterozoic strata. It consists of a tectonic domain with thin-skinned tectonic deformation and a domain further west with thick-skinned deformation (Alvarenga et al., 2014) (Fig. 2).

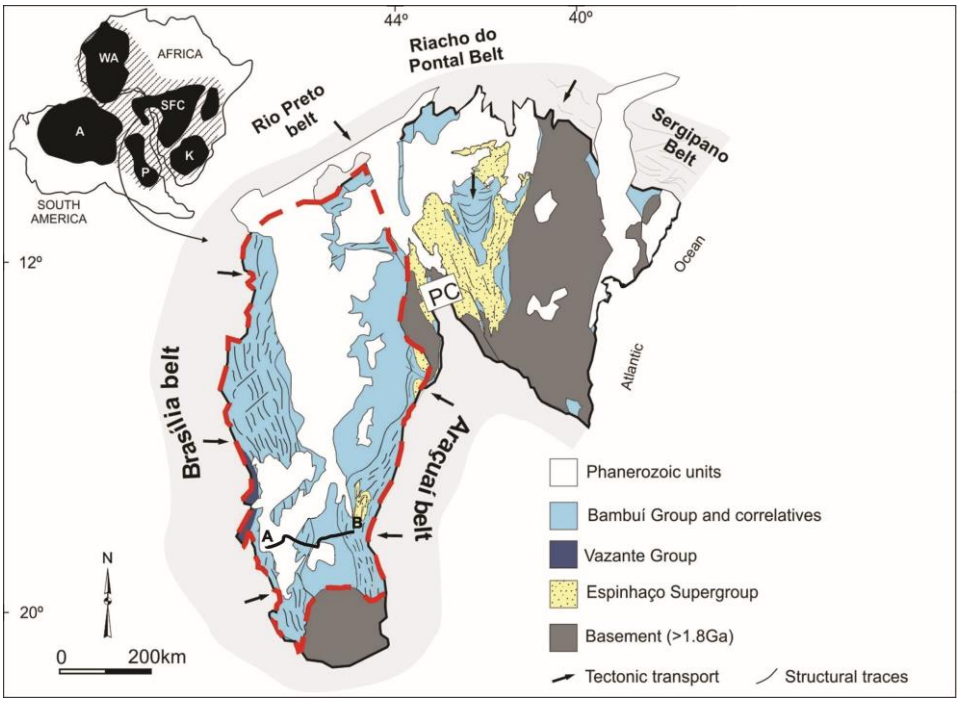

Figure 1: Geological map of the São Francisco basin (red dashed line) in the São Francisco craton. Inset map shows major cratons in the western Gondwana in a Neoproterozoic paleogeographic configuration: A, Amazonian; P, Rio de la Plata; K, Kalahari; WA, West Africa; SFC, São Francisco-Congo. PC: Paramirim Corridor. The AB cross-section refers to the area of the seismic line displayed in Fig. 2. (after Reis and Suss, 2016).

The São Francisco basin can be subdivided into five main domains regarding its chronostratigraphy: 1. the Archean/Paleoproterozoic basement, which consists of granite-gneissic rocks (Reis and Alkmim, 2015), 2. the Paleo/Mesoproterozoic/Early Neoproterozoic metasedimentary sequence represented by the Espinhaço Supergroup, and the Paranoá and Vazante groups (Guadagnin et al., 2015; Alvarenga et al., 2019), 3. The Neoproterozoic/Cambrian units are characterized by the Jequitaí Formation and Macaúbas and Bambuí groups (Caxito et al., 2012; Paula-Santos et al., 2015; Oliveira et al., 2021; Sanchez et al., 2021), 4. the Permian/Carboniferous Santa Fé Group (Campos and Dardenne, 1994), and 5. the Cretaceous sedimentary sequence, represented, from base to top, by Areado Group, Lower Cretaceous; and Mata da Corda and Urucuia groups, Upper Cretaceous (Campos and Do Carmo, 2005; Zalán and Silva, 2007).

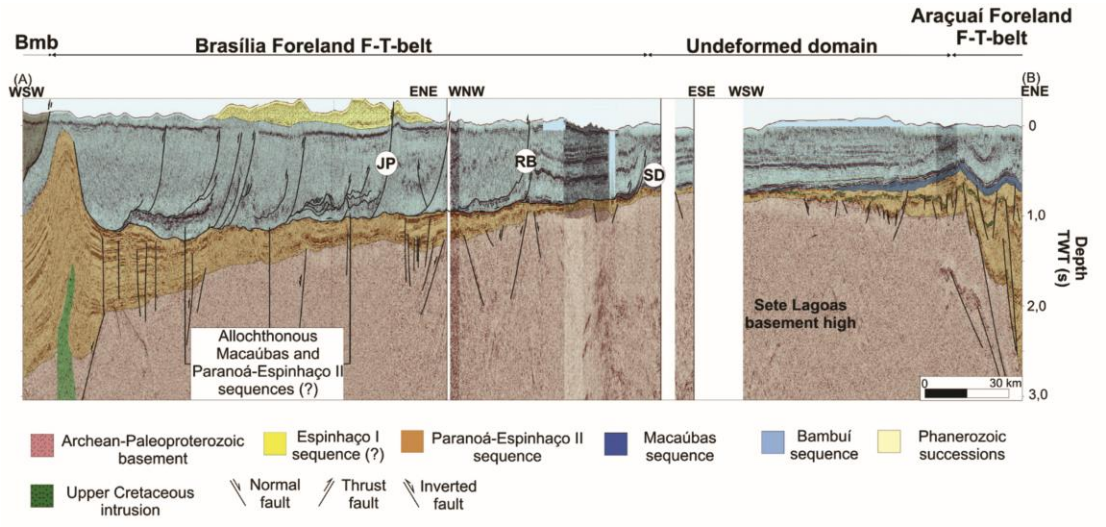

Figure 2: Composite seismic section "A-B", which location is shown in Fig. 1. Tectonic domains across the São Francisco basin, from the start point in west-southwest to the final point in east-northeast: Brasília foreland fold-thrust belt, undeformed domain, and Araçuaí foreland fold-thrust belt. Depth in two-way travel time (TWT). Thrust faults: JP e João Pinheiro; RB e Rio Borrachudo; SD e São Domingos. Bmb: Brasília metamorphic belt (after Reis and Suss, 2016).

The Neoproterozoic deposits in the West portion of the São Francisco basin, which was contiguous with the Congo craton (Fig. 1), are represented by the Jequitaí Formation and the Bambuí Group. The Bambuí Group, a mixed carbonate-siliciclastic platform, consists of, in ascending stratigraphic order, the Sete Lagoas Formation (limestones, dolostones, and pelite intercalations), Serra de Santa Helena Formation (siltstones and marl), Lagoa do Jacaré Formation (predominantly dark stromatolitic and oolitic limestone and shales), Serra da Saudade Formation (shales, siltstones, and sandstones), and Três Marias Formation (sandstones) (Dardenne, 1978).

The Sete Lagoas Formation, which is the main focus of this work, represents the basal unit of the Bambuí Group and consists of a sequence of carbonate-dominated sediments in the São Francisco basin. Those sediments are characterized by a low total organic carbon (TOC) content of less than 2% (Uhlein et al., 2019; Caetano-Filho et al., 2021) and relatively low thermal maturity (Reis & Suss, 2016). The Sete Lagoas Formation is interpreted to have been deposited in a shallow carbonate platform environment, perhaps with a limited connection with the open marine environment (Paula-Santos et al., 2015; Vieira et al., 2015).

Even though Dardenne (1978) formalized five formations within the Bambuí Group, the type sections of these lithostratigraphic units were never formally described. The International Stratigraphic Guide (Murphy and Salvador, 1999), which was developed to promote an international agreement on stratigraphic classification, establishes that a formal lithostratigraphic unit must have a type locality and a stratotype section with a clear characterization. Additionally, the designation of a hypostratotype section is a possibility to complement the definition of a lithostratigraphic unit (Murphy and Salvador, 1999; North American Commission on Stratigraphic Nomenclature, 2005).

The depositional age of the Bambuí Group has long been a matter of debate. The Bambuí Group was initially considered to be Cretaceous (Liais, 1872 in Couto et al., 1981), but recent studies show that it is probably Ediacaran–Cambrian (Pimentel et al., 2011; Warren et al., 2014; Paula-Santos et al., 2015; Moreira et al., 2020a; Sanchez et al., 2021; DaSilva et al., 2022). Geochronological constraints on the Bambuí Group are few and inconclusive. Carbonates of the lower Sete Lagoas Formation yielded Pb-Pb apparent ages of ~740 Ma (Babinski et al., 2007).

Nevertheless, Caxito et al. (2021) analyzed samples from crystal-fan-bearing limestone from the base of the Sete Lagoas Formation. The U-Pb ages obtained by Caxito et al. (2021) yielded lower intercept dates of 615.4 ± 5.9 Ma, when both the crystal-fans and matrix were analyzed together, 608.1 ± 5.1 Ma for crystal-fans, and 607.2 ± 6.2 Ma for the matrix. The youngest population of detrital zircons from the Sete Lagoas Formation gave U-Pb ages of ~557 Ma (Paula-Santos et al., 2015), and the youngest population of detrital zircons from the Três Marias Formation gave U-Pb ages of ~620 Ma (Pimentel et al., 2011; Rodrigues, 2008), providing maximum age constraints on the host strata. More recently, a zircon U–Pb age of 520.2 ± 5.3 Ma has been reported from a volcanic ash bed in the Serra da Saudade Formation (Moreira et al., 2020b), suggesting that the upper Bambuí Group may belong to the Stage 2 of the Cambrian System.

The occurrence of *Cloudina* sp. and *Corumbella werneri*—tubular fossils typically found in terminal Ediacaran rocks—in the lower Sete Lagoas Formation (Warren et al., 2014; Perrella Júnior et al., 2017) and the presence of *Treptichnus pedum*—a trace fossil whose first appearance is used to define the base of the Cambrian System—in the Três Marias Formation (Sanchez et al., 2021) further indicate that perhaps the entire Bambuí Group is Ediacaran–Cambrian. Although the conflict with the ~740 Ma Pb-Pb age from the Sete Lagoas Formation (Babinski et al., 2007) remains unresolved.

2.1. Fossil assemblage from the Sete Lagoas Formation

Studies of the fossiliferous assemblage of the Neoproterozoic that address the identification of fossils of this era are in real progress worldwide. The fossil occurrences comprehend organic-walled microfossils (Grey, 2005; Gaucher et al., 2008b, 2008a; Tang et al., 2015; Porter and Riedman, 2016; Denezine et al., 2022), the first skeletal metazoans (Beurlen and Sommer, 1957; Germs, 1972; Hahn et al., 1982; Adôrno et al., 2017, 2019), microbialites (Grotzinger et al., 2000; Sanchez et al., 2018; Santos et al., 2018), fossil embryos (Xiao and Knoll, 2000) and molecular fossils, also named biomarkers (Sousa Júnior et al., 2016; Bobrovskiy et al., 2018). All the above categories, except embryo fossils, were reported in lithostratigraphic units of the Neoproterozoic from Brazil.

The fossil record from the Sete Lagoas Formation consists of stromatolites and microbial mats occurrences (Fantinel et al., 2015), followed by organic-walled microfossils (Simonetti, 1994; Simonetti and Fairchild, 2000; Perrella Júnior et al., 2017; Denezine et al., 2022), also reported as permineralized specimens (Simonetti and Fairchild, 1989; Fairchild et al., 1996), and few records of metazoans (Warren et al., 2014). Thus, it comprises an assemblage that could provide subsidies for biostratigraphic correlation studies. In the Sete Lagoas Formation, there are records of cyanobacteria, protists, and metazoans (Tab. 1).

The first attempt at the chronostratigraphic positioning of the Sete Lagoas Formation from fossils was made by Marchese (1974). Marchese described stromatolites that outcrop on the BR-040 highway near the Municipality of Sete Lagoas, Minas Gerais State, and identified them as cf. *Gymnosolen* Steinmann, 1911. Marchese (1974) inferred from these occurrences an age of late Rifean for the Sete Lagoas Formation, an interval recognized as late Tonian. Furthermore, other studies analyzed and described several stromatolite microbialites, emphasizing a great diversity of

morphotypes, columnar, bulbs, and domes (Fairchild and Dardenne, 1978; Fairchild and Schorscher, 1985; Sanchez, 2014; Fantinel et al., 2015), in addition to microphytolites (Lopes, 1995; Nobre and Coimbra, 2000).

The first reports of organic-walled microfossils from the Sete Lagoas Formation were spherical vesicles, described by Sommer (1971) as *Bambuites erichsenii* Sommer, 1971. Sommer (1971) attributed this species to unicellular algae. Later on, several articles on organic-walled microfossils from the Sete Lagoas Formation were published (Simonetti and Fairchild, 1989, 2000; Fairchild et al., 1996, 2012; Sanchez and Fairchild, 2018), describing dozens of species from this unit (Table 1), although Sanchez and Fairchild (2018) invalidated one species, *Bambuites erichsenii* Sommer, 1971.

Simonetti and Fairchild (2000) bring the first systematic study of organic-walled microfossils from the Precambrian units of Brazil. This study analyzed samples of drill cores located in Montalvânia City, Minas Gerais State, Brazil. This research encompassed fossil recoveries from the Sete Lagoas Formation, as well as other formations of the Bambuí Group, comprising the Serra de Santa Helena, Lagoa do Jacaré, and Serra da Saudade formations. In addition to these units, the fossil content of the Conselheiro Mata Group was also analyzed. Nine species were identified in the Sete Lagoas Formation, comprising filamentous species, coccoidal colonies, and sphaeromorphs, however poorly preserved. Although the low recovery of specimens in this unit, it was possible to identify a domain of specimens of *Leiosphaeridia* spp. Eisenack, 1958.

Table 1: Fossils from the Sete Lagoas Formation. Articles: 1, Sommer (1971); 2, Marchese (1974); 3, Simonetti and Fairchild (1989); 4, Fairchild et al. (1996); 5, Simonetti & Fairchild (2000); 6, Fairchild et al. (2012); 7, Warren et al. (2014); 8, Perrella Júnior et al. (2017); 9, Sanchez and Fairchild (2018); 10, Denezine et al. (2022); 11, this study.

Species	**Articles**										
	1	2	3	4	5	6	7	8	9	10	11
cf. *Archaeotrichion contortum* Schopf, 1968				X							
cf. *Archaeotrichion* sp.				X							
Bambuites erichsenii Sommer, 1971	X								X		X
cf. *Biocatenoides*				X							
Cloudina sp.							X	X			
Corumbella werneri Hahn et al., 1982							X				
cf. *Cyanonema inflatum* Oehler, 1977				X							
cf. *Dictyosphaera macroreticulata* (Xing and Liu, 1972)				X							
Eomycetopsis sp. A			X								
Eomycetopsis sp. B			X								
cf. *Eomycetopsis* sp.				X							
cf. *Eomycetopsis*				X							
Eosynechoccus medius (Hofmann, 1976)					X						
Eosynechococcus moorei Hofmann, 1976			X								
Gymnosolen sp.		X									
Germinosphaera bispinosa Mikhailova, 1986										X	X
Glenobotrydion aenigmatis Schopf, 1968			X								
cf. *Gloeodiniopsis* sp.				X							
cf. *Gloeodiniopsis magna* (Nyberg and Schopf., 1984)				X							
Ghoshia sp.										X	
Ghoshia januarensis new species											X
Leiosphaeridia sp. 1					X						
cf. *Leiosphaeridia* sp.				X							
Leiosphaeridia crassa (Naumova, 1949)											X
Leiosphaeridia jacutica (Timofeev, 1966)											X
Leiosphaeridia minutissima (Naumova, 1949)										X	X
Leiosphaeridia tenuissima Eisenack, 1958										X	X
Leiosphaeridia ternata											X
Melanocyrillium sp.										X	
Myxococcoides cf. *M. cantabrigensis* Knoll, 1982			X								
Myxococcoides sp. A			X								
Myxococcoides sp. B			X								
cf. *Myxococcoides reticulata* Schopf, 1968				X							
cf. *Myxococcoides*				X							
cf. *Myxococcoides* sp.				X							
cf. *Myxococcoides globosa* Maithy and Shukla, 1977				X							
cf. *Oscillatoriopsis* sp.				X							
Palaeophycys sp.							X				
cf. *Rugosoopsis* sp.				X							
Siphonophycus robustum Schopf, 1968										X	X
Siphonophycus sp.			X								
cf. *Siphonophycus beltense* Horodyski, 1980				X							
cf. *Siphonophycus* sp.				X							
cf. *Siphonophycus*				X							
Trachyhystrichosphaera aimica Hermann, 1976						X					

Hidalgo (2007) also worked with organic-walled microfossils of the Sete Lagoas Formation, focusing on the Neoproterozoic glaciations and their influence on the paleobiota. Hidalgo (2007) corroborates the interpretation that the Sete Lagoas Formation was deposited after a glaciation event. Different preservation of organic-walled microfossils was also reported, such as permineralized filamentous organisms and some cocooids (Fairchild and Schorscher, 1985). All specimens studied by Fairchild and Schorscher (1985) were silicified but poorly preserved. In addition, Simonetti and Fairchild (1989) describe eleven species with occurrence in this unit, including coccoids, some solitary, others colonial, and rare eukaryotes or filamentous prokaryotes.

The occurrences of mineralized metazoans in the Sete Lagoas Formation are restricted to the occurrences reported by Warren et al. (2014) and Perrella-Júnior et al. (2017). Warren et al. (2014) report occurrences of *Cloudina* sp. and *Corumbella werneri* in the Sete Lagoas Formation from expositions in the Januária Municipality. Perrella-Júnior et al. (2017) also report occurrences of *Cloudina* sp. recovered from the same region, although the photomicrography of the occurrence is inconclusive (Perrella-Junior et al., 2017: fig.7G).

3. METHODOLOGY

The study of the Ediacaran portion of the São Francisco basin to describe the lectostratotype section and hypostratotype sections, as well as one additional section of the Sete Lagoas Formation, started with fieldworks carried out between 2018 and 2021. Lithostratigraphic columns are presented for each studied section, containing fossiliferous intervals, detailed sampling information, and the levels where organic-walled microfossils were recovered.

Standard petrographic thin sections were prepared and examined under a Zeiss Discovery.V20 stereomicroscope connected with an AxioCam ICc3 camera and a Zeiss Scope.A1

microscope connected with an AxioCam ICc1 camera. Organic-walled microfossils were extracted from thinly laminated mudstones and light to dark grey limestone and dolostones samples using acid maceration techniques. The samples were dissolved using HCl and HF acids. Residues were rinsed repeatedly in distilled water, and after the residues were settled following each rinse, the supernatant was decanted. No centrifugation was used to minimize mechanical damage to organic-walled microfossils. No oxidative procedure was applied to organic residues (Denezine et al., 2022) (Appendix 2). Transmitted-light photomicrographs were acquired using an Axio Imager.A2 microscope equipped with an AxioCam MRc digital camera (both Carl Zeiss).

Size analysis of *Leiosphaeridia* specimens is based on the measurement of their vesicle diameters. Vesicle diameter and wall thickness were used to identify four morphospecies of *Leiosphaeridia* present in the Sete Lagoas Formation: *Leiosphaeridia crassa*, *Leiosphaeridia jacutica*, *Leiosphaeridia minutissima*, *Leiosphaeridia tenuissima*. *Leiosphaeridia ternata* is the only *Leiosphaeridia* species that was identified due to its radially oriented acutely angled clefts along the vesicle. Abundance data were collected in this study. All palynological slides were examined thoroughly, and complete specimens were counted. Due to their colonial nature or frequent preservation as fragments, the abundance of *Siphonophycus robustum* and *Ghoshia januarensis* was not quantified.

Selected organic-walled microfossils from the Sete Lagoas Formation were analyzed using Raman spectroscopy. Specimens were placed on palynological slides and analyzed on a HORIBA JobinYvon LabRAM HR800 Raman microprobe equipped with a high-resolution 600 mm focal length spectrometer and a 514 nm argon laser source in the Department of Geosciences at Virginia Tech. The laser beam was less than 10 μm in diameter with a 40× objective lens. Raman spectra

were acquired using the software Labspec 5.0 with an acquisition time of less than one minute for each analysis.

Raman spectroscopy data were processed using Python modules. Baseline correction was applied to the raw data by adjusting a polynomial (third-order) curve using the Raman data from 200 to 800 and from 1900 to 2100 cm-1 that captures the Raman peaks of carbonaceous material. After baseline correction, the four Raman peaks of carbonaceous material, as in Kouketsu et al. (2014), were decomposed with the shape of a convolution between Gaussian and Lorentzian functions. The expected variations in the peaks are relatively small compared to the other parameters. Thus, two optimizations are performed. The first one finds amplitude and width parameters by letting them free and using fixed values for the frequencies. These frequency values are not the final ones but are close given the small variation expected, and the curve roughly is the desired shape. After this step, another optimization is performed, two frequencies are held at 1245 and 1510 cm-1 Kouketsu et al. (2014) and the other parameters are calculated more precisely. Raman data processing followed the procedures described in Kouketsu et al. (2014).

The processed Raman data were subjected to principal component analysis (PCA) in Python. The peak position, peak height, and full width at half-maximum (FWHM) of the four Raman peaks of carbonaceous material were used in PCA. The PCA allowed a dimensionality reduction to two principal components. The Python package for PCA is publicly available (Mazoni, 2021), and PCA in this study used the Python modules Numpy (Harris et al., 2020), Scipy (Virtanen et al., 2020), and Rampy (Le Rosq, 2021).

Types, figures, and other specimens examined in this study are deposited in the following institution: Museum of Geosciences (MGeo-UnB), University of Brasília, Brasília, Brazil.

4. STUDIED SECTIONS

The approached sections of the Sete Lagoas Formation, from the Minas Gerais State, are: 1. Lectostratotype section of the Sete Lagoas Formation, from the outcrop at the Conservation Unit Rei do Mato cave, Sete Lagoas County; 2. Hypostratotype section of the Federal Highway Police (PRF), Sete Lagoas County; 3. Hypostratotype section of the Barreiro, Januária County. The Fercal section was the only section studied in the Federal District, Brasília (Fig. 3).

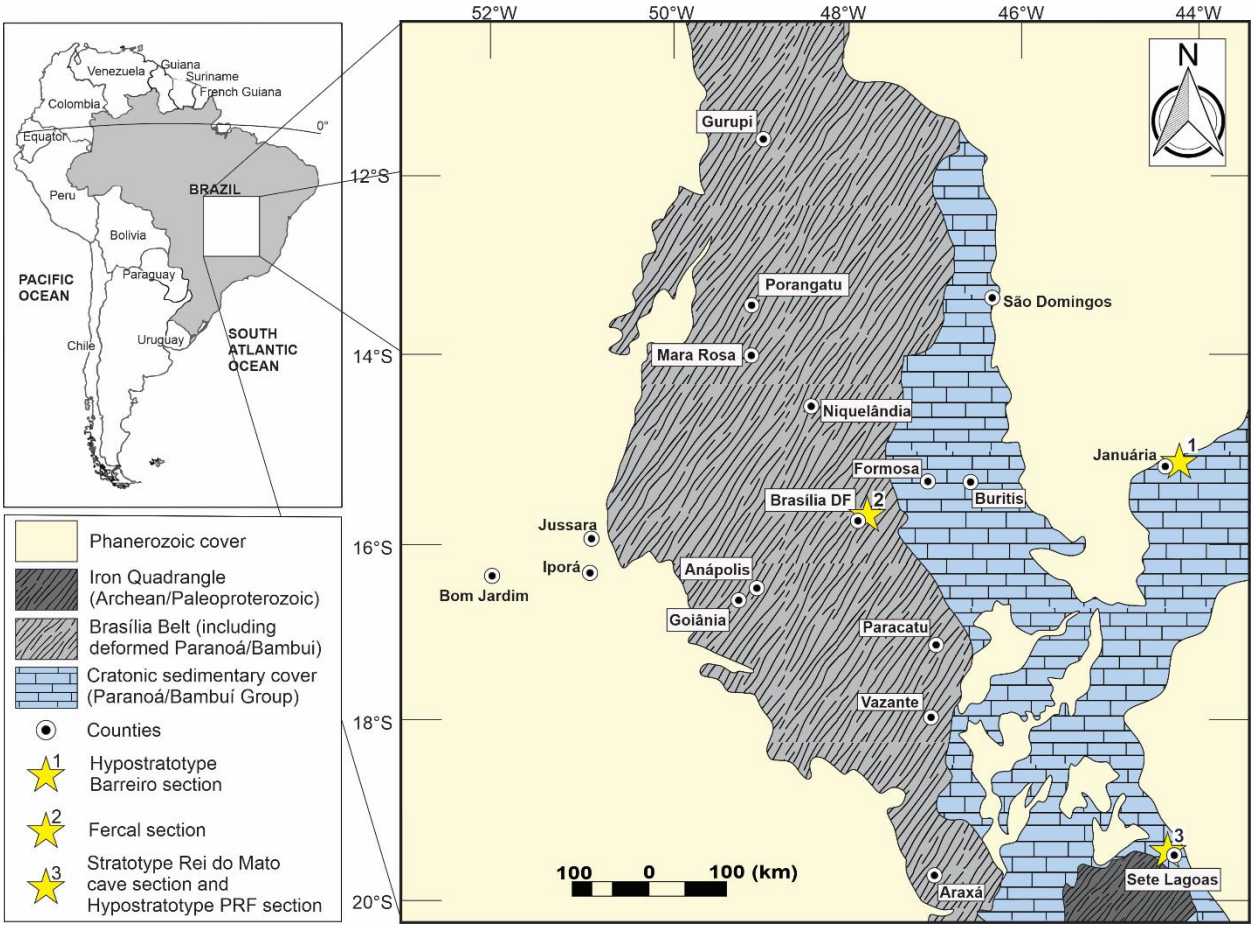

Figure 3: Geological map of studied areas in Brazil. (1) Barreiro section, Januária County, Minas Gerais State; (2) Fercal section, Brasília, Federal District; (3) Rei do Mato cave and PRF sections, Sete Lagoas County, Minas Gerais State.

The designation of the Rei do Mato cave section as a lectostratotype section complements the lithostratigraphic and chronostratigraphic definition of the lectostratotype section due to fossiliferous occurrences and great exposure of the sedimentary sequence of the Sete Lagoas Formation in the type locality. Additionally, the Rei do Mato cave section is located in an Environmental Conservation Unit. The Conservation Unit Rei do Mato cave is legally established by the Minas Gerais State Government to meet the requirements of protection and sustainable exploitation of bio and geodiversity.

4.1. Lectostratotype section of the Sete Lagoas Formation, Sete Lagoas County

The lectostratotype section of the Rei do Mato cave is located inside the borders of the Gruta Rei do Mato Conservation Unit, Sete Lagoas County, Minas Gerais State, southeastern Brazil (Fig. 3). The coordinates of the section (UTM), Datum WGS84 are: 23K, 575103 mE, 7844059 mN. The formations of the lower part of the Bambuí Group, Sete Lagoas and Serra de Santa Helena formations, outcrop in this locality. The stratigraphic thickness of the Sete Lagoas Formation in the studied area is about 125 m (Fig. 4). A total of 105 stratigraphic levels were sampled.

Although the basal boundary of the Sete Lagoas Formation with the lithostratigraphic unit below is not exposed, the carbonate rocks of the Sete Lagoas Formation rest on top of a Paleoproterozoic gneiss–migmatite basement in the surrounding area (Vieira et al., 2015).

The section studied is predominantly carbonate, with a predominance of limestone rocks with little or no contribution of siliciclastics. The section comprises metasedimentary rocks, mainly pure calcarenites of variable grain size and light gray to dark gray color. In the basal and intermediate portion of the section, there are structures such as hummocky and swaley cross-bedding, soft-sediment deformation structure comprising synforms, and convoluted bedding (Fig,

4). This facies association indicates deposition below the fair-weather baseline level in a transitional environment influenced by storm wave associated with a sloped carbonate ramp with high accumulation rates.

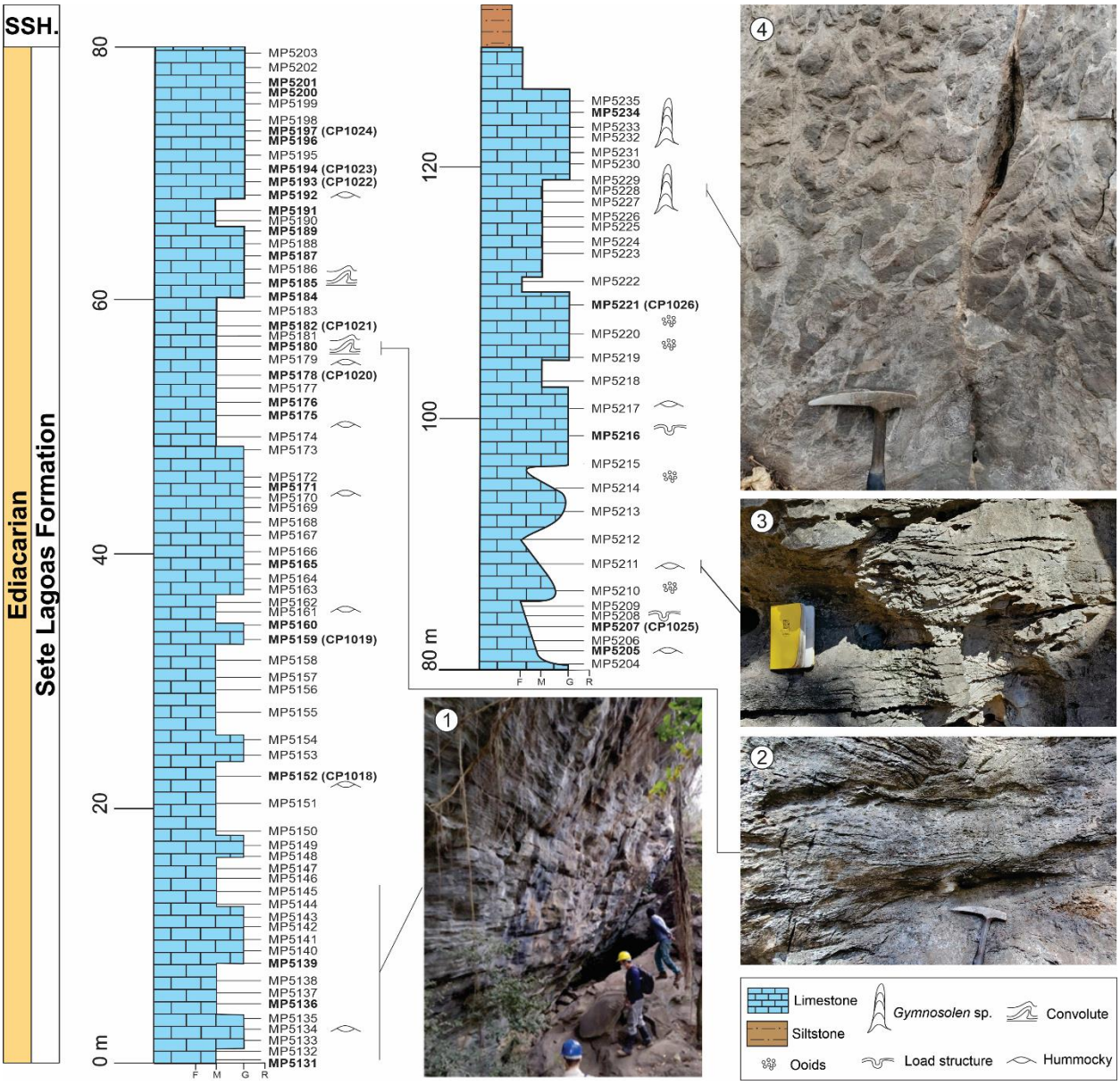

Figure 4: Lectostratotype section and field photographs of the Sete Lagoas Formation at the Rei do Mato cave, Sete Lagoas County, Minas Gerais State, Brazil. Sample horizons are marked with the sample number prefixes MP. **(1)** Lower portion of the lectostratotype; **(2)** Concolute structure; **(3)** Hummocky structure; **(4)** *Gymnosolen* sp.

In the upper portion of the section, the lithofacies display a greater amount of low-angle, tabular cross-bedding, climbing ripples, herringbone cross-stratification, and the occurrence of bifurcated columnar stromatolites. Such morphotype of microbialites was classified by Marchese (1974) as possibly belonging to the Genus *Gymnosolen* Steinmann, 1911. The occurrence of such stromatolites varies laterally, depending on the paleoecological conditions. From the set of these structures, it is possible to infer a paleoenvironment of stromatolitic internal carbonate ramp influenced by wave/tide (Vieira et al., 2007).

The interval above of the stromatolites presents a more significant contribution of siliciclastic material, represented by marls overlain by massive laminated siltstones, representing the transition to the Serra de Santa Helena Formation. It represents a short transition interval, of a few meters, in an internal carbonate ramp that undergoes marine transgression and becomes influenced by siliciclastic materials from the craton in an offshore environment of a siliciclastic platform (Vieira et al., 2007).

4.2. Hypostratotype section of the PRF, Sete Lagoas County

The hypostratotype section named PRF is located on the right side of the BR-040 highway, near the Federal Highway Police station at Sete Lagoas County, Minas Gerais State, southeastern Brazil, towards Brasília (Fig. 3). The coordinates of the section (UTM), Datum WGS84, are: 23K, 574314 mE, 7846482 mN. As in the lectostratotype, both the Sete Lagoas and Serra de Santa Helena formations are exposed in this section. It is important to highlight that the boundary between those two units also outcrops. Due to the exposure of the upper boundary of the Sete Lagoas Formation with the Serra de Santa Helena Formation and easy access, a hypostratotype is proposed for this section (Fig. 5). A total of 11 stratigraphic levels were sampled.

The Sete Lagoas Formation at the PRF section is represented by a thick interval of columnar stromatolites identified as *Gymnosolen* sp. Individual columns vary from < 5 to 52 cm and can be as large as 15 cm in diameter, with convex internal crescentic lamination. The inter-column spaces are filled with mudstone limestone or locally brecciated. This carbonate succession is covered by siltstones of the Serra de Santa Helena Formation, consisting of metric tabular layers of olive-green massive siltstones, subordinately carbonate lenses, and fine-grained sandstones, probably deposited in a deep-platform environment (Vieira et al., 2007).

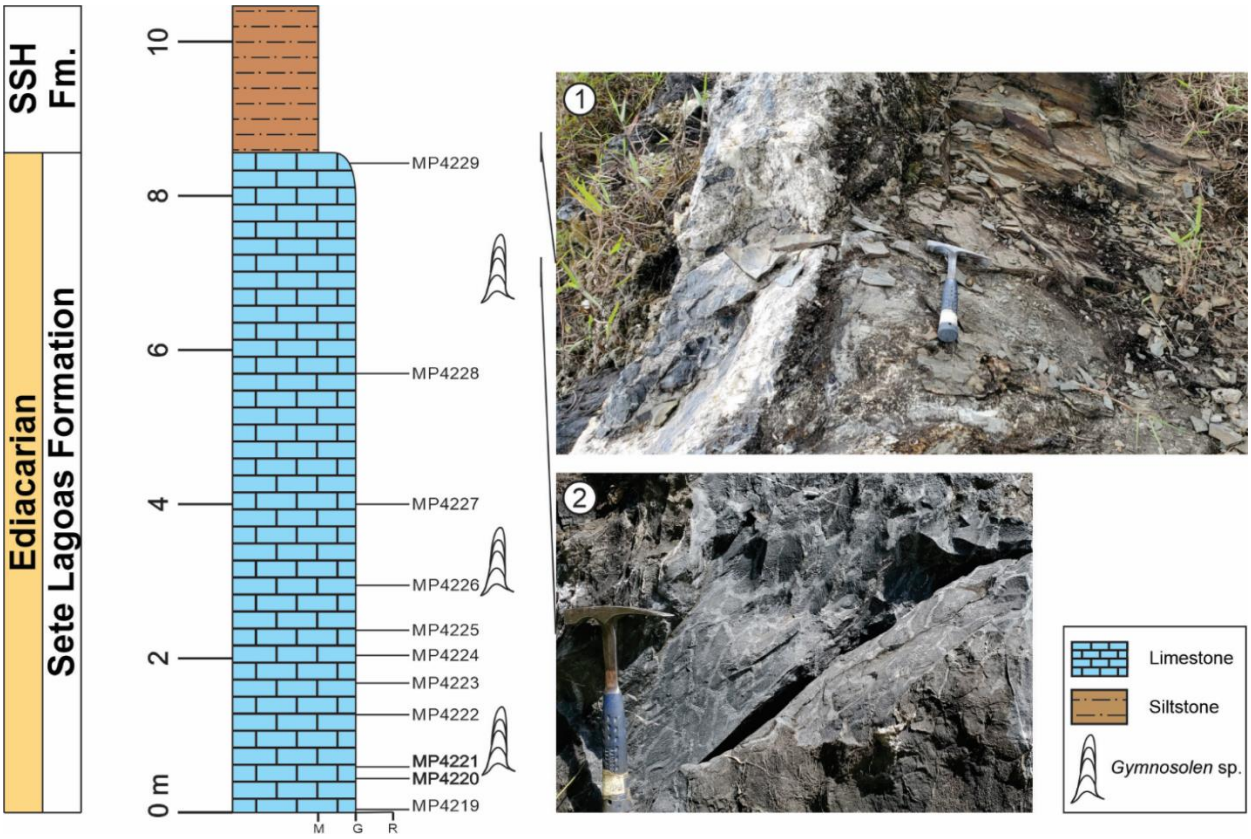

Figure 5: Hypostratotype section and field photographs of the Sete Lagoas Formation at the PRF, Sete Lagoas County, Minas Gerais State, Brazil. **(1)** Upper Sete Lagoas boundary. **(2)** *Gymnosolen* sp. Sample horizons are marked with the sample number prefixes MP. Sample numbers in bold mark fossiliferous horizons.

4.3. Hypostratotype section of the Barreiro, Januária County

The hypostratotype section named Barreiro is located in the Santa Luzia quarry near the Barreiro Community, western Januária Municipality, Minas Gerais State, Brazil (Fig. 3). The coordinates of the section (UTM), Datum WGS84, are: 23L, 560875 mE, 8290191 mN. Only the Sete Lagoas Formation is exposed in this section. The samples were collected from two different mining benches, as well as exposures on the hills where the Santa Luzia quarry is located. The stratigraphic thickness of the Sete Lagoas Formation in the studied area is about 70 m (Fig. 6). A total of 79 stratigraphic levels were sampled.

The lower 15 m consists mainly of crystalline laminated dark gray mudstones with a predominance of parallel plane bedding with microbial mats. However, there are cross-laminations in layers of fine calcareous grainstones. Microbial mats, silicified ooids, and dolomitic nodules are common at this level. Intraclastic carbonate breccias, with flat pebbles ranging from <1 to 50 cm and light gray micritic matrix are present at 16 m of the section and above, intercalated with limestones. The top of the section, at around 66 m, is composed of light gray crystalline dolomitic oolitic grainstones, sometimes with intraclasts. Such carbonates are cross-stratified. This packaging presents incipient flat stratification, about 2 cm thick, defined by the changes in the amount of sand size constituents (Fig. 6).

Occurrences of pseudo-tubular structures were identified as linear and crescentic stromatolites (Fig. 7.1–7.5). These microbialites were diagnosed based on macro analyses and thin sections. The length of the structures ranges from 2 to 10.5 cm, and diameters range from 2 to 6 mm. A single structure is commonly larger at the center than at the ends. They can be straight, slightly curved, or even tightly curved. Considering only these features, they could be interpreted as bioturbation, such as *Paleophycus tubularis* Hall, 1847, characterized by horizontal structures

with a cylindrical shape, generated by the activities of endobionts. *Paleophycus tubularis* can be linear or slightly sinuous without branches and presents full relief representing traces preserved within a bed (Hall, 1847). A similar structure in the Sete Lagoas Formation at the Barreiro section was presented by Warren et al. (2014). The tubular-like structure in Warren et al. (2014), which was tentatively assigned to *Paleophycus* sp., has the same dimensions and morphology as those presented herein.

Full reliefs typically represent active fills, which implies active manipulation of material by an organism (Lindholm, 1987). This sediment manipulation commonly results in textural contrasts between the trace and the host sediment. This contrast is not present in the structure from the Sete Lagoas Formation (Fig. 7.1–7.5) as it is present in a bioturbation specimen described by Xiao et al. (2019) (Fig. 7.6–7.8). Most commonly, active fill is produced by deposit and detritus feeders (Buatois and Mángano, 2011). In this case, no organic microlaminae would be preserved within the structure, which is not the case for the Barreiro section tubular structure (Fig. 7.3–7.4). Additionally, a full relief is not observed in the Sete Lagoas Formation material. On the other hand, the tubular-like structures are preserved as positive epirelief, again contrasting with the diagnosis of *Paleophycus* spp. At last, a tightly curved structure is unusual for bilaterian burrows (Fig. 7.1). Therefore, the tubular-like structures presented in this work lack evidence for bioturbation.

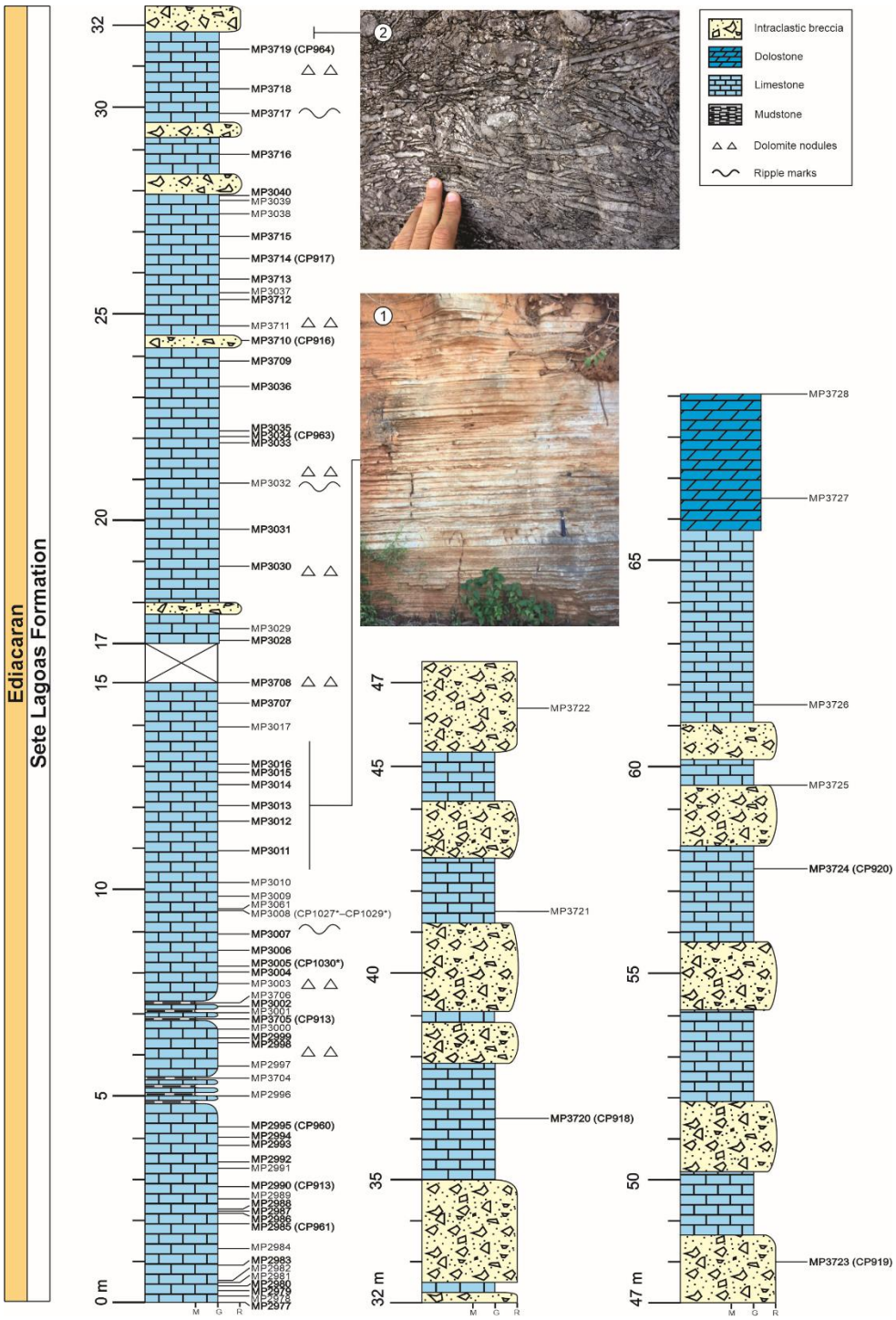

Figure 6: Lithostratigraphic section and field photographs of the Sete Lagoas Formation at the Barreiro section, Santa Luzia quarry, Januária Municipality, Minas Gerais State, Brazil. (1) Thin-bedded limestone; (2) Intraclastic breccia. Sample horizons are marked with the sample number prefixes MP. The CP numbers refer to the palynological slides of the illustrated specimens. CP numbers with * refer to thin sections illustrated. Sample numbers in bold mark fossiliferous horizons.

The thin section analysis conducted on the tubular-like structures showed a continuous accretion of sediments together with thin organic layers, interpreted here as organic microbial mats (Fig. 7.2–7.5).

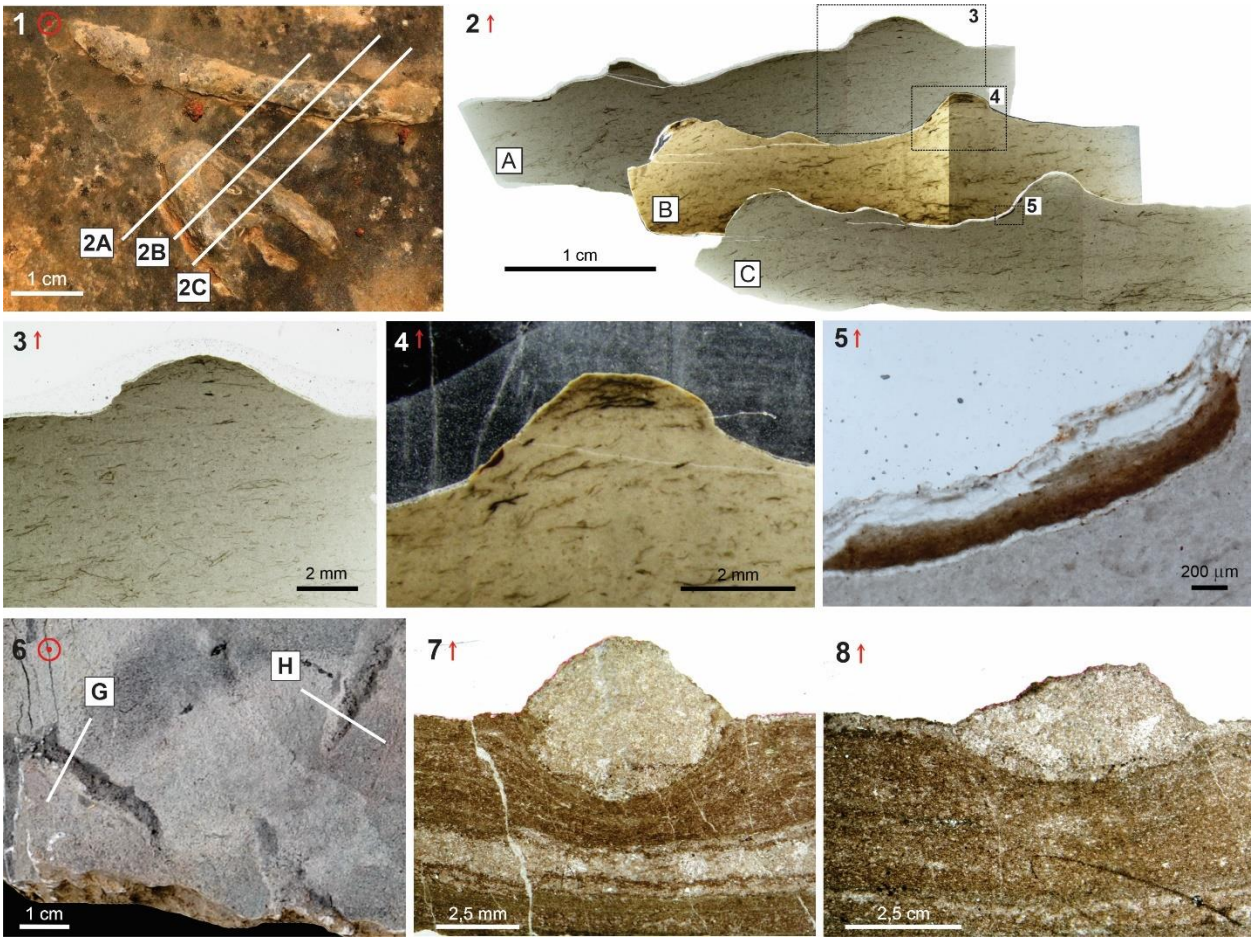

Figure 7: Comparison between microbialites and animal burrows. **(1–5)** Microbialites from the Sete Lagoas Formation, Bambuí Group, Barreiro section, Januária Municipality, Minas Gerais State, Brazil (MP3008). **(1)** Top bedding surface view. **(2)** Transmitted plane-polarized light photomontages of three petrographic thin sections cut perpendicularly to the bedding surface along labeled white lines in (1). **(2A)** CP1027; **(2B)** CP1028; **(2C)** CP1029.**(3–5)** Magnified views of labeled rectangles in (2) show microbial laminae details. Red arrows and circled dot mark stratigraphic up direction. **(6–8)** Animal burrows preserved in limestone of the terminal Ediacaran Dengying Formation at Wuhe, Yangtze Gorges area, South China (extracted from Xiao et al., 2019). **(7–8)** Transmitted plane-polarized light of petrographic thin sections cut perpendicularly to the bedding surface along labeled white lines in (6).

The microbial mats also follow the shape of the structure without any evidence of sediment manipulation made by water flow or even by organisms. When the edges of the structures were analyzed, remnants of organic layers were identified (Fig 7.2, 7.5). Those microbial remnant organic layers were comparable to the organic layers of thrombolites preserved at 1.4 meters below the stratigraphic level of the tubular-like structures (Fig. 8.1–8.3).

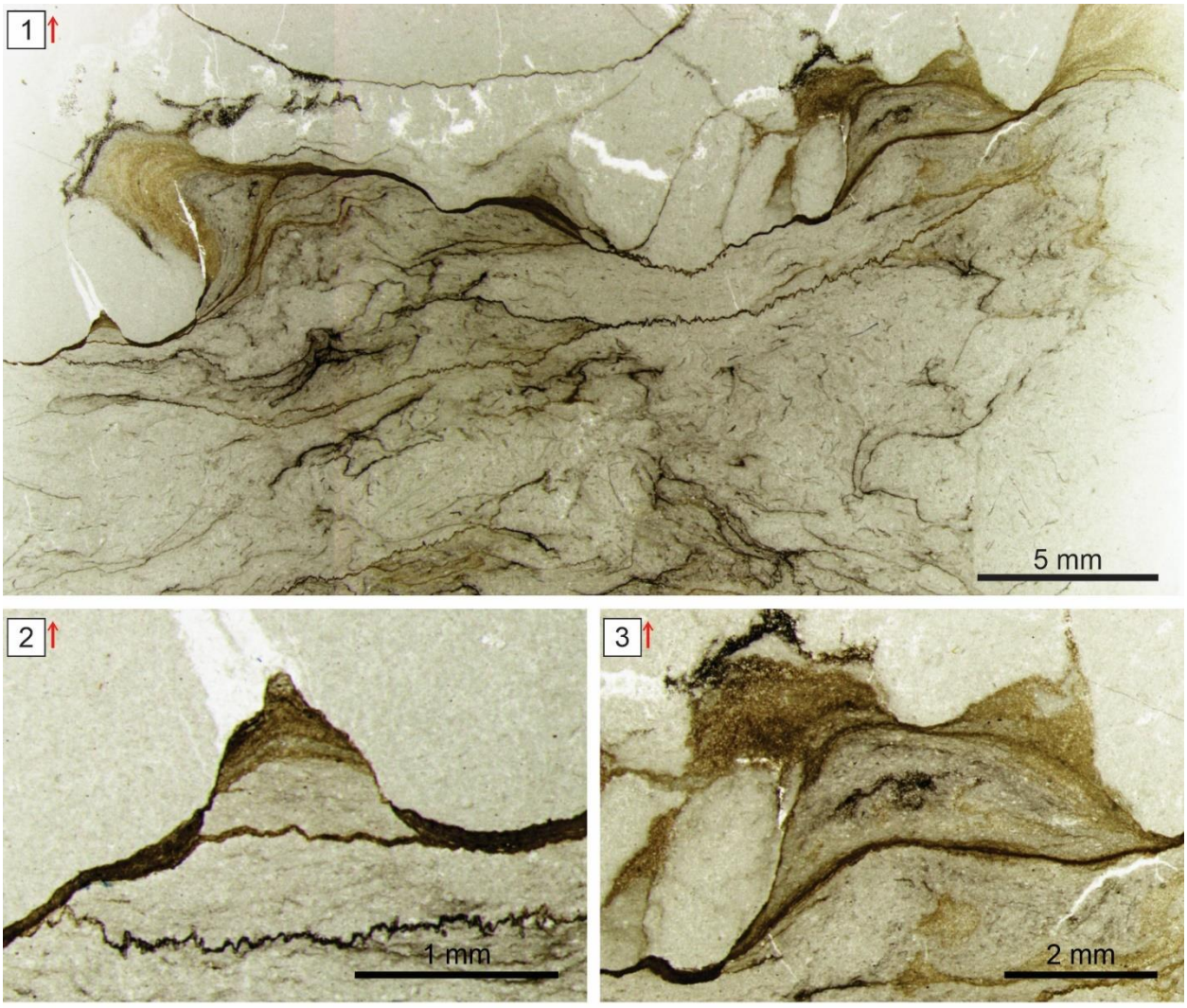

Figure 8: Comparison between microbialites and animal burrows. **(1-3)** Transmitted plane-polarized light photomicrographs of petrographic thin sections cut perpendicularly to the bedding surface, showing microbial fabrics of microbialites from the Sete Lagoas Formation, Bambuí Group, Barreiro section, Januária Municipality, Minas Gerais State, Brazil (CP1030).

The well-preserved microbialites at 8.1 m of the Barreiro section represent a calm environment where the microbial mats could easily grow and develop without disturbance. Also, a continuous micritic deposition without subaerial exposure could preserve the entire accretion structures (Fig. 8.1-8.3). If they are roll-ups or shrinkage microbial structures, then they were likely formed subaerially. If the discontinuous microlaminae represents fragments of microbial mats, then hydrodynamic energy must have been high enough to break up microbial mats. Regardless, the microbialites likely formed within the photic zone in shallow water and likely above fair weather wave base. Nevertheless, the poorly preserved and non-continuous organic laminations on the edge of the tubular-like structures could represent a poor preservation due to possible rework of the structure prior to the deposition of the overlying bed. The similarity of both organic lamination occurrences is strong evidence of the nature of the tubular-like structures preserved as positive epirelief: their genesis is related to microbialites.

4.4. Fercal section, Brasília

The Fercal section is located in the Federal District, midwestern Brazil (Fig. 3). The coordinates of the section (UTM), Datum WGS84, are: 23L, 201350 mE, 5284560 mN. This is the only section studied in this work in which both the lower and upper boundaries of the Sete Lagoas Formation are exposed. The Sete Lagoas Formation is about 230 meters thick in the Fercal composite section (Fig. 9). A total of 69 stratigraphic levels were analyzed.

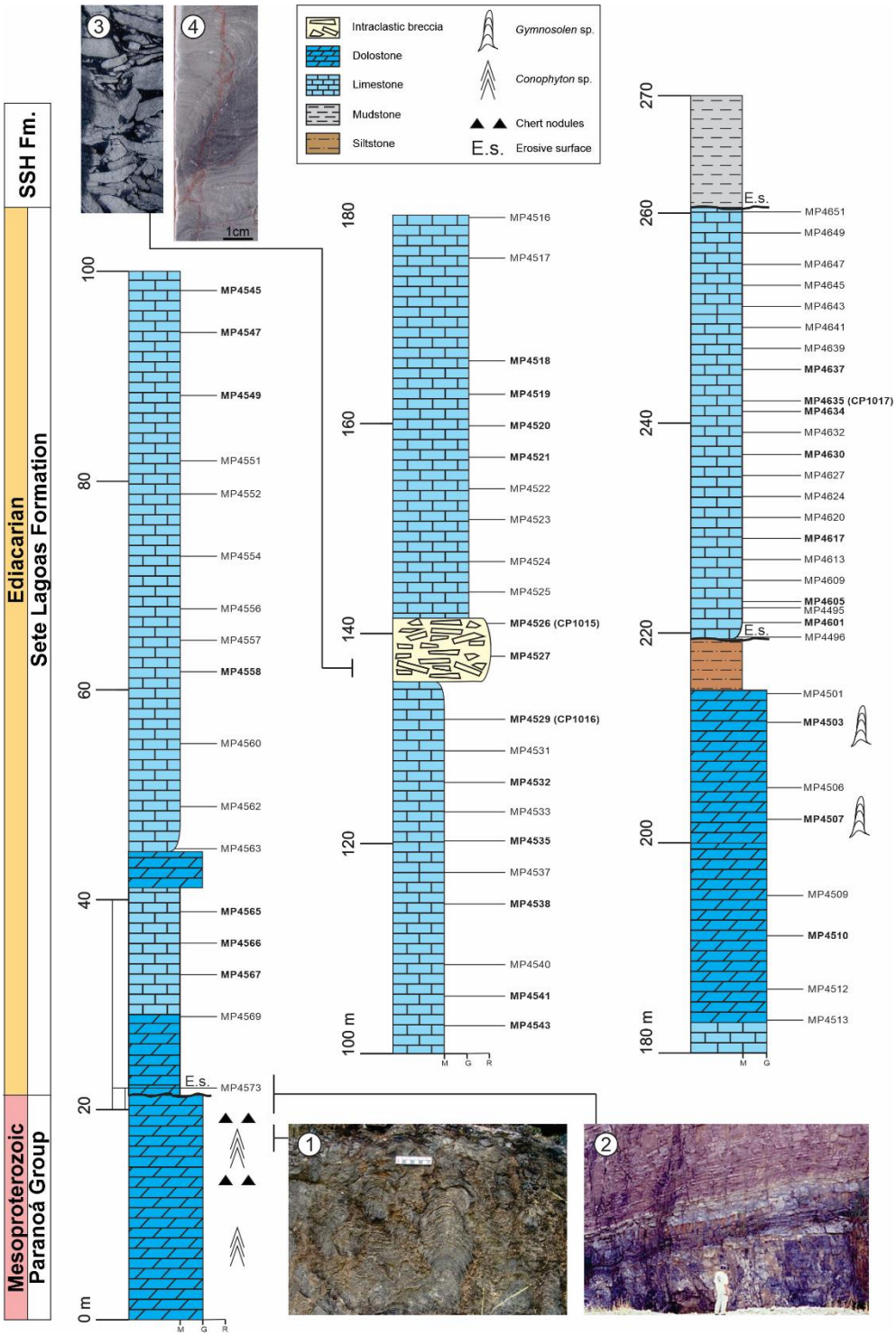

Figure 9: Lithostratigraphic section and field photographs of the Sete Lagoas Formation at the Fercal section, Federal District, Brazil. Extract from Carvalho (2018) and Carvalho and Alvarenga (2018). Sample horizons are marked with the sample number prefixes MP. The CP numbers refer to the palynological slides of the illustrated specimens. Sample numbers in bold mark fossiliferous horizons.

Carvalho (2018) studied this section with a chemostratigraphic approach, in which carbon and oxygen isotopes were analyzed to improve the establishment of chronostratigraphic correlations of the Sete Lagoas Formation. Carvalho and Alvarenga (2018) provided a detailed description of the lithofacies present in the Fercal section. A composite section was described, obtained from a drill core in the lower part, and a drill core and an outcrop at the Contagem quarry, in the upper part.

The lower part of the Sete Lagoas Formation succession, which overlies with erosional unconformity dolostone breccias of the Paranoá Group, is about 190 m thick and comprises three distinct lithostratigraphic units: 1, the lower part comprises a gray dolarenite overlain by a purple rhythmic succession of calcilutite to calcarenite alternated with claystone beds; 2, the middle part is dominated by pure calcarenites; 3, the upper part consists of crystalline dolostones with occurrences of *Gymnosolen* sp. An erosive surface marks the top of the first succession. The upper part of the Sete Lagoas succession begins with 1-2 meters of siltstone, followed by calcarenites with clay layers growing towards the top (Carvalho and Alvarenga, 2018).

5. TAXONOMY OF ORGANIC-WALLED MICROFOSSILS

The suprageneric taxonomy follows the system of modern cyanobacteria and the parataxonomic classification of acritarchs [e.g., Butterfield et al., (1994); Sergeev and Schopf, (2010)]. Nine organic-walled microfossils species were recovered: *Ghoshia januarensis* new species, *Germinosphaera bispinosa* Mikhailova, 1986, *Leiosphaeridia crassa* (Naumova, 1949), *Leiosphaeridia jacutica* (Timofeev, 1966), *Leiosphaeridia minutissima* (Naumova, 1949), *Leiosphaeridia tenuissima* Eisenack, 1958, *Leiosphaeridia ternata* (Timofeev, 1966), *Bambuites erichsenii* Sommer, 1971, and *Siphonophycus robustum* (Schopf, 1968). Two of them,

Siphonophycus robustum and *Ghoshia januarensis*, are considered cyanobacteria. Five of them, *Leiosphaeridia crassa*, *Leiosphaeridia jacutica*, *Leiosphaeridia minutissima*, *Leiosphaeridia tenuissima*, and *Leiosphaeridia ternata*, are sphaeromorphic acritarchs and probably represent protists. *Bambuites erichsenii* is an acanthomorph acritarch. The phylogenetic affinity of *Germinosphaera bispinosa* is uncertain.

Kingdom Eubacteria Woese and Fox, 1977

Phylum Cyanobacteria Stanier et al., 1978

Class Hormogoneae Thuret, 1875

Order Oscillatoriales Elenkin, 1949

Family Oscillatoriaceae Kirchner, 1900

Genus *Siphonophycus* Schopf, 1968

Type species.—*Siphonophycus kestron* Schopf, 1968 (holotype: Paleobot. Coll. Harvard Univ. No. 58469, stage coordinates 33.6 × 101.4) from the black chert facies in the middle third of Late Precambrian Bitter Springs Formation, exposed on the south slope of a ridge about 1 mile north of Ross River Tourist Camp (Love's Creek Homestead), 40 miles northeast of Alice Springs, Northern Territory, Australia, by original designation.

Other species.—*Siphonophycus thulenema* Butterfield, 1994 *in* Butterfield et al., 1994; *Siphonophycus septatum* (Schopf, 1968); *Siphonophycus robustum* (Schopf, 1968); *Siphonophycus typicum* (Hermann, 1974); *Siphonophycus kestron* Schopf, 1968; S*iphonophycus*

solidum (Golub, 1979); S*iphonophycus punctatum* Maithy, 1975; and S*iphonophycus gigas* Tang et al., 2013.

Original diagnosis by Schopf, 1968.—"Thallus broad, tubular, nonseptate, unbranched, commonly quite long, finely rugose in surface texture. Thallus cylindrical, somewhat tapered toward apices, solitary, straight to slightly bent, up to 180 µ long (incomplete specimen), occasionally folded and distorted. Apices apparently capitate, more-or-less constricted adjacent to expanded, broadly conical, bluntly pointed terminus. Thallus quite broad, 8.3–15.00 µ wide, commonly about 12.5 µ wide (based on five specimens), ornamented and ringed by finely punctate surficial ridges regularly spaced out 2/3 µ apart. Reproductive structures unknown."

Emended diagnosis by Knoll et al., 1991.—"Tubular, filamentous microfossils, nonseptate and unbranched, with little or no tapering toward filament termini; tubes truncated and open at ends or with closed, more or less hemispherical terminations; walls typically preserved as chagrenate to finely reticulate organic matter, but may be preserved as carbonate rinds."

Remarks.—The genus *Siphonophycus* is characterized by smooth and thin wall filaments without ornamentation. The taxon is traditionally interpreted as representing empty sheaths of filamentous cyanobacteria, but because of simple morphology, it could include a range of bacterial and eukaryotic organisms (Butterfield et al., 1994). Although it is here placed under cyanobacteria, we recognize that *Siphonophycus* is a form taxon, and several other genera of filamentous microfossils (e.g., *Eomycetopsis*, *Tenuofilum*, and *Leiotrichoides*) are regarded as synonyms of *Siphonophycus* (Knoll et al., 1991).

Siphonophycus robustum (Schopf, 1968) emend. Knoll et al., 1991

Figures 10.12–10.13, 13.1

1968 *Eomycetopsis robusta* Schopf, p. 685, pl. 82, figs. 2-3; pl. 83, figs. 1–4.

1968 *Eomycetopsis filiformis* Schopf, p. 685, pl. 82, figs. 1, 4; pl. 83, figs. 5–8.

1979 *Eomycetopsis robusta*; Knoll and Golubic, p.149, fig. 4a–b.

1982 *Eomycetopsis robusta*; Mendelson and Schopf, pp. 59–60, 62, pl. 1, figs. 9, 10.

1984 *Eomycetopsis robusta*; Sergeev, p. 436, fig. 2a–ã.

1991 *Eomycetopsis robusta*; Hofmann and Jackson, pp. 367–368, fig. 5.1–5.3, 5.8.

1991 *Siphonophycus robustum* (Schopf, 1968); Knoll et al., p. 565, fig. 10.3, 10.5.

1992 *Eomycetopsis robusta*; Zang and Walter, p. 314, pl. 17, figs. g–i, p. 308, pl. 18, fig. g.

1992 *Eomycetopsis robusta*; Sergeev, pp. 93–94, pl. 7, figs. 9–10; pl. 16, figs. 3, 6–7, 10; pl. 19, figs. 1, 5–10; pl. 24, fig. 7.

1993 *Eomycetopsis robusta*; Golovenok and Belova, pl. 2, fig. å.

1994 *Siphonophycus robustum*; Butterfield et al., pp. 64, 66, fig. 26a, 26g.

1994 *Siphonophycus robustum*; Hofmann and Jackson, p. 10, fig. 11.5.

1994 *Siphonophycus robustum*; Sergeev, pp. 250–251, fig. 8f.

1994 *Siphonophycus robustum*; Sergeev et al., pl. 3, fig. 6.

1995 *Siphonophycus robustum*; Kumar and Srivastava, p. 114, fig. 14c–e.

1995 *Siphonophycus robustum;* Zang, p. 172, figs. 26a, 32l-m.

1997 *Siphonophycus robustum*; Sergeev et al., p. 230, fig. 14a.

1998 *Siphonophycus robustum*; Kumar and Venkatachala, p. 63, fig. 6c.

2001 *Siphonophycus robustum*; Sergeev, p. 442, fig. 7.8–7.9.

2001 *Siphonophycus robustum*; Sergeev and Lee, p. 6, pl. 1, figs. 1–2, 7, 11–12.

2001 *Siphonophycus robustum*; Samuelsson and Butterfield, p. 240, figs. 2b, 9h.

2003 *Siphonophycus robustum*; Gaucher et al., fig. 6c–d.

2003 *Siphonophycus robustum*; Gaucher and Germs, fig. 7.12.

2004 *Siphonophycus robustum*; Sharma and Sergeev, figs. 3c, 4a, 6b, 6e, 7c, 7f, 9e, 11f.

2004 *Siphonophycus robustum*; Sergeev and Lee, pl. 2, fig. 4.

2004 *Siphonophycus robustum*; Tiwari and Pant, fig. 3i, 3n.

2005 *Siphonophycus robustum*; Prasad et al., pl. 1, fig. 7; pl. 5, fig. 12.

2006 *Siphonophycus robustum*; Sergeev, p. 213, pl. 6, figs. 9–10; pl. 17, fig. 1; pl. 19, figs. 8– 9; pl. 22, figs. 1–2, 7–8, 11–12; pl. 25, figs. 1, 3; pl. 27, figs. 4–5; pl. 28, fig. 2; pl. 36, fig. 1–2; pl. 44, figs. 1–7, 13; pl. 46, figs. 7–10; pl. 48, fig. 4.

2008 *Siphonophycus robustum*; Kumar and Pandey, fig. 3a–b.

2008 *Siphonophycus robustum*; Sergeev et al., pl. 6, figs. 1, 5–6; pl. 9, figs. 1–3, 5–7.

2009 *Siphonophycus robustum*; Tiwari and Pant, fig. 6a–c.

2009 *Siphonophycus robustum*; Dong et al., p. 30, fig. 6.12.

2010 *Siphonophycus robustum*; Sergeev and Schopf, p. 387, fig. 6.4.

2012 *Siphonophycus robustum*; Sergeev et al., pp. 309–310, pl. 21, figs. 2, 4, 8–10.

2013 *Siphonophycus robustum*; Pandey and Kumar, p. 504, fig. 4e.

2013 *Siphonophycus robustum*; Knoll et al., fig. 4c.

2013 *Siphonophycus robustum*; Tang et al., fig. 13b, 13m.

2014 *Siphonophycus robustum*; Babu et al., fig. 3q.

2014 *Siphonophycus robustum*; Liu et al., fig. 110.1.

2015 *Siphonophycus robustum*; Vorob'eva et al., fig. 9.14.

2015 *Siphonophycus robustum*; Tang et al., fig. 18c.

2015 *Siphonophycus robustum*; Schopf et al., pp. 716, 718, fig. 11.11.

2016 *Siphonophycus robustum*; Porter and Riedman, p. 837, fig. 16.4.

2016 *Siphonophycus robustum*; Sergeev et al., fig. 8.4.

2016 *Siphonophycus robustum*; Baludikay et al., fig. 11n.

2017 *Siphonophycus robustum*; Tang et al., fig. 8a, 8c–d.

2017a *Siphonophycus robustum*; Shi et al., fig. 6.3, 6.5.

2017b *Siphonophycus robustum*; Shi et al., p. 721, fig. 3e–f.

2017 *Siphonophycus robustum*; Javaux and Knoll, p. 212, fig. 5.11.

2017 *Siphonophycus robustum*; Beghin et al., pl. 3, fig. i.

2017a *Siphonophycus robustum*; Sergeev et al., p. 290, fig. 5.10–5.11.

2019 *Siphonophycus robustum*; Li et al., fig. 15h.

2019 *Siphonophycus robustum*; Loron et al., fig. 3f.

2019 *Siphonophycus robustum*; Arrouy et al., fig. 6f.

2020 *Siphonophycus robustum*; Knoll et al., p. 6, fig. 3n–o.

2020 *Siphonophycus robustum*; Arvestål and Willman, p. 22, fig. 10f.

2020 *Siphonophycus robustum*; Shukla et al., pp. 496–497, fig. 5e.

2021 *Siphonophycus robustum*; Miao et al., p. 17, fig. 9e.

2022 *Siphonophycus robustum*; Denezine et al., fig. 11.6.

For additional synonyms, see Butterfield et al. (1994).

Holotype.—Paleobotanical collections, Harvard University (thin section Bit. Spr. 10-1, number 58491), from Neoproterozoic Bitter Springs Formation, Amadeus Basin, Australia (Schopf, 1968, pl. 83, fig. 1).

Original diagnosis.—"Filaments commonly solitary, occasionally in groups of a few entangled filaments, rarely showing plectenchymatous organization. Lateral walls approximately1/3-3/4 μ thick, markedly coriaceous, coarsely and irregularly granular in surface texture. Filaments up to 135 μ long (incomplete filament), more-or-less regularly cylindrical with a variance in diameter of less than 0.8 μ from the widest to the most narrow portion of the filament; 2.8-4.2 μ in diameter with an average width (20 filaments measured of 3.5 μ. Septate portions of filament vary in length, commonly less than 25 μ long, with filaments commonly constricted or overlapping at the septa; overlapping portions commonly with rounded ends. Reproductive structures unknown." (Schopf, 1968).

Emended diagnosis by Knoll and Golubic (1979).—"Filaments cylindrical; unbranched; tubular (nonseptate); bent, sinuous and tortuous; partially flattened, circular to elliptical in cross-section; intertwined to form more or less dense meshworks; long. Surface coarsely to irregularly granular in texture. Occasional cylindrical and evenly spaced inclusions, homogeneously filled with fine-grained carbonaceous matter and centrally located in the "bore" of the tube. Filaments tubular with average diameters expressed as mean ± standard deviation 2.95 ±μm (range 2.0-4.4, n = 60). Occasional long cylindrical inclusions, 1.09 ± 0.36 μm (n = 8) in diameter, 3-4 μm long located centrally within tubular filaments."

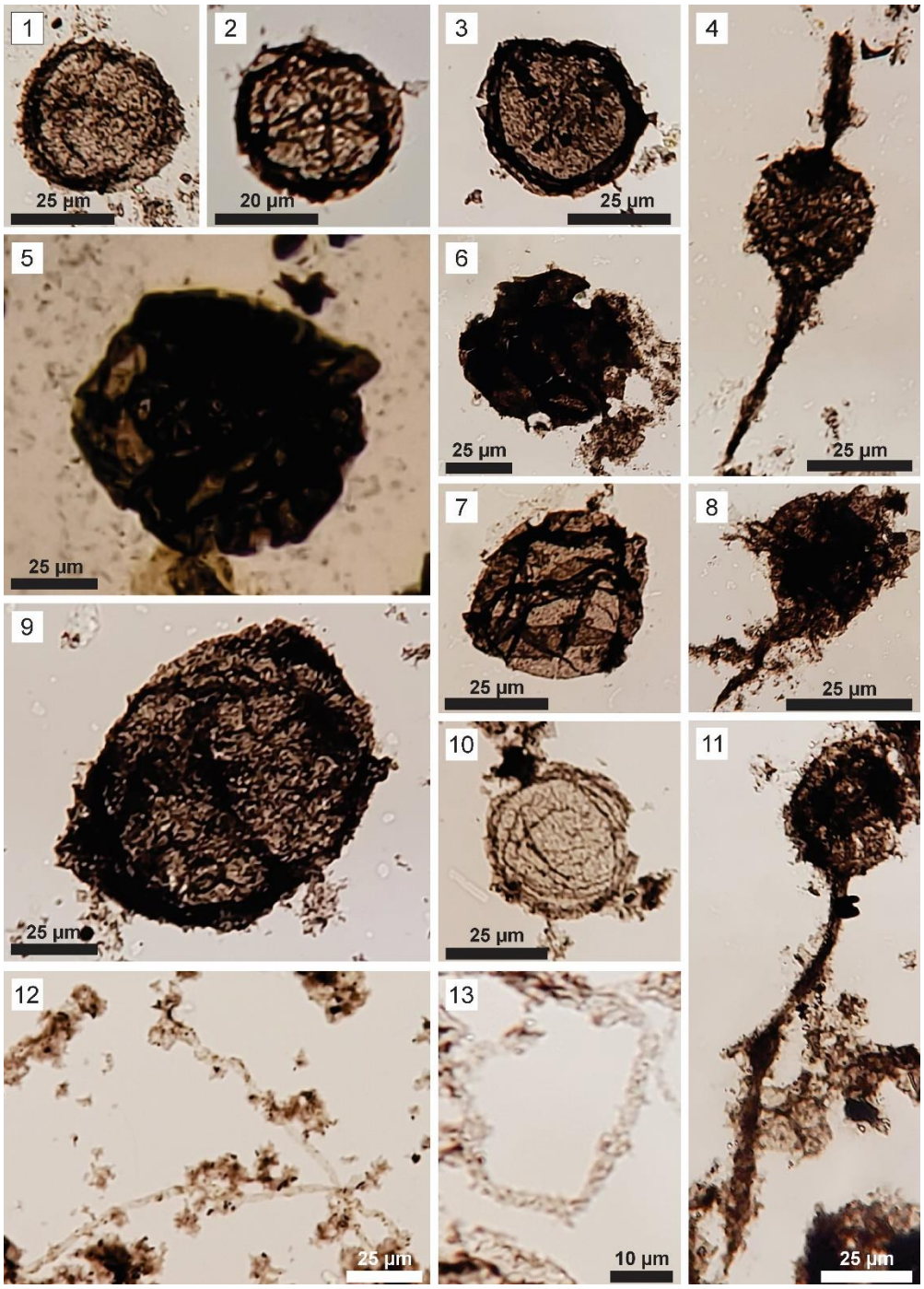

Figure 10: Organic-walled microfossils from the Sete Lagoas Formation at the Barreiro section. Slide number and England Finder coordinates (in parentheses) are given for each illustrated specimen. **(1–3, 7, 10)** *Leiosphaeridia minutissima*, **(1)** CP962 (S32); **(2)** CP962 (F48); **(3)** CP918 (K22); **(7)** CP964 (P29); **(10)** CP963 (F33). **(4, 8, 11)** *Germinosphaera bispinosa*, all in slide CP917 (EF coordinates: S26, I43, and O28, respectively). **(5)** *Leiosphaeridia jacutica*, CP913 (Y23). **(6)** *Leiosphaeridia crassa*, CP964 (H29). **(9)** *Leiosphaeridia tenuissima*, CP914 (Q30). **(12-13)** *Siphonophycus robustum*, **(12)** CP960 (I50); **(13)** CP961 (H24).

Emended diagnosis by Knoll et al. (2020).—"A species of *Siphonophycus* with tubes 2–4 μm in cross-sectional diameter."

Illustrated materials.—CP960, CP961, and CP1019.

Occurrence in the studied sections.—**Barreiro section:** MP2985, MP2995, MP3040, MP3708, MP3709, and MP3710. **Fercal section:** MP4510, MP4543, and MP4634. **Rei do Mato section:** MP5159.

Remarks.—Filamentous microfossils from the Sete Lagoas Formation that are 2 to 4 μm in diameter are identified as *Siphonophycus robustum* (Schopf, 1968).

Order Stigonematales Geitler, 1925

Family Capsosiracea Geitler, 1925

Genus *Ghoshia* Mandal & Maithy, 1984 in Mandal et al., 1984

Type species.—*Ghoshia bifurcata* Mandal & Maithy, 1984 in Mandal et al., 1984.

Original diagnosis presented by Mandal & Maithy in Mandal et al., 1984.—"Thallus heterotrichous, erect filaments arising from basal horizontally creeping thallus, densely packed, truly laterally branched, with cells in one or two series; sheath absent; reproduction not observed."

Ghoshia januarensis new species

Figures 11.1–11.9, 13.10, 13.15

2017 Fossil filaments consisting of aligned rounded cells, Perrella Júnior et al., p. 138. fig. 7h.

2022 *Ghoshia* sp.; Denezine et al., fig. 11.5.

Holotype.—*Ghoshia januarensis* (CP916). Paratypes: CP919 and CP920. Specimens are housed in the Research Collection, Museum of Geosciences, Institute of Geosciences, University of Brasília, Federal District, Brazil.

Type locality.—Specimens recovered from the Sete Lagoas Formation, Bambuí Group, Santa Luzia quarry, Municipality of Januária, Minas Gerais State, Brazil.

Type horizon.—Intraclastic breccia from the Sete Lagoas Formation, Bambuí Group. Stratigraphic level: between 31.5 to 36.4 m.

Diagnosis.—A species of *Ghoshia* characterized by spherical to dolliform cells that are 3–10 μm in diameter. Cells are organized to form uniserial chains that branch irregularly.

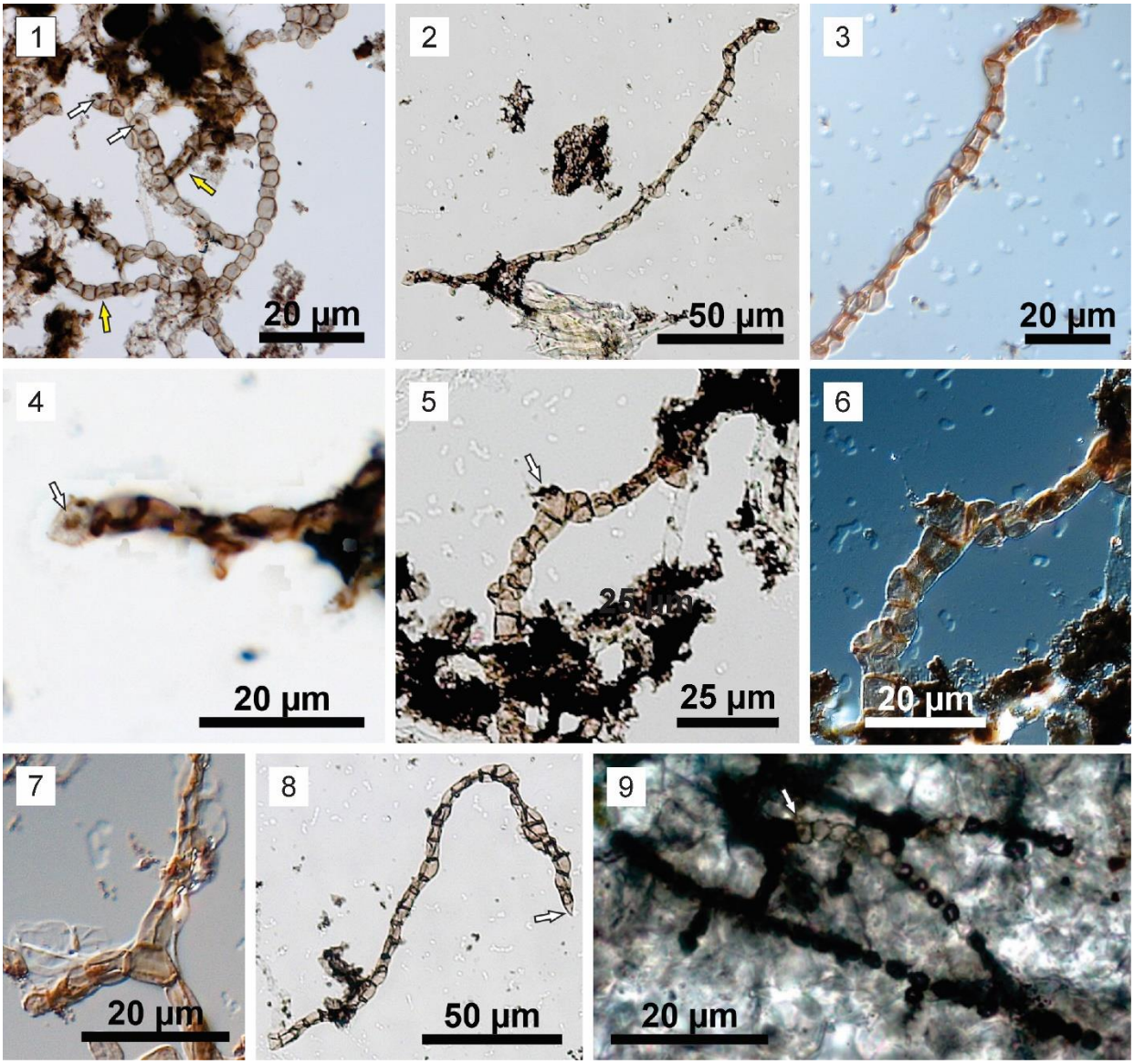

Figure 11: *Ghoshia januarensis* new species from the Sete Lagoas Formation in the Barreiro section. Slide number and England Finder coordinates (in parentheses) are given for each illustrated specimen. **(1)** Holotype: CP916 (E46). Note dark spots inside cells indicated by white arrows. Yellow arrows indicate slightly deflated and deformed cells. **(2–8)** Paratypes; **(2–6)** CP919 (E18); 3 is a magnified view of the upper right part of 2, showing slightly deflated and deformed cells; 4 is a magnified view of the lower left part of 2, showing dark spot in terminal cell (arrow); **(5–6)** CP919 (J16), 6 is a dark-field view of the central part of 5, showing a polyhedral cell (arrow in 5). **(7)** CP919 (J26), note polyhedral cell at a branching point. **(8)** CP920 (N18/3), showing pointed terminal cell (arrow). **(9)** Specimen identified in a thin section of the Sete Lagoas Formation at the Barreiro section in the Januária area. Reproduced from Perrella Júnior et al. (2017) with permission.

Description.—Uniserial cell chains that branch irregularly. Cells are spherical (Fig. 11.1), dolliform (Fig. 11.3), or polyhedral in shape (Fig. 11.7), with smooth cell walls. Side branches arise more or less perpendicularly to the rom main branches. Cells at the branch points are often polyhedral in shape (Fig. 11.7). Cells 3–10 μm in diameter. Deformation folds, likely resulting from compression, are present in some cells (Fig. 11.2, 11.7, 11.8).

Etymology.—In reference to the Municipality of Januária, Minas Gerais State, Brazil.

Illustrated materials.—CP916, CP919, CP920, CP1016, and CP1018.

Occurrence on the studied sections.—**Barreiro section:** MP2980, MP3013, MP3015, MP3040, MP3710, MP3714, MP3718, MP3723, and MP3724. **Fercal section:** MP4518, MP4529, MP4541, and MP4605. **Rei do Mato section:** MP5152, MP5159, MP5196, and MP5234.

Remarks.—The Sete Lagoas specimens are somewhat similar to *Arctacellularia* German *in* Timofeev et al., 1976 in their uniserial filaments consisting of spherical, dolliform, and polyhedral cells. However, unlike the Sete Lagoas specimens, *Arctacellularia* does not branch. The Sete Lagoas specimens are also similar to the Devonian cyanobacteria *Langiella* Croft and George, 1959, *Kidstoniella* Croft and George, 1959, and *Rhyniella* Croft and George, 1959, in having branching filaments. However, these Devonian genera can be distinguished by the presence of morphologically differentiated heterocysts and akinetes or by the presence of a sheath (Croft and George, 1959). The Sete Lagoas specimens are best placed in the Genus *Ghoshia*, which is characterized by branching uniserial filaments consisting of largely undifferentiated cells. The new

species proposed here, *Ghoshia januarensis*, resembles *Ghoshia bifurcata* Mandal & Maithy, 1984 in cell size but differs in its more variable cell shape; *Ghoshia januarensis* has spherical, dolliform, and polyhedral cells, whereas *Ghoshia bifurcata* is said to have "drum-shaped to rectangular" cells (Mandal et al., 1984). In addition, some specimens of *Ghoshia bifurcata* (including the holotype, plate 4, fig. 30 of Mandal et al., 1984) seem to have cell aggregates that are not uniserially organized.

A specimen from the Sete Lagoas Formation in the Januária area is illustrated as "fossil filaments consisting of aligned rounded cells" (Perrella Júnior et al., 2017, fig. 7H) shares the exact characteristics of *Ghoshia januarensis*, including uniserial and branching filamentous consisting of spherical cells. Thus, this specimen is here identified as *Ghoshia januarensis*. It is important to highlight that the specimen illustrated in Perrella Júnior et al. (2017) was observed in a petrographic thin section, ruling out the possibility of modern contamination (Fig. 11.9).

Raman data show that the four analyzed specimens of *Ghoshia januarensis*, including the holotype, are distinct from other organic-walled microfossils from the Sete Lagoas Formation (Fig. 12). Relative to other organic-walled microfossils from the Sete Lagoas Formation, *Ghoshia januarensis* specimens exhibit broader peaks characteristic of carbonaceous material (Fig. 12.1). PCA analysis of Raman parameters also shows that *Ghoshia januarensis* specimens are separated from other organic-walled microfossils from the Sete Lagoas Formation (Fig. 12.2). Such differences in Raman characteristics could be taken as evidence for different degrees of thermal maturation (Kouketsu et al., 2014). However, recent studies show that differences in organic precursors could also lead to differences in Raman characteristics of carbonaceous material (Qu et al., 2015; Pang et al., 2020).

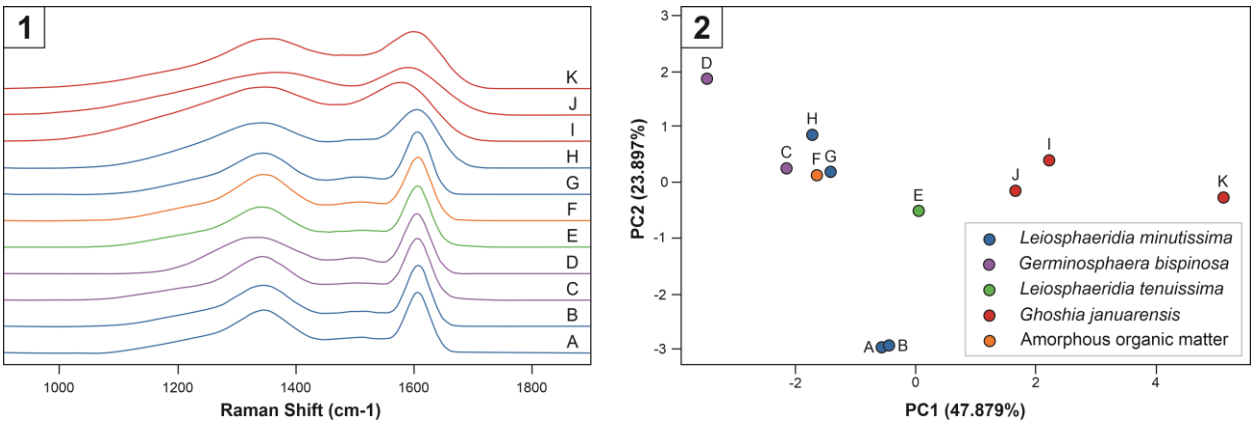

Figure 12: Raman spectroscopic data of organic-walled microfossils and amorphous organic matter from the Sete Lagoas Formation at the Barreiro section. **(1)** Baseline-corrected and fitted Raman spectra. Different colors mean different species. Each Raman spectra corresponds to the data of principal component analysis showed in 12.2. Note that Raman spectra of *Ghoshia januarensis* (J from holotype and I, K from paratypes) have broader peaks of carbonaceous matter around 1350 cm^{-1} and 1600 cm^{-1} relative to other Sete Lagoas organic-walled microfossils. **(2)** Principal component analysis of deconvolved Raman data. Samples: A–B and J, CP916; C–D, CP917; E, I, K, CP920; F, H, MP3728; G, MP3723.

Indeed, *Ghoshia januarensis* seems to occupy the end member of a continuum of Raman characteristics of organic-walled microfossils from the Sete Lagoas Formation (Fig. 12). Thus, we favor the interpretation that the difference in organic precursors, as opposed to the difference in organic maturation, underlies the observed difference in Raman spectra. This consideration, coupled with the previous report of *Ghoshia januarensis* from a petrographic thin section of the Sete Lagoas Formation (Perrella Júnior et al., 2017), led us to believe that *Ghoshia januarensis* is indigenous to the Sete Lagoas Formation, rather than later contamination.

Group Acritarcha Evitt, 1963

Group Acritarcha Evitt, 1963

Subgroup Acanthomorphitae Downie et al., 1963

Genus *Bambuites* Sommer, 1971

Type species.—Bambuites erichsenii Sommer, 1971.

Other species.—The Genus *Bambuites* is monospecific.

Original diagnosis presented by Sommer (1971) in Portuguese.—"Configurações arredondadas, solitárias, de substância carbonosa opaca provida de lacunas irregulares, quando observada à luz transmitida; por vêzes ressalta parede de contôrno mais denso; diâmetro de dimensões variáveis."

Original diagnosis presented by Sommer (1971) translated.—"Rounded morphotypes, opaque carbonaceous composition of irregular gaps, when observed, the transmitted light sometimes pops up the wall of denser contour; and diameter of dimensions variables."

Bambuites erichsenii Sommer, 1971

Figures 13.2–13.3, 13.12

1971a *Bambuites erichsenii* Sommer; Sommer, p.136, pl. 1, figs. 1–15.

1971b *Bambuites* sp.; Sommer, figs. 1–2.

2017 *Leiosphaeridia jacutica*; Sanchez & Fairchild, fig. 8.

2020 *Bambuites erichsenii*, Baptista, p. 82–83, figs. 4.2.4a–d, 4.2.5.

Holotype.—Micropaleontological Collection, slide number S.70/1, Section of Paleontology and Stratigraphy, D.G.M - D.N.P.M., Museum of Earth Science, Rio de Janeiro County, Rio de Janeiro State, Brazil, from upper Ediacaran, Bambuí Group, Sete Lagoas Formation, Brazil (Sommer, 1971, pl. 1, fig. 2, and pl. 2, fig. 2).

Original diagnosis by Sommer (1971) in Portuguese.— "*Configurações arredondadas, entre 70 a 200 µ de diâmetro; dos espécimes encontrados, 10 entre 100 e 140 µ de diâmetro; há fragmentos que sugerem diâmetro hem maior. Parede de contôrno, quando conspícua, cêrca de 20 µ de espessura; em geral, o indivíduo é completamente opaco, raramente inteiro, a margem sempre provida de ornamento crenulado"*.

Original diagnosis by Sommer (1971) translated.— "*Rounded morphotypes, between 70 and 200 micrometers in diameter; of the specimens found, 10 are between 100 and 140 micrometers in diameter; there are fragments that suggest a much larger diameter. Contour wall, when conspicuous, about 20 micrometers thick; in general, the individual is completely opaque, rarely whole, the margin always provided with crenulated ornamentation."*

Emended diagnosis by Baptista (2020).—Round microfossils with 10 to 200 micrometers in diameter, being that described fragments suggest the possibility of larger individuals. There are

two types of processes: triangular processes with about 1 micrometer of length and triangular processes at the top and squared at the base, with 3 to 5 micrometers in diameter.

Illustrated materials.—CP1016 and CP1022.

Occurrence in the studied sections.—**Fercal section:** MP4527, MP4529, and MP4637. **Rei do Mato section:** MP5136, MP5192, MP5193, and MP5194.

Remarks.—The main contribution to the original diagnosis of *Bambuites erichsenii* made by *Baptista (2020)* is the characterization of processes along the vesicle. The presence of these processes excludes the possibility of *Bambuites erichsenii* being a junior synonym of *Leiosphaeridia jacutica* (Timofeev, 1966), as previously proposed by Sanchez & Fairchild (2017).

Genus *Germinosphaera* Mikhailova, 1986

Type species.—*Germinosphaera bispinosa* Mikhailova, 1986.

Other species.—*Germinosphaera guttaformis* Mikhailova in Jankauskas et al., 1989, *Germinosphaera alveolata* Miao et al. (2019).

*Original diagnosis presented by Mikhailova (1986) in Russia*n.—"Оболочки округлые, округло-овальные, плотные, толстые, гладкие или шагреневые, проросшие. Отростки, которые могут ветвиться, наблюдаются на одном или двух поолюсах."

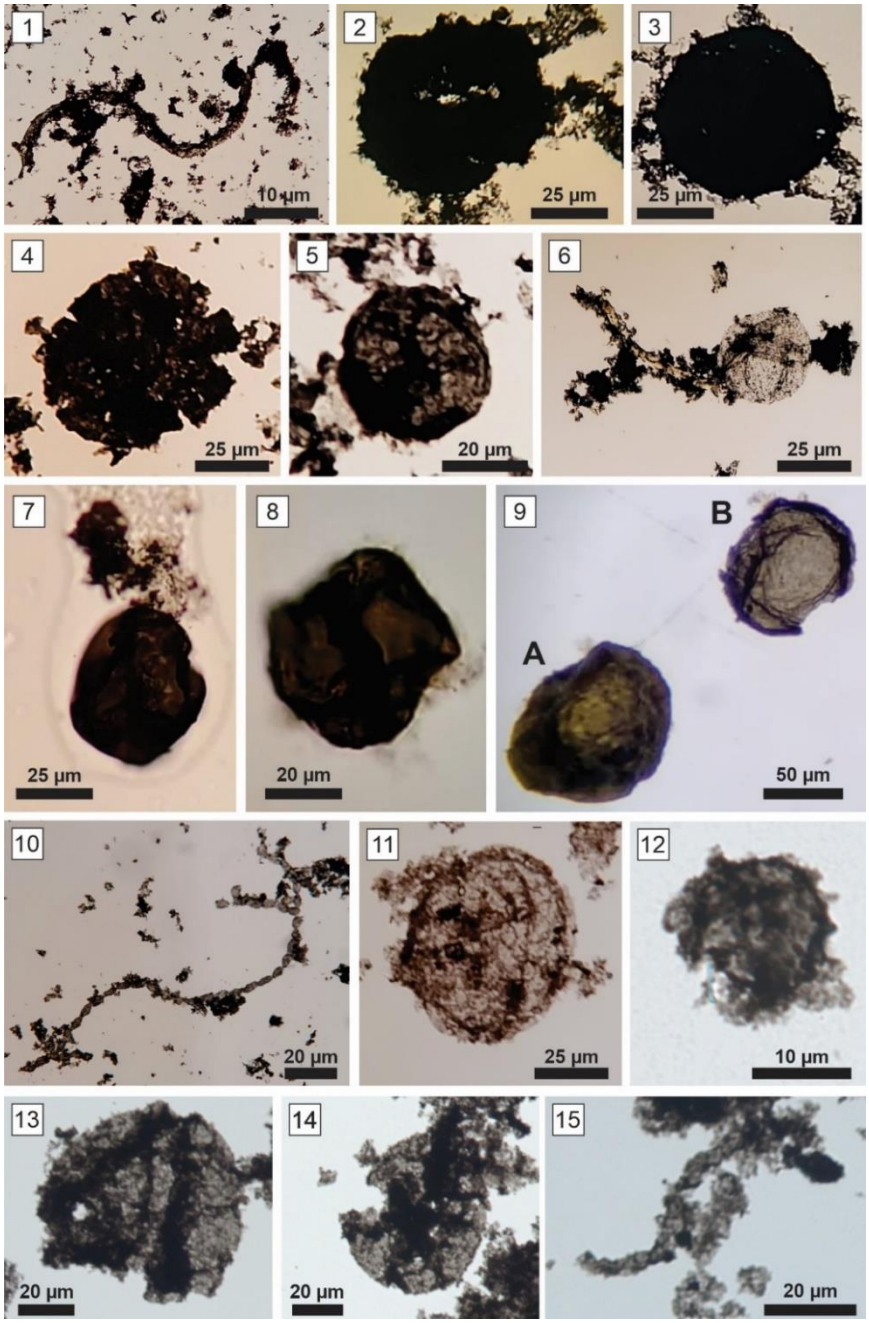

Figure 13: Organic-walled microfossils from the Sete Lagoas Formation. **(1–11)** specimens from the Rei do Mato section. **(12–15)** specimens from the Fercal section. Slide number and England Finder coordinates (in parentheses) are given for each illustrated specimen. **(1)** *Siphonophycus robustum*, CP1019 (R45). **(2–3, 12)** *Bambuites erichsenii*, **(2)** CP1022 (M57); **(3)** CP1022 (E24); **(12)** CP1016 (J50). **(4)** *Leiosphaeridia ternata*, CP1020 (N31). **(5, 14)** *Leiosphaeridia minutissima*, **(5)** CP1021 (S15); **(14)** CP1017 (L19). **(6)** *Germinosphaera bispinosa*, CP1025 (G29). **(7–8)** *Leiosphaeridia crassa*, **(7)** CP1023 (L55); **(8)** CP1023 (C33). **(9B, 11, 13)** *Leiosphaeridia tenuissima*, **(9B)** CP1024; **(11)** CP1026 (G19); **(13)** CP1015 (J26). **(9A)** *Leioshpaeridia jacutica*, CP1024. **(10, 15)** *Ghoshia januarensis*, **(10)** CP1018 (S27); **(15)** CP1016 (O39).

Original diagnosis presented by Mikhailova (1986) translated.—"The shells are round, round-oval, dense, thick, smooth or shagreen, sprouted. Processes are observed at one or two poles."

Emended diagnosis by Butterfield et al. (1994).—" Spheroidal vesicles with 1–6 open-ended, tubular, and occasionally branched processes that communicate freely with the vesicle. Multiple processes usually restricted to a single 'equatorial' plane, but otherwise non-uniformly distributed on the vesicle."

Emended diagnosis by Miao et al. (2019).—"Vesicle spheroidal, teardrop-shaped to slightly irregular outline, having psilate or low relief sculptured alveolar wall surface and bearing a single to multiple processes. Processes are simple tubular or occasionally branching and open-ended. Processes are distributed [irregularly] on the vesicle wall, if multiple, and may be predominantly, but not exclusively, distributed in the equatorial plane of the vesicle."

Germinosphaera bispinosa Mikhailova, 1986

Figures 10.4, 10.8, 10.11, 13.6

1986 *Germinosphaera bispinosa* Mikhailova, p. 33, fig. 6.

1986 *Germinosphaera unispinosa* Mikhailova, p.33, fig. 5.

1989 *Germinosphaera bispinosa*; Jankauskas et al., p. 142, pl. 47, fig. 2.

1989 *Germinosphaera tadasii* Weis *in* Jankauskas et al., p. 143, pl. 47, figs. 3–5.

1989 *Germinosphaera unispinosa* Jankauskas et al., p. 143, pl. 47, fig. 1.

1991 *Germinosphaera* sp.; Knoll et al., p. 557, fig. 19.6.

1993 *Gemmispora rudis* Yan in Yan and Liu, pl. I, figs. 6–7.

1994 *Germinosphaera fibrilla* (Ouyang et al., 1974); Butterfield et al., p. 38, fig. 17a–h.

1994 *Germinosphaera bispinosa*; Butterfield et al., p. 38, fig. 16d–e.

1994 *Germinosphaera jankauskasii* Butterfield *in* Butterfield et al., pp. 38, 40, fig. 16a–c.

1995 *Germinosphaera* sp. cf. *G. unispinosa*; Zang, p. 164, fig. 26k–l.

1999 *Germinosphaera unispinosa*; Yin and Guan, pp. 128, 130, fig. 5.2, 5.4, 5.6, 5.9.

2005 *Germinosphaera bispinosa* Prasad et al., pp. 44, 46, pl. 11, fig. 3.

2005 *Germinosphaera unispinosa* Prasad et al., p. 44, pl. 11, figs. 1–2.

2007 *Germinosphaera unispinosa*; Yin and Yuan, fig. 2.11.

2009 *Germinosphaera* sp.; Vorob'eva et al., p. 191, fig. 13.13–13.15, 13.17.

2016 *Germinosphaera bispinosa*; Baludikay et al., fig. 6a–c.

2017 *Germinosphaera bispinosa*; Loron and Moczydłowska, pp. 24-25, pl. 1, fig. 3.

2019 *Germinosphaera bispinosa*; Li et al., fig. 10c–g.

2019 *Germinosphaera bispinosa*; Loron et al., fig. 8e–f.

2019 *Germinosphaera bispinosa*; Miao et al., pp. 187–188, fig. 5d–f.

2021 *Germinosphaera bispinosa*; Miao et al., p. 14, fig. 5d–e.

2022 *Germinosphaera bispinosa*; Denezine et al., fig. 11.4.

Holotype.—No 882/2 from the Krasnoyarsk region, River Uderei; Upper Riphean, Dashkin Formation (Mikhailova, 1986, fig. 6).

Diagnosis by Butterfield in Butterfield et al. (1994).—"Spheroidal vesicles with 1–6 open-ended, tubular, and occasionally branched processes that communicate freely with the vesicle. Multiple

processes usually restricted to a single 'equatorial' plane, but otherwise non-uniformly distributed on the vesicle."

Emended diagnosis by Miao et al. (2019).—"Spheroidal to slightly elongate or irregular vesicle with one to multiple tubular processes. Vesicle wall psilate. Processes may [be] arranged irregularly or equatorially on the vesicle wall when multiple."

Description.—Vesicles are 23.4–34.8 µm in diameter, bearing 1–2 processes. When two processes are present, they are inserted at two opposing ends of the vesicle (Fig. 3.4). Processes typically taper slightly toward their distal end (Fig. 3.4, lower process; Fig. 3.8) or are more or less cylindrical (Fig. 3.11). The upper process in the specimen illustrated in Fig. 3.4 is apparently constricted at the base. Still, it is uncertain whether this constriction is a taphonomic feature related to the twisting of the process. Processes are 1–3 µm in maximum diameter and 22.6–123 µm in preserved length.

Illustrated material.—CP917 and CP1025.

Occurrence in the studied sections.—**Barreiro section:** MP3036 and MP3714. **Rei do Mato section:** MP5207.

Remarks.—Mikhailova (1986) established two species of *Germinosphaera*, *Germinosphaera unispinosa*, and *Germinosphaera bispinosa*. Two additional species were published in Jankauskas et al. (1989), *Germinosphaera guttaformis* Mikhailova *in* Jankauskas et al. (1989) and

Germinosphaera tadasii Weiss *in* Jankauskas et al, 1989. These species were distinguished by the number of processes and the psilate versus shagrinate nature of vesicle walls. However, Butterfield et al. (1994) considered the possibility that the processes in *Germinosphaera* represent growth structures in vegetative stages, analogous to the modern xanthophyte *Vaucheria*. As such, they emended the diagnosis of *Germinosphaera* and the diagnosis of *G. bispinosa*, and they synonymized *G. unispinosa* with *G. bispinosa*. Miao et al. (2019) further emended the diagnosis of *Germinosphaera* and considered shagrinate vesicle walls to represent taphonomic alteration. Furthermore, they noted that the vesicle diameter of different species could overlap each other. Thus, they proposed that *G. tadasii* and *G. jankauskasii*, characterized by shagrinate vesicle walls, were junior synonyms of *G. bispinosa*. Following Miao et al. (2019), *Germinosphaera* currently has three species: *Germinosphaera bispinosa* Mikhailova, 1986, *Germinosphaera guttaformis* Mikhailova *in* Jankauskas et al., 1989, and *Germinosphaera alveolata* Miao et al., 2019.

Subgroup Sphaeromorphitae Downie et al., 1963

Genus *Leiosphaeridia* Eisenack, 1958

Type species.—Leiosphaeridia baltica Eisenack, 1958.

Other species.—Fensome et al. (1990) revised all *Leiosphaeridia* species and listed 167 valid species.

Original diagnosis presented by Eisenack (1958b) in German.—"Hohlkugelförmige, dünnwandige und aus einer sehr widerstandsfähigen, hellgelb bis dunkelrotbraun

durchscheinenden organischen Substanz bestehende Organismenreste, die oft in scheibenförmig zusammengepreßtem Zustande oder auch unregelmäßig verfaltet überliefert sein können. Wand, auch in erwachsenem Zustande, stets ohne Wandporen (Unterschied zu Tasmanites). Pylome vorhanden."

Original diagnosis presented by Eisenack (1958b) translated.—"Hollow spherical, thin-walled organism consisting of a very resistant, light yellow to dark red-brown translucent, organic substance, which can often be preserved as a disc-shaped compressed state or irregularly folded. Even when fully grown, walls are always without wall pores (in contrast to *Tasmanites*). Pylome present."

Emended diagnosis by Downie and Sarjeant (1963).—"Spherical to ellipsoidal bodies without processes, often collapsed or folded, with or without pylomes. Walls granular, punctate or unornamented, thin. Without divisions into fields and without transverse or longitudinal furrows or girdles."

Emended diagnosis by Jankauskas et al. (1989) in Russian.—"Сфероидальные оболочки с гладкой, точеечной или зеррнистой поверхиостью размером от 2—3 до 750 мкм. Толщина стенки от долей микрометра до 3—10 мкм. В ископаемом состоянии сплющены и осложнены складками смятия различной формы и размеров."

Emended diagnosis by Jankauskas et al. (1989) translated.—" Spheroidal vesicle with a smooth, punctate, or granular surface ranging in size from 2–3 to 750 µm. The wall thickness varies from

fractions of a micrometer to 3–10 µm. The specimens are flattened and can present folds of crushing of various shapes and sizes."

Remarks.—A significant number of species of the genus *Leiosphaeridia* have been reported from the Proterozoic. Many have very long stratigraphic ranges, e.g., from the Paleoproterozoic to the Mesozoic (Lamb et al., 2009). There are even reports of *Leiosphaeridia* species from the Miocene (Hannah et al., 2000). Because of its simple morphologies, the genus *Leiosphaeridia* is regarded as a form taxon with diverse phylogenetic affinities, and it is classified in the Acritarcha (Grey, 2005; Sergeev and Schopf, 2010; Jankauskas et al., 1989), although Sergeev and Schopf (2010) consider this taxon belonging to the Kingdom Protista, a proposition followed here. Downie and Sarjeant (1963) emended the diagnosis of the Genus *Leiosphaeridia* to exclude the reference of the vesicle color since it could reflect diagenetic features. Moreover, the maceration protocol could affect the color of organic vesicles due to oxidizing solutions. Jankauskas et al. (1989) limited the diameter of the vesicle of *Leiosphaeridia* species ranging in size from 2–3 to 750 µm. Furthermore, Jankauskas et al. (1989) divided the smooth-walled *Leiosphaeridia* species into four species according to vesicle diameter and wall thickness, a form-taxonomical scheme followed in the present work. Butterfield et al. (1994) suggested that *Leiosphaeridia* should be restricted to spherical fossils with vesicle walls less than 2 µm thick to be differentiated from *Chuaria circularis* Walcott, 1899, which has thicker vesicle walls (2-3 µm single-wall thickness).

Leiosphaeridia crassa (Naumova, 1949) Jankauskas *in* Jankauskas et al., 1989

Figures 10.6, 13.7

1949 *Leiotriletes crassus* Naumova, p. 54, pl. 1, figs. 5–6, pl. 2, figs. 5–6.

1973 *Leiopsophosphaera crassa*; Pykhova, p. 99, pl. 2, fig. 3.

1989 *Leiosphaeridia crassa* (Naumova, 1949) Jankauskas *in* Jankauskas et al., pp. 75–76, pl. 9, figs. 5–10.

1992 *Leiosphaeridia crassa*; Zang and Walter, pp. 289, 291, 293, pl. 9, figs. a–k, pl. 12, fig. k, pl. 14, figs. e, h.

1994 *Leiosphaeridia crassa*; Butterfield et al., pp. 40, 42, figs. 16f, 23k.

1994 *Leiosphaeridia crassa*; Hofmann and Jackson, p. 22, fig. 1.19–29.

1994 *Leiosphaeridia crassa*; Knoll, fig. 4b.

1995 *Leiosphaeridia crassa;* Zang, p. 166, figs. 21d, 28c–d.

1999 *Leiosphaeridia crassa*; Yin and Guan, p. 131, figs. 3.8, 4.5, 5.3, 5.5, 5.7, 5.11, 6.2–6.6, 6.9, 6.12.

2004 *Leiosphaeridia crassa*; Javaux et al., fig. 4e–i.

2004 *Leiosphaeridia crassa*; Sergeev and Lee, pp. 21, 23, pl. 3, figs. 4–5.

2004 *Leiosphaeridia crassa*; Tiwari and Pant, p. 1736, fig. 3v.

2005 *Leiosphaeridia crassa*; Grey, pp. 179–182, figs. 63a–c, 64a–d.

2005 *Leiosphaeridia crassa;* Marshall et al., fig. 1e.

2005 *Leiosphaeridia crassa*; Prasad et al., pl. 1, figs. 1–2; pl. 4, fig. 16, pl. 5, fig. 18, pl. 9, figs. 10–11.

2006 *Leiosphaeridia crassa*; Javaux and Marshal, fig. 3.4–3.6.

2006 *Leiosphaeridia crassa*; Sergeev and Seong-joo, p. 15, pl. 2, figs. 2a–c, 5.

2008a *Leiosphaeridia crassa*; Moczydłowska, p. 84, figs. 7a, 8g.

2008b *Leiosphaeridia crassa*; Moczydłowska, fig. 2g.

2008 *Leiosphaeridia crassa*; Sergeev et al., pl. 7, figs. 5–6.

2009 *Leiosphaeridia crassa*; Yin et al., figs. 3a, 3h, 3l, 4d, 4f, 4h, 5a, 5c.

2009 *Leiosphaeridia crassa*; Tiwari and Pant, figs. 7d–e, 8h, 8o–p.

2009 *Leiosphaeridia crassa*; Stanevich et al., p. 32, pl. 3, figs. 3–4.

2010 *Leiosphaeridia crassa*; Sergeev and Schopf, p. 395, fig. 15.3–15.6.

2011 *Leiosphaeridia crassa*; Strother et al., fig. 1a, 1e.

2011 *Leiosphaeridia crassa*; Couëffé and Vecolii, figs. 6.2, 7.1, 7.7.

2013 *Leiosphaeridia crassa*; Tang et al., fig. 4b.

2014 *Leiosphaeridia crassa*; Lottaroli et al., fig. 10.2.

2014 *Leiosphaeridia crassa*; Babu et al., fig. 3f.

2015 *Leiosphaeridia crassa*; Tang et al., fig. 4d.

2015 *Leiosphaeridia crassa*; Nagovitsin and Kochnev, fig. 1.55–1.56.

2016 *Leiosphaeridia crassa*; Baludikay et al., fig. 8a–c.

2016 *Leiosphaeridia crassa*; Porter and Riedman, p. 833, fig. 13.2, 13.6.

2016 *Leiosphaeridia crassa*; Sergeev et al., fig. 4.2.

2017 *Leiosphaeridia crassa*; Javaux and Knoll, p. 209, fig. 4.6.

2017 *Leiosphaeridia crassa*; Agic et al., p. 110, fig. 8a–c.

2017a *Leiosphaeridia crassa*; Sergeev et al., fig. 3.14.

2017b *Leiosphaeridia crassa*; Sergeev et al., pl. I, fig. 6.

2017 *Leiosphaeridia crassa*; Beghin et al., pl. 2, figs. c–d.

2017 *Leiosphaeridia crassa*; Suslova et al., fig. 3.1–3.4.

2018 *Leiosphaeridia crassa*; Anderson et al., pp. 10, 12, fig. 8a–e.

2018 *Leiosphaeridia crassa*; Riedman et al., fig. 5.15.

2019 *Leiosphaeridia crassa*; Arrouy et al., fig. 6d–e.

2019 *Leiosphaeridia crassa*; Li et al., fig. 4f.

2020 *Leiosphaeridia crassa*; Arvestål and Willman, p. 11, fig. 6j–k, 6m.

2020 *Leiosphaeridia crassa*; Knoll et al., p. 6, fig. 3g.

2020 *Leiosphaeridia crassa*; Shukla et al., p. 502, fig. 6g.

2020 *Leiosphaeridia crassa*; Pang et al., fig. 2m.

For additional synonyms also see Jankauskas et al. (1989) and Zang and Walter (1992).

Type material.—Naumova (1949) did not designate a holotype for *Leiotriletes crassus*. Subsequently, Jankauskas in Jankauskas et al. (1989) designated one specimen of *Leiotriletes crassus* published by Naumova (1949) as a "holotype" (Naumova, 1949, pl. 1, fig. 3). Additionally, he designated another specimen from a different locality and stratigraphic unit as a "lectotype" (Jankauskas et al., 1989, LitNIGRI, N 16-800-2942/9, specimen 2, tab. 9, fig. 5). By so doing, the assumption of a holotype by Jankauskas can, according to the International Code of Nomenclature for algae, fungi, and plants, be taken as the designation of a lectotype (Turland et al., 2018). In addition, the specimen designated by Jankauskas as a "lectotype" should be regarded as a neotype. Based on the same code, when there is a lectotype, it always takes precedence over a neotype. Although in this case, the lectotype, strictly speaking, designated by Jankauskas was a specimen of *Leiotriletes simplicissimus*, a species he synonymized with a different species of *Leiosphaeridia*, *Leiosphaeridia minutissima*. Considering the aforementioned, the lectotype designated by Jankauskas is not valid. Due to the presented circumstances, the neotype designated by Jankauskas in Jankauskas et al. (1989) is considered the valid type material of *Leiosphaeridia crassa*.

Original diagnosis presented by Naumova (1949) in Russian.—“В очертании спора округлой или округло-овальной формы. Поверхность экзины гладкая, экзина очень толстая и плотная. Форма имеет складки смятия, щель разверзания, простая. Широко распространена в нижнем кембрии Прибалтики.”

Original diagnosis presented by Naumova (1949) translated.—“ In outline, the spore is round or round-oval. The surface of the exine is smooth, the exine is very thick and dense. The form has crumpled folds, an opening gap, and is simple. Widespread in the Lower Cambrian of the Baltic.”

Emended diagnosis by Javaux and Knoll (2017) and Knoll et al. (2020).—“A species of *Leiosphaeridia* with smooth, pliant walls with lanceolate folds and a modal diameter of less than 70 μm.”

Illustrated materials.—CP964 and CP1023.

Occurrence in the studied sections.—**Barreiro section:** MP3719 and MP3720. **Fercal section:** MP4510, MP4535, MP4541, MP4549, and MP4566. **Rei do Mato section:** MP5159, MP5165, MP5171, MP5184, MP5191, MP5192, MP5193, MP5194, and MP5196.

Remarks.—Leiotriletes crassus Naumova, 1949 was originally described supported only by a description, without a diagnosis. Even though the International Code of Nomenclature for algae, fungi, and plants states that either a description or a diagnosis is enough for the valid publication of a name (Art. 38.1 in Turland et al., 2018), it is strongly recommended that both the diagnosis

and description be presented when describing a new species (Hassemer et al., 2020). Later, Jankauskas *in* Jankauskas et al. (1989) reviewed some species of *Leiosphaeridia*, transferred *Leiotriletes crassus* Naumova, 1949 to the genus *Leiosphaeridia*. When *Leiotriletes crassus* was transferred to the genus *Leiosphaerida*, the epithet was changed to *crassa*, so the gender of the epithet agrees with the gender of the genus name. Thus, this species became *Leiosphaeridia crassa* (Naumova, 1949) Jankauskas *in* Jankauskas et al., 1989. In addition, Jankauskas et al. (1989) did not include in their synonym list the species *Leiopsophosphaera crassa* Pykhova, 1973. Finally, Fensome et al. (1990), also in a work of taxonomic revision, transferred *Leiopsophosphaera crassa* Pykhova, 1973 to *Leiosphaeridia crassa* (Pykhova, 1973). However, Fensome et al. (1990) did not take into account the study of Jankauskas et al. (1989) and regarded *Leiotriletes crassus* Naumova, 1949 as taxonomically uncertain (Grey, 2005). Thus, *Leiosphaeridia crassa* (Pykhova, 1973) is a junior homonym of *Leiosphaeridia crassa* (Naumova, 1949) Jankauskas *in* Jankauskas et al., 1989. Nonetheless, *Leiopsophosphaera crassa* Pykhova, 1973 is considered by some authors (Grey, 2005; Yin and Guan, 1999) as a synonym of *Leiosphaeridia crassa* (Naumova, 1949), a synonymy followed in this study. *Leiosphaeridia crassa* differs from *Leiosphaeridia minutissima* in its thicker vesicle wall and from *Leiosphaeridia tenuissima* and *Leiosphaeridia jacutica* in vesicle size (Jankauskas et al., 1989).

Leiosphaeridia jacutica (Timofeev, 1966) Mikhailova and Jankauskas in Jankauskas et al., 1989

Figures 10.5, 13.9A

1966 *Kildinella jacutica* Timofeev, p. 30, pl. 7, fig. 2; pl.19, fig 9; pl. 61, fig. 5; pl. 67, fig. 8; pl. 72, fig. 1.

1989 *Leiosphaeridia jacutica* (Timofeev, 1966), Mikhailova and Jankauskas in Jankauskas et al., pp. 77–78, pl. 12, figs. 3, 7, 9.

1992 *Leiosphaeridia jacutica*; Butterfield and Chandler, fig. 5e.

1994 *Leiosphaeridia jacutica*; Butterfield et al., p. 42, fig. 16h.

1994 *Leiosphaeridia jacutica*; Hofmann and Jackson, p. 22, fig. 17.1–17.4.

1995 *Leiosphaeridia jacutica*; Kumar and Srivastava, p. 106, fig. 11k.

2001 *Leiosphaeridia jacutica*; Sergeev, p. 444, fig. 8.7–8.10.

2004 *Leiosphaeridia jacutica*; Javaux et al., fig. 4a–d, 4m.

2005 *Leiosphaeridia jacutica*; Grey, pp. 183–184, fig. 63g.

2005 *Leiosphaeridia jacutica*; Marshall et al., fig. 1c.

2005 *Leiosphaeridia jacutica*; Prasad et al., pl. 3, figs. 13–14; pl. 4, fig. 12; pl. 9, fig. 25; pl. 10, fig. 6.

2006 *Leiosphaeridia jacutica*; Sergeev and Seong-joo, pp. 14–15, pl. 2, fig. 6.

2006 *Leiosphaeridia jacutica*; Javaux and Marshal, fig. 3.1–3.3.

2009 *Leiosphaeridia jacutica*; Stanevich et al., p. 32, pl. 3 fig. 2.

2009 *Leiosphaeridia jacutica*; Vorob'eva et al., p. 185, fig. 14.13.

2010 *Leiosphaeridia jacutica*; Nemerov et al., fig. 6.8–6.9.

2010 *Leiosphaeridia jacutica*; Prasad et al., pl. 1, fig. 3.

2013 *Leiosphaeridia jacutica*; Tang et al., fig. 4d.

2014 *Leiosphaeridia jacutica*; Babu et al., fig. 3l.

2015 *Leiosphaeridia jacutica*; Chiglino et al., p. 643, fig. 5b.

2015 *Leiosphaeridia jacutica*; Tang et al., figs. 4f–g, 5a.

2015 *Leiosphaeridia jacutica*; Nagovitsin and Kochnev, fig. 4.43.

2015 *Leiosphaeridia jacutica*; Vorob'eva et al., fig. 7.6.

2016 *Leiosphaeridia jacutica*; Baludikay et al., fig. 8d.

2016 *Leiosphaeridia jacutica*; Porter and Riedman, pp. 833–834, fig. 13.3.

2016 *Leiosphaeridia jacutica*; Sergeev et al., fig. 4.1, 4.6–4.7.

2016 *Leiosphaeridia jacutica*; Singh and Sharma, p. 80, pl. 1, figs. 9–10.

2017 *Leiosphaeridia jacutica*; Javaux and Knoll, pp. 209–210, fig. 4.4–4.5.

2017a *Leiosphaeridia jacutica*; Sergeev et al., fig. 3.1, 3.9–3.11.

2017b *Leiosphaeridia jacutica*; Sergeev et al., pl. I, fig. 5.

2017 *Leiosphaeridia jacutica*; Beghin et al., pl. 2, fig. e.

2017 *Leiosphaeridia crassa*; Tang et al., fig. 3c.

2017 *Leiosphaeridia jacutica*; Tang et al., fig. 3d.

2018 *Leiosphaeridia jacutica*; Anderson et al., p. 12, fig. 8f–k.

2019 *Leiosphaeridia jacutica*; Arrouy et al., fig. 6b–c.

2019 *Leiosphaeridia jacutica*; Li et al., fig. 4h.

2020 *Leiosphaeridia jacutica*; Arvestål and Willman, p. 11, fig. 6i, 6l.

2020 *Leiosphaeridia jacutica*; Knoll et al., p. 6, fig. 2g.

2020 *Leiosphaeridia jacutica*; Shukla et al., pp. 502–503, fig. 6l.

2020 *Leiosphaeridia jacutica*; Pang et al., fig. 2f.

2021 *Leiosphaeridia jacutica*; Han et al., fig. 3a–d.

Holotype.—IGD Russian Academy of Sciences No. 451/1, from upper Riphean, Lakhanda Group, Neryuen Formation, Siberia (Timofeev, 1966, pl. 7, fig. 2).

Original description by Timofeev (1966) in Russian.—"Оболочки диаметром 150–250 мк, сферические, толстые, однослойные, с поверхностью от гладкой до грубошагреневой, с резко очерченными, крупными, серповидными, иногда угловатымц складками. Цвет темно-желтый, желто-коричневый."

Original description by Timofeev (1966) translated.—"The vesicles are 150–250 microns in diameter, spherical, thick, single-layered, with a surface from smooth to coarse shagreen, with sharply defined, large, crescent-shaped, sometimes angular folds. Color dark yellow, yellow-brown."

Emended diagnosis by Javaux and Knoll (2017).—"A species of *Leiosphaeridia* characterized by smooth, pliant walls with lanceolate folds and a modal diameter greater than 70 µm."

Illustrated materials.—CP913 and CP1024.

Occurrence in the studied sections.—**Barreiro section:** MP2990, MP3719, and 3714**. Fercal section:** MP4510, MP4532, and MP4549. **Rei do Mato section:** MP5187, MP5192, MP5193, and MP5197.

Remarks.—Timofeev (1966) described the new species *Kinidella jacutica* Timofeev, 1966, also designated a holotype but did not present the diagnosis of this species, only the description. Later on, Mikhailova and Jankauskas in Jankauskas et al., 1989 verified that *Kinidella jacutica* should be transferred to *Leiosphaeridia jacutica* (Timofeev, 1966). They also designated a lectotype for

Leiosphaeridia jacutica. This lectotype is invalid since Timofeev (1966) had designated a holotype in its publication. The synonym list of Jankauskas et al. (1989) includes *Leiosphaeridia warsanofiewii* (Naumova, 1950) in (Shepeleva, 1963). Therefore, the synonymy is restricted to the specimen illustrated in Shepeleva (1963) and not the species proposed by Naumova (1950). *Leiosphaeridia jacutica* differs only by the larger size compared to *Leiosphaeridia crassa* (Jankauskas et al., 1989). The specimen illustrated by Tang et al. (2017) in their fig. 3c is not *Leiosphaeridia crassa* but *Leiosphaeridia jacutica* because its diameter is around 90 µm. *Leiosphaeridia jacutica* differs from *Bambuites erichsenii* in its sphaeromorphic vesicle without processes.

Leiosphaeridia minutissima (Naumova, 1949) Jankauskas in Jankauskas et al., 1989

Figures 10.1–10.3, 10.7, 10.10, 13.5, 13.14

1949 *Leiotriletes minutissimus* Naumova, p. 52, pl. 1, figs. 1–2, pl. 2, figs. 1–2.

1989 *Leiosphaeridia minutissima* (Naumova, 1949) Jankauskas in Jankauskas et al., pp. 79–80, pl. 9, figs. 1–4, 11.

1992 *Leiosphaeridia minutissima*; Butterfield and Chandler, fig. 3a, 3i.

1994 *Leiosphaeridia minutissima*; Hofmann and Jackson, p. 21, fig. 23.9–23.15.

2003 *Leiosphaeridia minutissima*; Gaucher and Germs, fig. 6.10–6.12.

2005 *Leiosphaeridia minutissima*; Grey, p. 184, fig. 63d.

2005 *Leiosphaeridia minutissima*; Blanco and Gaucher, fig. 11b.

2005b *Leiosphaeridia minutissima*; Gaucher et al., fig. 6d.

2005 *Leiosphaeridia minutissima*; Prasad et al., pl. 9, figs. 1, 3.

2008 *Leiosphaeridia minutissima*; Gaucher et al., p. 491, fig. 3a.

2008a *Leiosphaeridia minutissima*; Moczydłowska, pp. 84–85, fig. 8h.

2008b *Leiosphaeridia minutissima*; Moczydłowska, figs. 2f, 6d.

2010 *Leiosphaeridia minutissima*; Nemerov et al., fig. 6.7.

2011 *Leiosphaeridia minutissima*; Couëffé and Vecolii, fig. 7.3.

2013 *Leiosphaeridia minutissima*; Tang et al., fig. 4a.

2015 *Leiosphaeridia minutissima*; Chiglino et al., p. 642, fig. 5a.

2015 *Leiosphaeridia minutissima*; Tang et al., fig. 4c.

2015 *Leiosphaeridia minutissima*; Nagovitsin and Kochnev, fig. 4.57–4.58.

2015 *Leiosphaeridia minutissima*; Schopf et al., p. 724, fig. 13.10.

2016 *Leiosphaeridia minutissima*; Baludikay et al., fig. 8e.

2016 *Leiosphaeridia minutissima*; Porter and Riedman, p. 834, fig. 13.1, 13.5.

2017 *Leiosphaeridia minutissima*; Javaux and Knoll, p. 210, fig. 4.7–4.8.

2017a *Leiosphaeridia minutissima*; Shi et al., fig. 11.6–11.7.

2017 *Leiosphaeridia minutissima*; Beghin et al., pl. 2, figs. g–h.

2017 *Leiosphaeridia minutissima*; Tang et al., fig. 3a.

2017 *Leiosphaeridia minutissima*; Suslova et al., fig. 3.6–3.11.

2017 *Leiosphaeridia minutissima*; Agic et al., pp. 110–112, fig. 8g–h.

2018 *Leiosphaeridia minutissima*; Yin et al., fig. 4h, 4j, 4l.

2018 *Leiosphaeridia minutissima*; Javaux and Lepot, fig. 2e.

2019 *Leiosphaeridia minutissima*; Lei et al., fig. 3.13–3.14.

2019 *Leiosphaeridia minutissima*; Arrouy et al., fig. 5a–g, 5j.

2019 *Leiosphaeridia minutissima*; Li et al., fig. 4e.

2019 *Leiosphaeridia minutissima*; Shang et al. , p. 24, fig. 21a.

2020 *Leiosphaeridia minutissima*; Arvestål and Willman, pp. 11–12, fig. 6c–g.

2020 *Leiosphaeridia minutissima*; Knoll et al., p. 6, fig. 2a, 2c.

2020 *Leiosphaeridia minutissima*; Shukla et al., p. 502, fig. 6e, 6k, 6m.

2020 *Leiosphaeridia minutissima*; Pang et al., fig. 2n.

2021 *Leiosphaeridia minutissima*; Loron et al., fig. 6.2.

2022 *Leiosphaeridia minutissima*; Denezine et al., fig. 11.1–11.2.

Type material.— Naumova (1949) did not designate a holotype for *Leiotriletes minutissimus*. Afterward, Jankauskas in Jankauskas et al. (1989) designated one of the specimens published by Naumova (1949) as a "holotype" (Naumova, 1949, pl. 1, fig. 1). Additionally, he designated another specimen from a different locality and stratigraphic unit as a "lectotype" (Jankauskas et al., 1989, LitNIGRI, N 16-800-2942/9, tab. 9, fig. 1). According to the International Code of Nomenclature for algae, fungi, and plants, the "holotype" mentioned by Jankauskas should be regarded as a lectotype and the "lectotype" regarded as a neotype. Based on the same code, when a lectotype is designated, it always takes precedence over a neotype. In light of the aforementioned, the lectotype designated by Jankauskas in Jankauskas et al. (1989) (Naumova, 1949, pl. 1, fig. 1) is the valid type material of *Leiosphaeridia minutissima*.

Description presented by Naumova (1949) in Russian.—"Очертание споры округлое. Экзина очень тонкая, прозрачная, наблюдаются многочисленные складки смятия. Поверхность экзины гладкая. Щель разверзания трехлучевая, простая, плохо различимая нз-за складок смятия."

The description presented by Naumova (1949) translated.—"The outline of the vesicle is rounded. The exine is very thin and transparent, with numerous crumpled folds. The surface of the exine is smooth. The opening slit is three-beam, simple, poorly distinguishable due to the crumpling folds."

Diagnosis presented by Javaux and Knoll (2017).—"A species of *Leiosphaeridia* characterized by smooth walls with sinuous folds and a modal diameter less than 70 µm."

Emended diagnosis presented by Knoll et al. (2020).—"A species of *Leiosphaeridia* characterized by thin, smooth walls with sinuous folds and a modal diameter less than 70 µm."

Illustrated materials.—CP918, CP962, CP963, CP964, CP1017, and CP1021.

Occurrence in the studied sections.— **Barreiro section:** MP3719, MP2977, MP2979, MP2980, MP2983, MP2985, MP2986, MP2987, MP2988, MP2992, MP2993, MP2994, MP2995, MP2998, MP2999, MP 3002, MP 3004, MP 3005, MP 3006, MP 3007, MP 3011, MP 3012, MP 3013, MP 3015, MP 3016, MP3028, MP 3030, MP3031, MP3033, MP3034, MP3035, MP3036, MP3705, MP3707, MP3708, MP3709, MP3710, MP3712, MP3713, MP3714, MP3715, MP3716, MP3719, and MP3720. **Fercal section:** MP4503, MP4507, MP4510, MP4519, MP4520, MP4521, MP4526, MP4527, MP4535, MP4538, MP4545, MP4547, MP4549, MP4565, MP4566, MP4567, MP4601, MP4617, MP4630, MP4634, and MP4635. **Rei do Mato section:** MP5131, MP5136, MP5139, MP5159, MP5160, MP5175, MP5178, MP5180, MP5182, MP5184, MP5185, MP5189, MP5191, MP5193, MP5196, MP5200, MP5201, MP5205, MP5207, MP5216, and MP5221. **PRF section:** MP4220 and MP4221.

Remarks.— The basionym of *Leiosphaeridia minutissima* (Naumova, 1949) is *Leiotriletes minutissimus* Naumova, 1949. As for *Leiotriletes* crassus, Naumova (1949) did not present a diagnosis for this species but provided a detailed description. Subsequently, Jankauskas *in* Jankauskas et al. (1989) transferred this species to *Leiosphaeridia minutissima* (Naumova, 1949) without presenting a diagnosis. When *Leiotriletes minutissimus* was transferred to the genus *Leiosphaerida*, the epithet was changed to *minutissima*, so the gender of the epithet agrees with the gender of the genus name. The first formal diagnosis for *Leiosphaeridia minutissima* was presented by Javaux and Knoll (2017), emended later on by Knoll et al. (2020).

Leiosphaeridia tenuissima Eisenack, 1958

Figures 10.9, 13.8, 13.9B, 13.11, 13.13

1958a *Leiosphaeridia tenuissima* Eisenack, p. 391, pl.1, figs. 2–3.

1958b *Leiosphaeridia tenuissima*; Eisenack, pl. 2, figs. 1–2.

1989 *Leiosphaeridia tenuissima*; Jankauskas et al., p. 81, pl. 9, figs. 12–13.

1994 *Leiosphaeridia tenuissima*; Butterfield et al., p. 42, fig. 16i.

1994 *Leiosphaeridia tenuissima*; Hofmann and Jackson, p. 22, fig. 15.16–15.18.

1998 *Leiosphaeridia tenuissima*; Zhang et al., p. 32, fig. 9.7.

1998 *Leiosphaeridia* spp. div.; Zhang et al., p. 32, fig. 9.8–9.9

1999 *Leiosphaeridia tenuissima*; Turnau and Racki, p. 267, pl. 5, fig. 1.

2000 *Leiosphaeridia tenuissima*; Gaucher, p. 68, pl. 11, fig. 5.

2003 *Leiosphaeridia tenuissima*; Gaucher and Germs, fig. 6.6.

2004 *Leiosphaeridia tenuissima*; Javaux et al., fig. 4j–l.

2004 *Leiosphaeridia tenuissima*; Gaucher et al., fig. 4d.

2005a *Leiosphaeridia tenuissima*; Gaucher et al., p. 549, fig. 8g–h.

2005b *Leiosphaeridia tenuissima*; Gaucher et al., fig. 6a–b, 6e–h.

2005 *Leiosphaeridia tenuissima*; Blanco and Gaucher, fig. 11a.

2005 *Leiosphaeridia tenuissima*; Grey, pp. 184–185, fig. 63h.

2005 *Leiosphaeridia tenuissima*; Marshall et al., fig. 1d.

2005 *Leiosphaeridia tenuissima*; Prasad et al., pl. 1, figs 3; pl. 2, fig. 10; pl. 3, fig. 15; pl. 4, fig. 17; pl. 8, figs. 16–17.

2006 *Leiosphaeridia tenuissima*; Gaucher and Germs, pp. 207–208, figs. 7d, 7f–g, 8b–f.

2007 *Leiosphaeridia tenuissima*; Javaux, figs. 1.18–1.19.

2008 *Leiosphaeridia tenuissima*; Gaucher et al., pp. 491–493, fig. 3b–i.

2009 *Leiosphaeridia tenuissima*; Stanevich et al., p. 32, pl. 3, fig. 5.

2010 *Leiosphaeridia tenuissima*; Prasad et al., pl. 1, fig. 1.

2010 *Leiosphaeridia tenuissima*; Buick, fig. 1e.

2013 *Leiosphaeridia tenuissima*; Tang et al., fig. 4c.

2014 *Leiosphaeridia tenuissima*; Liu et al., fig. 101.

2014 *Leiosphaeridia tenuissima*; Vorob'eva and Petrov, fig. 6b.

2015 *Leiosphaeridia tenuissima*; Schopf et al., p. 724, fig. 13.9.

2015 *Leiosphaeridia tenuissima*; Nagovitsin and Kochnev, fig. 4.59.

2015 *Leiosphaeridia tenuissima*; Chiglino et al., pp. 640, 642, fig. 4a–c.

2015 *Leiosphaeridia tenuissima*; Tang et al., fig. 4e.

2015 *Leiosphaeridia tenuissima*; Vorob'eva et al., fig. 7.8.

2016 *Leiosphaeridia tenuissima*; Baludikay et al., fig. 8f.

2016 *Leiosphaeridia tenuissima*; Porter and Riedman, p. 834, fig. 13.4.

2016 *Leiosphaeridia tenuissima*; Sergeev et al., fig. 4.2.

2016 *Leiosphaeridia tenuissima*; Singh and Sharma, p. 81, pl. 1, figs. 12, 15.

2017 *Leiosphaeridia tenuissima*; Beghin et al., pl. 2, fig. j.

2017 *Leiosphaeridia tenuissima*; Tang et al., fig. 3b.

2017 *Leiosphaeridia tenuissima*; Agic et al., p. 112, fig. 8d–f.

2017 *Leiosphaeridia tenuissima*; Suslova et al., fig. 3.13–3.14.

2017a *Leiosphaeridia tenuissima*; Sergeev et al., fig. 3.12.

2017a *Leiosphaeridia minutissima*; Sergeev et al., fig. 3.13.

2017b *Leiosphaeridia tenuissima*; Sergeev et al., pl. 1, figs. 7, 9.

2018 *Leiosphaeridia tenuissima*; Anderson et al., p. 12, figs. 8l–m, 15k.

2019 *Leiosphaeridia tenuissima*; Arrouy et al., figs. 6a, 7a–d.

2019 *Leiosphaeridia tenuissima*; Li et al., fig. 4g.

2019 *Leiosphaeridia tenuissima*; Tang et al., fig. 1.2–1.5.

2019 *Leiosphaeridia tenuissima*; Wan et al., fig. 4f.

2020 *Leiosphaeridia tenuissima*; Arvestål and Willman, p. 12, fig. 6a–b.

2020 *Leiosphaeridia tenuissima*; Shukla et al., p. 502, fig. 6a–d, 6f.

2020 *Leiosphaeridia tenuissima*; Pang et al., fig. 2c.

2021 *Leiosphaeridia tenuissima*; Han et al., fig. 3e.

2021 *Leiosphaeridia tenuissima*; Tang et al., fig. 9a.

2021 *Leiosphaeridia tenuissima*; Loron et al., fig. 6.1, 6.3.

2022 *Leiosphaeridia tenuissima*; Denezine et al., fig. 11.3.

Holotype.—Preparation A3, 3 number 4, from the Dictyonema shales of the Ordovician Baltic, Nikolskaya on the Tossna, SE Leningrad (Eisenack, 1958a: pl. 1, fig. 2).

Original diagnosis presented by Eisenack (1958) in German.—"Wand äußerst dünn und zart, glasklar durchscheinend, ohne Wandporen; nur in flachgedrücktem Zustand in Form von fast kreisrunden Scheibchen überliefert. Pylome nicht beobachtet. Ø um rd 100 µ schwankend."

Original diagnosis presented by Eisenack (1958) translated.—"Wall extremely thin and delicate, crystalline translucent, without wall pores; only preserved in the flattened state in the form of almost circular disks. Pyloma was not observed. Size around 100 µ."

Emended diagnosis by Javaux and Knoll (2017).—"A species of *Leiosphaeridia* characterized by smooth walls with sinuous folds and a modal diameter (rather than maximum diameter) greater than 70 µm; the wall color is not a diagnostic criteria."

Illustrated materials.—CP914, CP1015, CP1024, and CP1026.

Occurrence in the studied sections.—**Barreiro section:** MP3002, MP3007, MP2994, MP3707, MP3709, MP3013, MP3714, MP3719, and MP3720. **Fercal section:** MP4503, MP4510, MP4527, MP4558, MP4566, and MP4634. **Rei do Mato section:** MP5131, MP5152, MP5160, MP5180, MP5194, MP5197, MP5207, and MP5221.

Remarks.— *Leiosphaeridia tenuissima* Eisenack, 1958 and *Leiosphaeridia minutissima* (Naumova, 1949) are simple sphaeromorphs and have a thin and translucent wall less than 0.5 µm thick. However, Jankauskas et al. (1989) differentiated them based on vesicle size, defining specimens smaller than 70 µm as *Leiosphaeridia minutissima* and specimens larger than 70 µm as *Leiosphaeridia tenuissima*. The specimen illustrated by Sergeev et al. (2017b, fig. 3.13) as *Leiosphaeridia minutissima* is better identified as *Leiosphaeridia tenuissima* due to its greatest diameter of about 105 µm.

Leiosphaeridia ternata (Timofeev, 1966), Mikhailova and Jankauskas in Jankauskas et al., 1989

Fig. 13.4

1966 *Turuchanica ternata* Timofeev, 1966, Timofeev, p. 45, pl. 9, fig. 8.

1989 *Leiosphaeridia ternata* (Timofeev, 1966), Jankauskas et al.: pl. 11, figs. 2–4; pl. 12, figs. 4–5, 8.

1994 *Leiosphaeridia ternata*; Hofmann and Jackson, p. 26, figs. 17.5–17.7.

1992a *Leiosphaeridia ternata*; Zang & Walter, p. 296, pl. 12, figs. f–i.

1992b *Leiosphaeridia ternata*; Zang & Walter, p. 68, pl. 53, figs. a–e.

1995 *Leiosphaeridia ternata*: Zang, p. 166, figs. 28k, 28l.

1997 *Leiosphaeridia ternata*: Cotter, p. 264, fig. 7j.

2000 *Leiosphaeridia ternata*: Simonetti and Fairchild, p. 21, fig. 8f.

2003 *Leiosphaeridia ternata*; Ragozina et al., p. 57, pl. 2, fig. 1.

2016 *Leiosphaeridia ternata*; Baludikay et al., fig. 8g.

2016 *Leiosphaeridia ternata*; Strother and Wellman, figs. 7a, 7f–g.

2016 *Leiosphaeridia ternata*; Sergeev et al., figs. 4.3–4.4.

2016 *Leiosphaeridia ternata*; Singh and Sharma, p. 80, pl. 1, fig. 11.

2017a *Leiosphaeridia ternata*; Sergeev et al., fig. 3.8.

2017b *Leiosphaeridia ternata*; Sergeev et al., pl. 1, fig. 2.

2017 *Leiosphaeridia ternata*; Javaux & Knoll, p. 211, fig. 4.9.

2017 *Leiosphaeridia ternata*; Beghin et al., pl. 2, fig. k.

2017 *Leiosphaeridia ternata*; Loron and Moczydłowska, p. 12–14, pl. 2, figs. 1–2.

2019 *Leiosphaeridia ternata*; Loron et al., fig. 2e.

2020 *Leiosphaeridia ternata*; Arvestål and Willman, p. 12, fig. 6h.

2020 *Leiosphaeridia ternata*; Shukla et al., p. 503, fig 6h.

2021 *Leiosphaeridia ternata*; Miao et al., p. 15, fig. 3c.

Holotype.—IGD Russian Academy of Sciences No. 169/1, from late Precambrian, Miroedikhinsk series, Turukhansk District (Timofeev, 1966, pl. 9, fig. 8).

Original description by Timofeev (1966) in Russian.—"Толстые грубые уплощенно-сферические оболочки, слабо расчлененные по краям, как правило, на три сегмента. Размеры 50–80 мк. Цвет коричневый."

Original description by Timofeev (1966) translated.—"Thick flat spherical vesicles, slightly dissected along the edges, as a rule, in three segments. Sizes 50–80 microns. Brown color."

Illustrated materials.—CP1020.

Occurrence in the studied sections.—**Rei do Mato section**: MP5176 and MP5178.

Remarks.—Timofeev (1966) described the new species *Turucharica ternata* Timofeev, 1966, also designated a holotype but did not present the diagnosis of this species, only the description. Later on, Mikhailova and Jankauskas in Jankauskas et al., 1989 redesignated *Turucharica ternata* as *Leiosphaeridia ternata* (Timofeev, 1966). They also designated a lectotype for *Leiosphaeridia jacutica*. This lectotype is invalid since Timofeev (1966) had designated a holotype.

6. STRATIGRAPHIC DISTRIBUTION OF THE FOSSIL ASSEMBLAGE

Nine species of organic-walled microfossils were recovered in the four studied sections: 1. Lectostratotype section of the Sete Lagoas Formation, Rei do Mato section; 2. Hypostratotype section Barreiro section; 3. Hypostratotype PRF section; 4. Fercal section. In addition to this assemblage, important occurrences of stromatolites are also reported in all studied sections.

The analysis of 264 samples from the four analyzed sections, 109 of which contained microfossils, yielded a modest diversity assemblage of organic-walled microfossils from the Sete Lagoas Formation, including nine species of five genera:: 1. *Ghoshia januarensis* new species; 2. *Germinosphaera bispinosa* Mikhailova, 1986; 3. *Leiosphaeridia crassa* (Naumova, 1949); 4. *Leiosphaeridia jacutica* (Timofeev, 1966); 5. *Leiosphaeridia minutissima* (Naumova, 1949); 6. *Leiosphaeridia tenuissima* Eisenack, 1958; 7. *Leiosphaeridia ternata* (Timofeev, 1966); 8. *Siphonophycus robustum* (Schopf, 1968); 9. *Bambuites erichsenii* Sommer, 1971. In addition, two morphotypes of stromatolites were also described: ridges and columnar stromatolites, which the last one was classified as *Gymnosolen* sp.

In the lectostratotype section of the Sete Lagoas Formation, Rei do Mato section, 105 stratigraphic levels were studied, of which 30 yielded the recovery of nine organic-walled microfossils species: 1. *Ghoshia januarensis*; 2. *Germinosphaera bispinosa*; 3. *Leiosphaeridia crassa*; 4. *Leiosphaeridia jacutica*; 5. *Leiosphaeridia minutissima*; 6. *Leiosphaeridia tenuissima*; 7. *Leiosphaeridia ternata*; 8. *Siphonophycus robustum*; 9. *Bambuites erichsenii*. *Bambuites erichsenii* has the greatest range of all species recovered in this section, occurring at four stratigraphic levels from 5 m to 71 m. As a minor component of the assemblage of the lectostratotype Rei do Mato section, *Siphonophycus robustum* and *Germinosphaera bispinosa* were recovered in one level only, simultaneously at 34 m, 83 m, and 84 m (Fig. 14). The occurrence of three main species characterizes the basal portion of the section: *Leiosphaeridia minutissima*, *Leiosphaeridia tenuissima*, and *Bambuites erichsenii.* The complete organic-walled assemblage recovered in this study occurs in the lower portion of the Rei do Mato section, between 30 and 89 m. This interval also has the greatest abundance of species and the greatest number of specimens in this section. It comprehends the most diversified interval of all sections studied. In addition to the occurrence of these microfossils, columnar stromatolites are reported in the upper portion of the section.

In the hypostratotype Barreiro section, 79 stratigraphic levels were studied, of which 48 yielded the recovery of seven organic-walled microfossils: 1. *Ghoshia januarensis*; 2. *Germinosphaera bispinosa*; 3. *Leiosphaeridia crassa*; 4. *Leiosphaeridia jacutica*; 5. *Leiosphaeridia minutissima*; 6. *Leiosphaeridia tenuissima*; 7. *Siphonophycus robustum*. *Ghoshia januarensis* has the greatest range of all species recovered in this section, occurring at nine stratigraphic levels from 0.4 m to 57.5 m (Fig. 14). *Leiosphaeridia minutissima* is the longest-ranging sphaeromorph, occurring at 45 stratigraphic levels from the base of the section to 36.4 m.

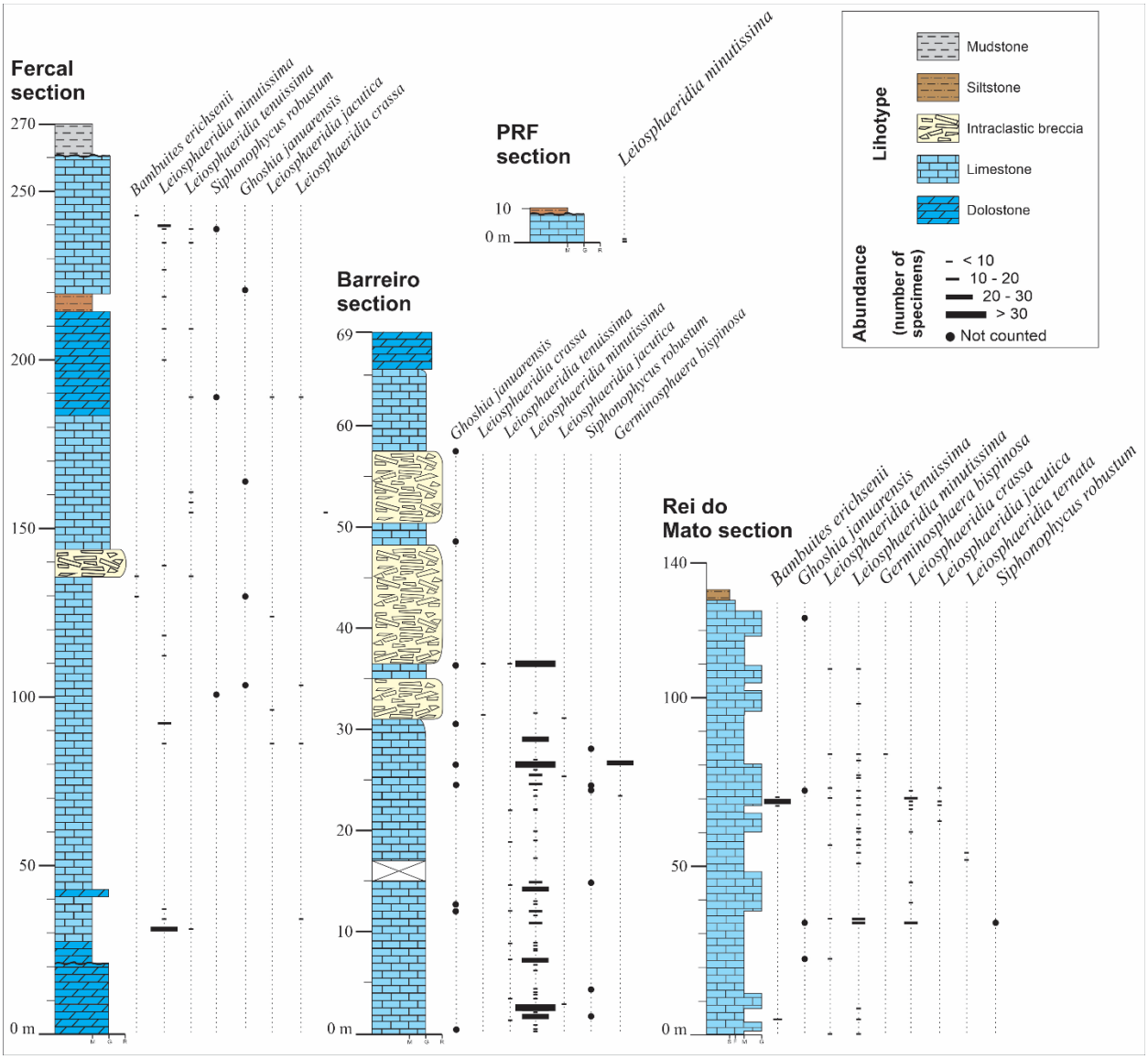

Figure 14: Stratigraphic distribution and relative abundance of organic-walled microfossils from the Sete Lagoas Formation at the studied sections.

With almost the same stratigraphic range as *Leiosphaeridia minutissima* but present only at nine horizons, *Leiosphaeridia tenuissima* ranges from 1.3 to 36.4 m. As a minor component of the assemblage of the Barreiro section, *Leiosphaeridia jacutica* was recovered from three levels in the interval of 2.8–31.5 m, *Leiosphaeridia crassa* from two levels in 31.5–36.4 m, *Germinosphaera bispinosa* from two horizons in 23.5–26.5 m, and *Siphonophycus robustum* from four levels in

1.9–28 m. Except for *Leiosphaeridia crassa* and *Germinosphaera bispinosa*, all other recovered species have their first appearance within 2 m above the base of the studied section, where there is a predominance of mudstone limestone. *Leiosphaeridia crassa* and *Germinosphaera bispinosa* first emerge in the middle part of the section below the intraclastic breccia beds.

The disappearance of organic-walled microfossils in the Barreiro section is gradual, although three species (*Leiosphaeridia crassa*, *Leiosphaeridia minutissima*, and *Leiosphaeridia tenuissima*) disappear at approximately 37 m. No organic-walled microfossils other than *Ghoshia januarensis* were recovered above 37 m. The disappearance of organic-walled microfossils is likely related to taphonomic and environmental factors. The greater abundance of intraclastic breccias in the upper portion of the sampled section is not conducive to fossil preservation. These breccias may also indicate a greater influence of storm activities in shallower environments relative to the thinly bedded limestone in the lower part of the sampled section. These taphonomic and environmental changes may have selectively affected the abundance of organic-walled microfossils other than *Ghoshia januarensis*. In addition, microbial ridges were described in this section.

In the Fercal section, eight organic-walled microfossils species were recovered: 1. *Ghoshia januarensis*; 2. *Bambuites erichsenii*; 3. *Leiosphaeridia crassa*; 4. *Leiosphaeridia jacutica*; 5. *Leiosphaeridia minutissima*; 6. *Leiosphaeridia tenuissima*; 7. *Siphonophycus robustum*. *Leiosphaeridia minutissima* and *Leiosphaeridia tenuissima* have the greatest range of all species recovered in this section, occurring from 32.8 m to ~ 242 m (Fig. 14). The minor components of the assemblage of the Fercal section have their occurrences restricted to three levels: *Bambuites erichsenii* at 131.875, 137.85, and 245.1, *Leiosphaeridia jacutica* at 88.2, 125.85, and 191.1, and *Siphonophycus robustum* at 102.7, 191.1, and 241.1. *Ghoshia januarensis* ranges from 105.5 to 223.1, while *Leiosphaeridia crassa* occurs from 36.6 to 191.1. The basal portion of the section is

characterized by the occurrence of three main species: *Leiosphaeridia minutissima*, *Leiosphaeridia tenuissima*, and *Leiosphaeridia crassa*. The middle levels are represented by the assemblage from the lower level plus the occurrence of *Leiosphaeridia ternata*, *Ghoshia januarensis*, *Leiosphaeridia jacutica*, *Bambuites erichsenii*, and *Siphonophycus robustum*. The upper portion of the Fercal section is characterized by the occurrence of the species listed above, except by *Leiosphaeridia jacutica* and *Leiosphaeridia crassa*. In addition to the occurrence of organic-walled microfossils, columnar stromatolites are reported in the upper portion of this section, identified as *Gymnosolen* sp.

Among the four studied sections, the one with more reduced exposition is the hypostratotype PRF section. With almost five meters of exposition, the hypostratotype PRF section is restricted to the occurrence of two levels of *Leiosphaeridia minutissima*, at 0.45 m and 0.6 m, and to the occurrence of *Gymnosolen* sp., columnar stromatolites throughout the carbonate rocks. Of the nine organic-walled microfossil species, only *Leiosphaeridia minutissima* occurs in all four studied sections, while *Leiosphaeridia ternata* is exclusive of the lectostratotype Rei do Mato section.

Table 2: Fossiliferous occurrences in the studied sections. Due to their colonial nature or frequent preservation as fragments, the abundance of *Siphonophycus robustum* and *Ghoshia januarensis* was not quantified.

Species	**Fossiliferous occurrences**			
	Barreiro section	Fercal Section	Rei do Mato section	PRF section
Leiosphaeridia minutissima	359 specimens	89 specimens	87 specimens	4 specimens
Ghoshia januarensis	Present	Present	Present	Absent
Leiosphaeridia crassa	14 specimens	9 specimens	45 specimens	Absent
Leiosphaeridia jacutica	4 specimens	4 specimens	5 specimens	Absent
Leiosphaeridia tenuissima	14 specimens	13 specimens	10 specimens	Absent
Germinosphaera bispinosa	23 specimens	Absent	1 specimen	Absent
Siphonophycus robustum	Present	Present	Present	Absent
Leiosphaeridia ternata	Absent	Absent	3 specimens	Absent
Bambuites erichsenii	Absent	Present	Present	Absent
Gymnosolen sp.	Absent	Present	Present	Present

7. BIOSTRATIGRAPHY

Of all four sections of the Sete Lagoas Formation approached in this study, the only one with lower and upper boundaries is the Fercal section, which is located in Brasília, Federal District. The studied sections at Sete Lagoas Municipality, the lectostratotype Rei do Mato section and the hypostratotype PRF section, comprise only the upper boundary of the Sete Lagoas Formation The hypostratotype Barreiro section in Januária Municipality, Minas Gerais State, lacks both the lower and upper boundaries of the Sete Lagoas Formation. After the taxonomic analysis, a first detailed biozonation for the Sete Lagoas Formation is herein proposed.

7.1. Biostratigraphic zoning

The succession of two biostratigraphic units is recognized based on organic-walled microfossils: 1. *Leiosphaeridia minutissima* Zone (Lm), and 2. *Bambuites erichsenii* Zone (Be):

***Leiosphaeridia minutissima* Zone, interval of lowest occurrence**

Stratotype.—Fercal section (Fig. 3), from level 32.8 m until level 131.85 m (Fig. 9).

Index species.—Leiosphaeridia minutissima.

Description.—The *Leiosphaeridia minutissima* Zone is a lowest occurrence interval zone. The lower and upper boundaries are defined by the first occurrences of *Leiosphaeridia minutissima* and *Bambuites erichsenii*, respectively. Seven species occur in this zone: 1. *Leiosphaeridia crassa*, 2. *Leiosphaeridia jacutica*, 3. *Leiosphaeridia tenuissima*, 4. *Leiosphaeridia minutissima*, which name this zone, 5. *Ghoshia januarensis*, 6. *Siphonophycus robustum*, and 7. *Germinosphaera bispinosa*. The stratotype is characterized mainly by a sequence of mudstone limestones.

Type Locality.—Fercal quarry, Brasília, Federal District, Brazil.

Remarks.—Zone recognized in the stratotype Fercal section, Barreiro and Rei do Mato sections (Fig. 15).

Bambuites erichsenii Zone, range

Stratotype.—Fercal section (Fig. 3), from level 131.85 m until level 245.1 m (Fig. 9).

Index species.—*Bambuites erichsenii*.

Description.—The *Bambuites erichsenii* Zone is a range zone in which the lower and upper boundaries are defined by the first and last occurrence of *Bambuites erichsenii*. Nine species occur in this zone: 1. *Ghoshia januarensis;* 2. *Germinosphaera bispinosa;* 3. *Leiosphaeridia crassa;* 4. *Leiosphaeridia jacutica;* 5. *Leiosphaeridia minutissima;* 6. *Leiosphaeridia tenuissima;* 7. *Leiosphaeridia ternata;* 8. *Siphonophycus robustum;* 9. *Bambuites erichsenii*, which name this zone. The stratotype of this zone is characterized by a sequence of intraclastic limestone breccia, followed by mudstones limestones, siltstones, grainstone dolostones, and grainstone limestones.

Type Locality.—Fercal quarry, Brasília, Federal District, Brazil.

Remarks.—Zone recognized in the stratotype Fercal section and the Rei do Mato section (Fig. 15).

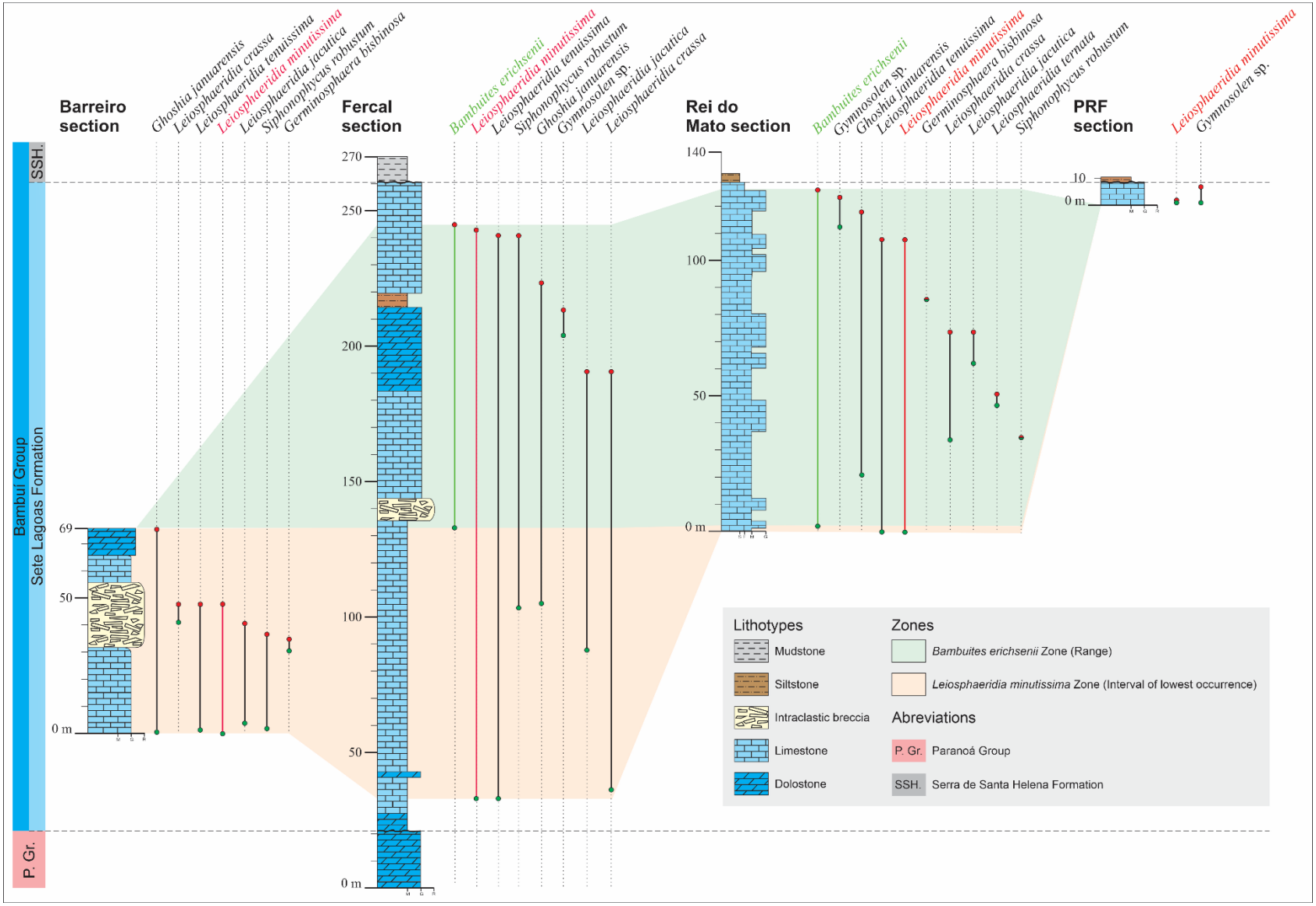

Figure 15: Lithostratigraphic logs of the lectostratotype section of the Sete Lagoas Formation, Rei do Mato section, the hypostratotypes sections of the Barreiro and PRF sections, and the Fercal section with fossiliferous occurrences and biostratigraphic zones.

Seven out of nine organic-walled microfossils from the Sete Lagoas Formation recorded in this work have wide stratigraphic ranges when global data are considered, i.e., *Leiosphaeridia crassa*, *Leiosphaeridia jacutica*, *Leiosphaeridia minutissima* and *Leiosphaeridia tenuissima* range from the Mesoproterozoic to the Cambrian (Grey, 2005), and *Leiosphaeridia ternata* has the wider range, from Paleoproterozoic to Cambrian (Shukla et al., 2020). *Germinosphaera bispinosa* and *Siphonophycus robustum* are known from the late Paleoproterozoic to the Paleozoic (Butterfield et al., 1994; Sergeev et al., 2012; Miao et al., 2019) (Fig. 16).

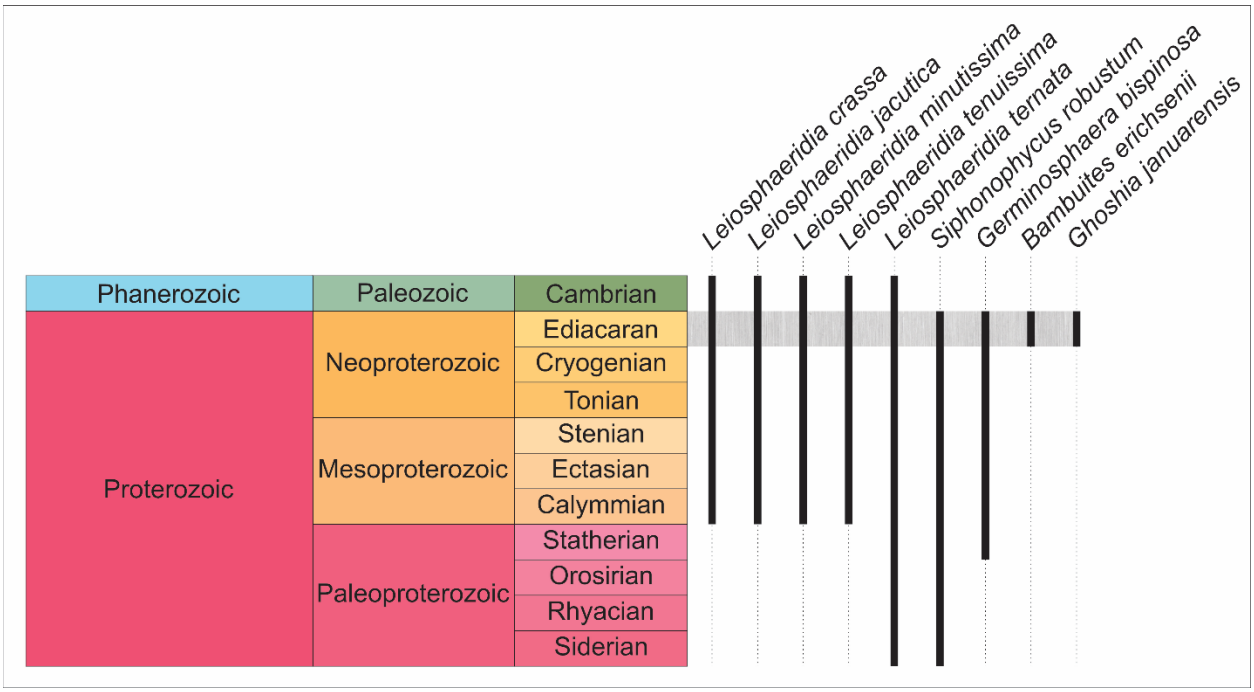

Figure 16: Chronostratigraphic distribution of the organic-walled species recovered from the Sete Lagoas Formation, Bambuí Group, Brazil (Butterfield et al., 1994; Grey, 2005; Sergeev et al., 2012; Javaux and Knoll, 2017; Miao et al., 2019; Shukla et al., 2020).

Nevertheless, *Ghoshia januarensis* and *Bambuites erichsenii* have additional occurrences only in Tamengo Formation, Corumbá Group, restricted to the upper Ediacaran (Adôrno, 2019). In this lithostratigraphic interval of the Tamengo Formation, these two organic-walled species

occur associated with occurrences of *Cloudina lucianoi* and *Corumbella werneri*. This association of *Ghoshia januarensis* and *Bambuites erichsenii* distribution and the appearance of basal mineralized invertebrates are evidence of their chronostratigraphic position in the upper Ediacaran (Fig. 16).

7.2. Other proxies from the Sete Lagoas Formation

Proxies for chronostratigraphic studies from the Sete Lagoas Formation include geochronological and paleontological data. Carbonates of the lower portion of Sete Lagoas Formation yielded Pb-Pb ages of ~740 ± 22 Ma, Tonian/Cryogenian (Babinski et al., 2007). Nevertheless, Caxito et al. (2021) analyzed samples from crystal-fan-bearing limestone from the base of the Sete Lagoas Formation. The ages obtained with U-Pb data by Caxito et al. (2021) yielded lower intercept dates of 615.4 ± 5.9 Ma, when both the crystal-fans and matrix were analyzed together, 608.1 ± 5.1 Ma for crystal-fans, and 607.2 ± 6.2 Ma for the matrix. The conflict between the data published by Caxito et al. (2021) and the ~740 Ma Pb-Pb age from the Sete Lagoas Formation (Babinski et al., 2007) remains under debate. The youngest population of detrital zircons from the Sete Lagoas Formation gave U-Pb ages of ~557 Ma (Paula-Santos et al., 2015). Caxito et al. (2021) also analyzed the topmost strata of this unit within dark stromatolitic carbonates and yielded a 566 ± 15 Ma U–Pb date. Caxito et al. (2021) suggest a ca. 20 Ma hiatus or a stratigraphic condensed deposition to explain the different ages between the basal and upper portion of the Sete Lagoas Formation. In addition, the occurrences of *Cloudina* sp. and *Corumbella werneri* in the lower Sete Lagoas Formation (Warren et al., 2014; Perrella Júnior et al., 2017), tubular fossils typically found in terminal Ediacaran rocks, also indicate an Ediacaran age for this unit.

In addition to the data mentioned above, the youngest population of detrital zircons from the Três Marias Formation gave U-Pb ages of ~620 Ma (Pimentel et al., 2011; Rodrigues, 2008), providing maximum age constraints on the host strata. Furthermore, a zircon U–Pb age of 520.2 ± 5.3 Ma has been reported from a volcanic ash bed in the Serra da Saudade Formation (Moreira et al., 2020b), suggesting that the upper Bambuí Group may be already Cambrian. Furthermore, occurrences of *Treptichnus pedum*, a trace fossil whose first appearance is used to define the base of the Cambrian System, were reported in the Três Marias Formation (Sanchez et al., 2021). Based on this geochronological and paleontological evidence, the entire Bambuí Group is Ediacaran–Cambrian in age.

7.3. Correlation and remarks

Leiospheres (sphaeromorphs) have wide stratigraphic ranges and limited applicability as a global biostratigraphic toll, which can make correlations with chronobiostratigraphic significances based on leiosphere zones a difficult task. For example, Grey (2005) established the Ediacaran Leiosphere-dominated Palynoflora (ELP), represented by the *Leiosphaeridia jacutica* - *Leiosphaeridia crassa* Assemblage Zone, lower Ediacaran. Later on, Gaucher and Sprechmann (2009) renamed the ELP designated by Grey (2005) as Early Ediacaran Leiosphere Palynoflora (EELP) (Fig. 17).

Considering Gaucher and Sprechmann (2009), this palynoflora EELP is dominated by large sphaeromorphs, which comprise leiosphaerids (> 200 µm). The great size of the acritarchs of this assemblage could be a response to a eukaryotic plankton recovery from the late Cryogenian environmental changes. The EELP is regarded as a lower Ediacaran acritarch assemblage (ca. 635–580 Ma) (Fig. 17).

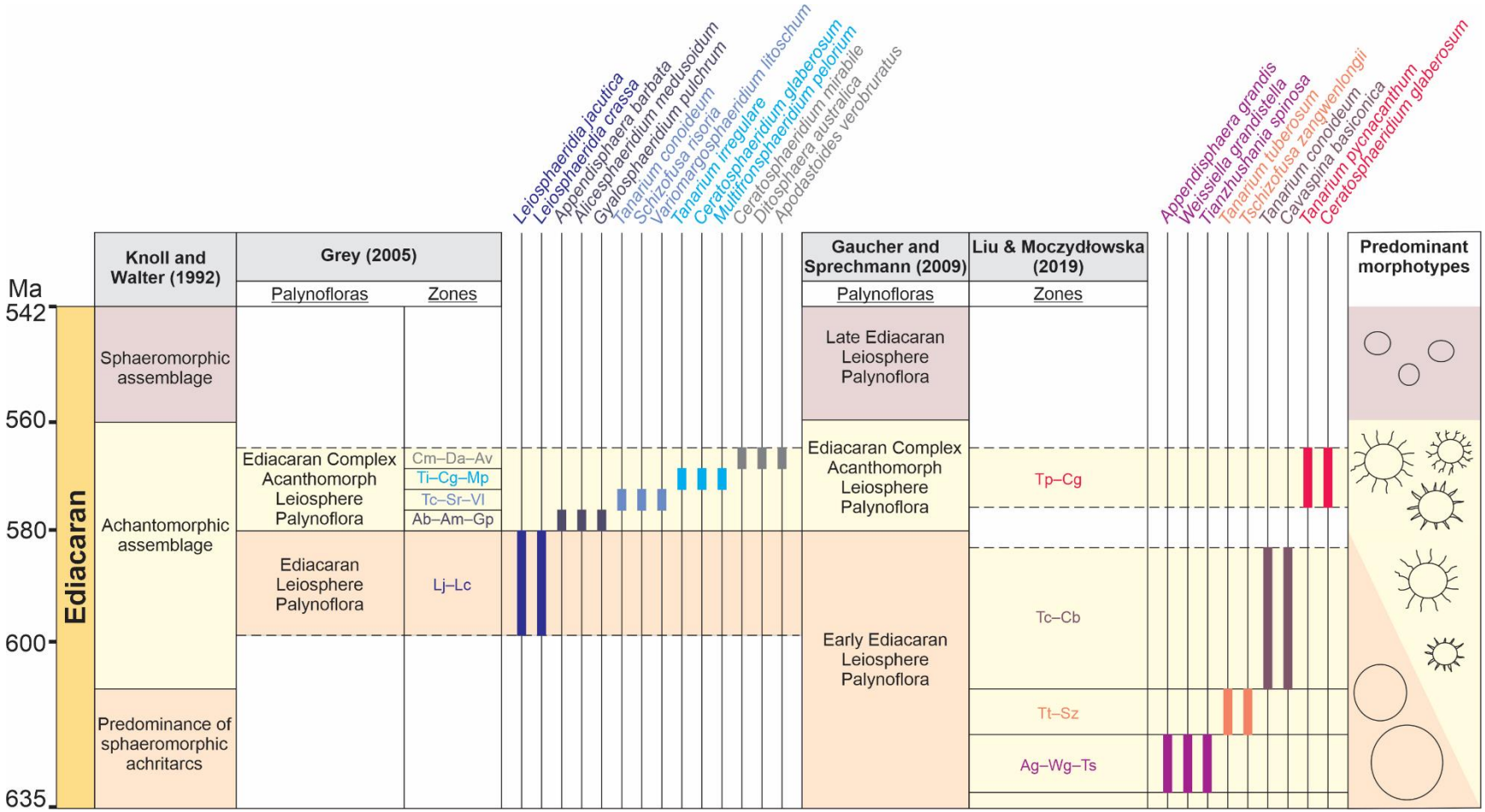

Figure 17: Ediacaran acritarch assemblages (data extracted from Knoll and Walter (1992), Grey (2005), Gaucher and Sprechmann (2009), and Liu and Moczydłowska (2019). All recognized biostratigraphic units by Grey (2005) and Liu and Moczydłowska (2019) are assemblage zones. Zones abbreviations correspond to the species which characterize each zone.

In contrast to the data of the predominance of sphaeromorphs in the lower Ediacaran (Grey, 2005; Gaucher and Sprechmann, 2009), studies from South China recovered abundant and diverse acanthomorphic acritarchs from lower Ediacaran strata (Zhou et al., 2007; Liu and Moczydłowska, 2019; Ouyang et al., 2021). Liu and Moczydłowska (2019) recognized three acanthomorphs assemblage zones in the lower Ediacaran from China: 1. Zone *Appendisphaera grandis – Weissiella grandistella – Tianzhushania spinosa*, 2. Zone *Tanarium tuberosum – Schizofusa zangwenlongii*, and 3. Zone *Tanarium conoideum – Cavaspina basiconica*, all of them refered as assemblage zones. These occurrences indicate that the Ediacaran Leiosphere Palynoflora of Grey (2005), renamed Early Ediacaran Leiosphere Palynoflora by Gaucher and Sprechmann (2009), could be controlled by local environments, regional biogeography, or taphonomic factors.

It is perceived that the terminal Ediacaran (ca. 550-539 Ma) is characterized by a leiosphere assemblage (Knoll and Walter, 1992; Gaucher and Sprechmann, 2009) (Fig. 17). Gaucher and Sprechmann (2009) presented the Late Ediacaran Leiosphere Palynoflora, which is a low-diversity assemblage characterized by smaller sphaeromorphs (< 150 µm) such as *Leiosphaeridia minutissima*, *Leiosphaeridia tenuissima*, among others (Fig. 17). In addition, there are also occurrences of *Chuaria circularis*, as well as *Bavlinela faveolata*, *Soldadophycus bossii*, and small acanthomorphs, such as *Asteridium* spp. The Late Ediacaran Leiosphere Palynoflora, sensu Gaucher and Sprechmann (2009), has been documented in the Nama Group in Namibia (Germs et al., 1986), the Holgat Formation of the Port Nolloth Group in Namibia (Gaucher et al., 2005a), the Mulden Group in Namibia (Gaucher and Germs, 2007), the Tent Hill Formation in Australia (Damassa and Knoll, 1986), Cijara Formation in Spain (Palacios, 1989), the Cango Caves and Gamtoos groups in South Africa (Gaucher and Germs, 2006), the Dengying Formation in South China (Yin and Yuan, 2007), the Arroyo del Soldado Group in Uruguay (Gaucher, 2000; Gaucher

et al., 2003), the Sierras Bayas Group in Argentina (Cingolani et al., 1991; Gaucher et al., 2005b), the La Providencia Group in Argentina (Arrouy et al., 2019), and the Corumbá Group in Brazil (Zaine, 1991; Gaucher et al., 2003; Tobias, 2014). In Namibia, Argentina, Uruguay and Brazil (Germs et al., 1986; Gaucher et al., 2003, 2005b; Tobias, 2014), the Late Ediacaran Leiosphere Palynoflora occurs associated with tubular fossils such as the invertebrates *Cloudina lucianoi* (Beurlen and Sommer, 1957), *Cloudina riemkeae* Germs, 1972, and *Corumbella werneri* Hahn et al., 1982, considered index fossils for the late Ediacaran.

Based on the predominance of small leiospheres in the Sete Lagoas Formation from the studied sections (< 150 µm) (Fig. 18), it is possible to consider the position of the *Bambuites erichsenii* Zone in the Late Ediacaran Leiosphere Palynoflora (Fig. 19). While the *Bambuites erichsenii* Zone would be restricted to the upper Ediacaran, it is tempting to consider that the *Leiosphaeridia minutissima* Zone extends to lower chronostratigraphic units.

Besides the predominance of small specimens of *Leiosphaeridia* spp. and considering the divergent geochronological dating of the lower portions of the Sete Lagoas Formation, the *Leiosphaeridia minutissima* Zone could extend to the lower/mid Ediacaran, based on Paula-Santos et al. (2015) and Caxito et al. (2021), or even to the Tonian/Cryogenian if the data of Babinski et al. (2007) is considered (Fig. 19).

Indeed, *Leiosphaeridia minutissima* has a wide stratigraphic range with occurrences from Mesoproterozoic to Cambrian (Grey, 2005) (Fig. 16). Considering that the lower boundary of the *Leiosphaeridia minutissima* Zone is marked by the first occurrence of *Leiosphaeridia minutissima* after the cap carbonate in the Sete Lagoas Formation, the global range of this species would imply an older geochronological interval for the zone. The micropaleontological analyses of the cap carbonate herein studied include the Fercal section, which led no fossiliferous recovery. So, further

detailed micropaleontological studies of the cap carbonate of the Sete Lagoas Formation are strongly recommended in order to evaluate biodiversity and biostratigraphic signature for a better age constraint of the lower boundary of the *Leiosphaeridia minutissima* Zone.

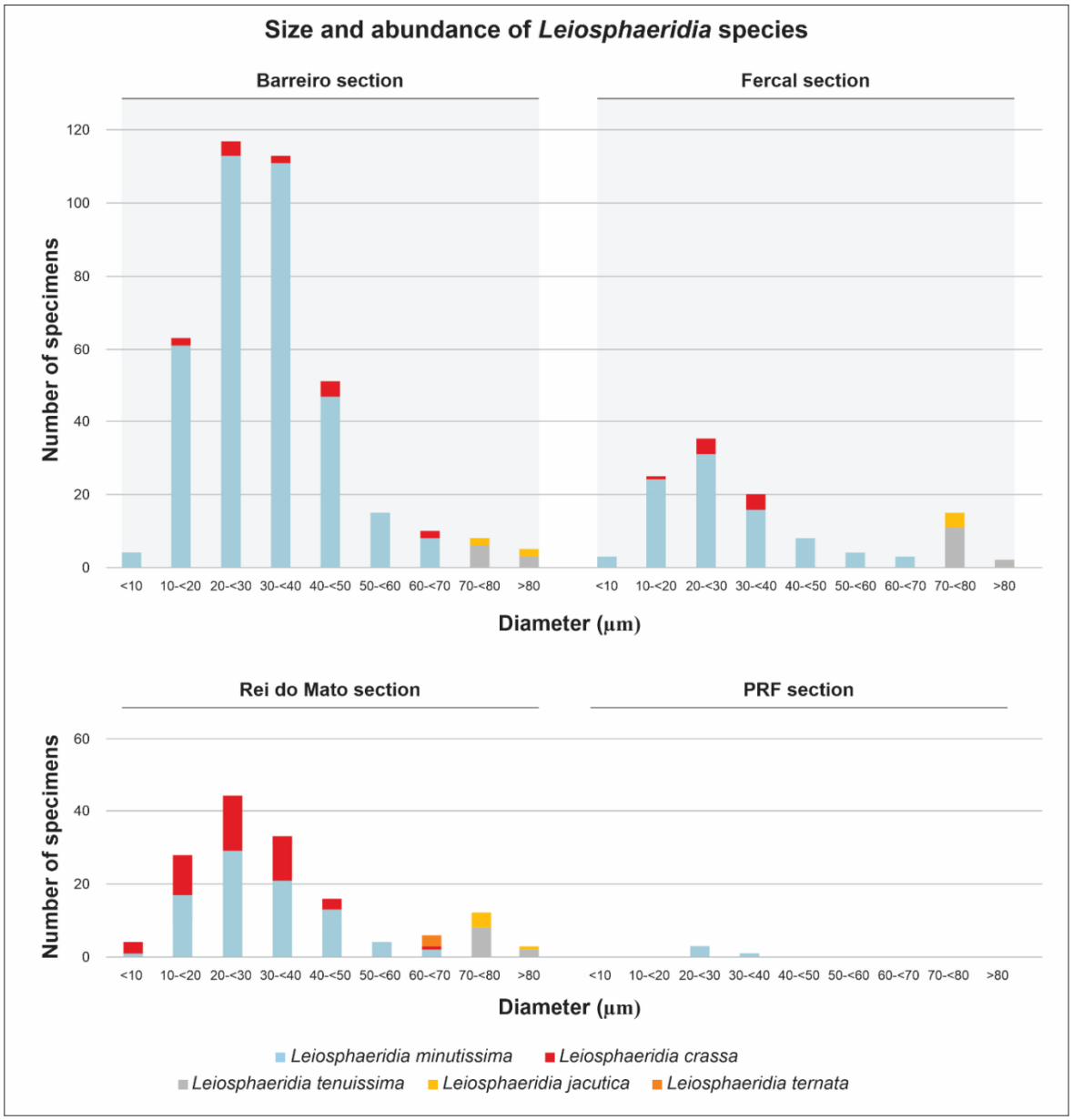

Figure 18: Abundance and size distribution of *Leiosphaeridia* species from the studied sections comprising both biostratigraphic unities: *Leiosphaeridia minutissima* Zone and *Bambuites erichsenii* Zone.

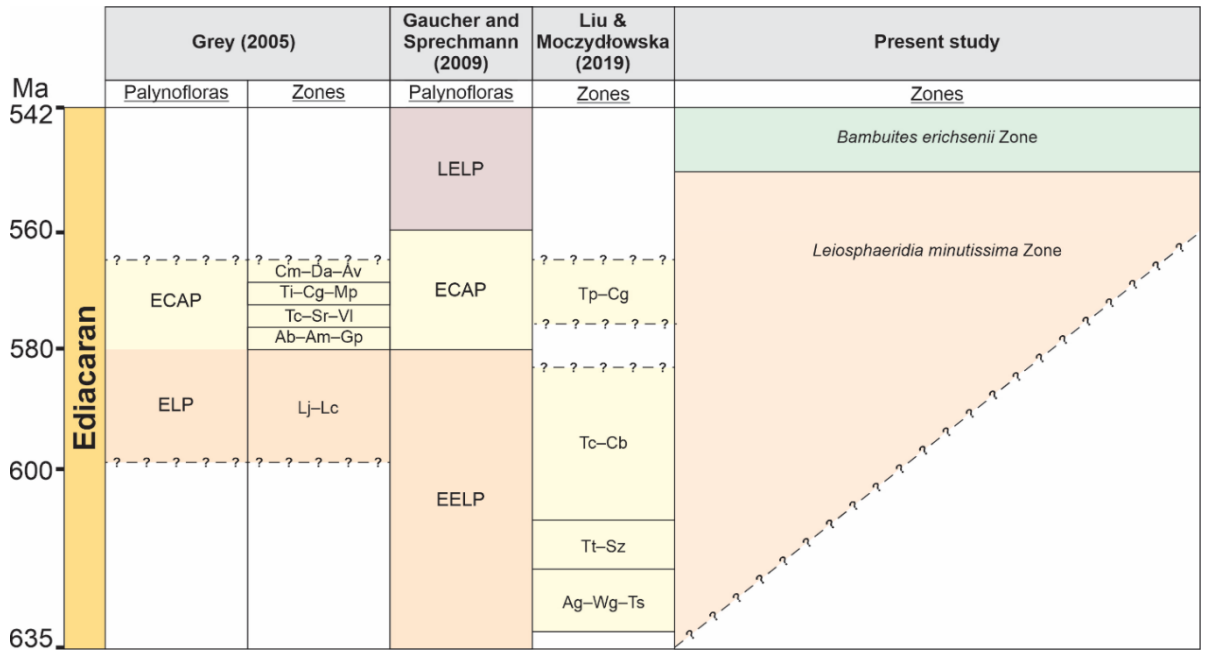

Figure 19: Simplified chart of zones identified in the Ediacaran Period. Lm: *Leiosphaeridia minutissima* Interval of Lowest Occurrence Zone, Be: *Bambuites erichsenii* Range Zone (see figure 14 for other abbreviations).

Additionally, carbon isotope studies of three out of the four studied sections have shown fluctuations throughout the Sete Lagoas Formation (Vieira et al., 2007; Carvalho, 2018; Okubo et al., 2022). When these isotopic data are integrated into the biozones presented herein, a most robust subdivision of the Sete Lagoas Formation can be accessed (Fig. 20). Two $\delta^{13}C$ signatures can be observed within the *Leiosphaeridia minutissima* Zone, from bottom to top: 1. Bottom - a negative signature with $\delta^{13}C$ values ranging from -3.8‰ to -0.33‰; 2. Top - a lower positive signature with $\delta^{13}C$ values ranging from +0.09‰ to +3.64‰. Two $\delta^{13}C$ signatures can also be recognized within the *Bambuites erichsenii* Zone, from bottom to top: 1. Bottom – a lower positive signature with $\delta^{13}C$ ranging from +0.73‰ to +3‰; 2. Top – greater positive $\delta^{13}C$ values ranging from +4.94‰ to +8.96‰ (Fig. 20). As it was possible to see, the biostratigraphic data integrated with the chemostratigraphic ones could be a good parameter to refine the subdivision of the Sete Lagoas

Formation. In order to evaluate this integrated correlation, further isotopic analyses from the Rei do Mato section is planned for the future.

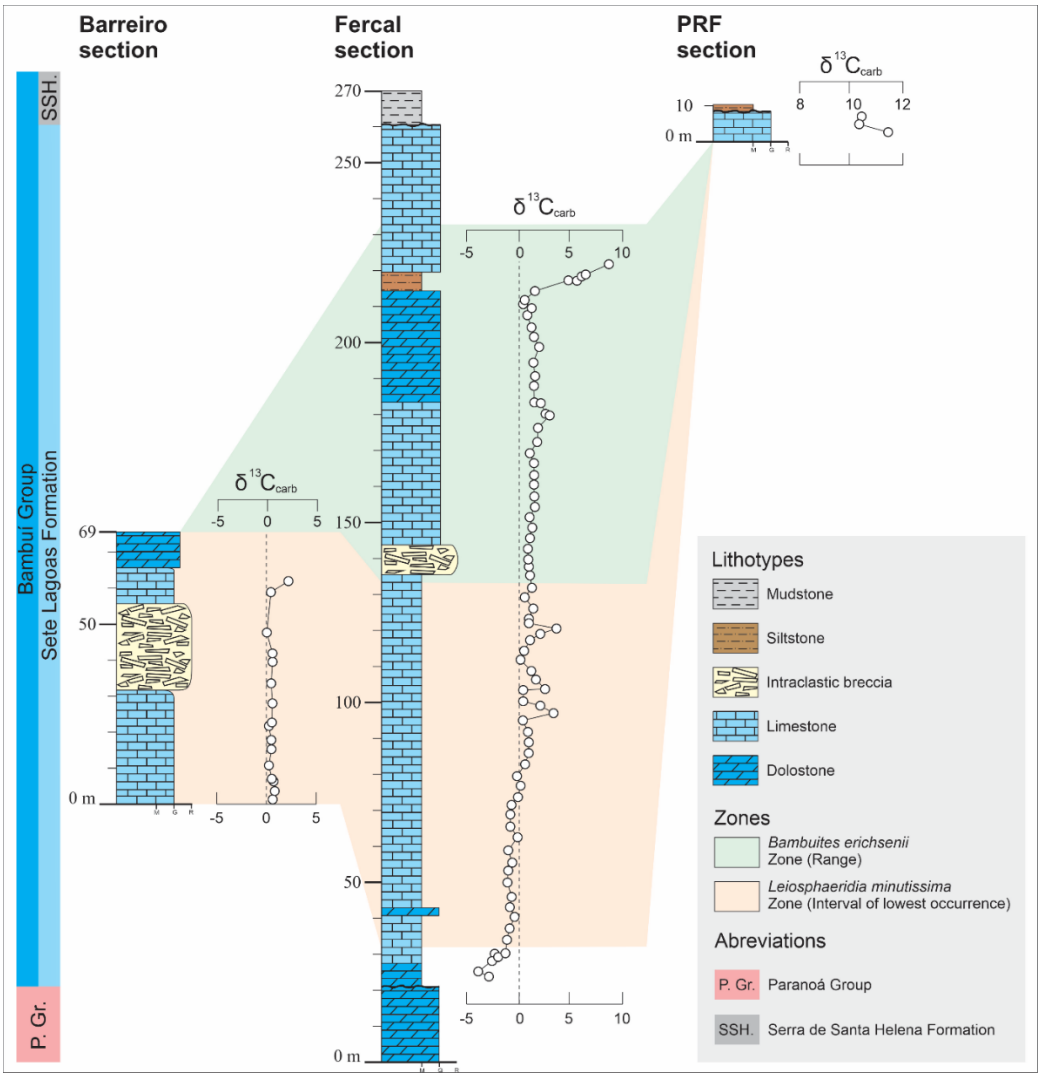

Figure 20: Stratigraphic sections of the Sete Lagoas Formation coupled with $\delta^{13}C$ profiles. Isotopic values are in ‰. Isotopic data extracted from: Barreiro section (Okubo et al., 2022), Fercal section (Carvalho, 2018), PRF section (Vieira et al., 2007).

To conclude, the succession of *Leiosphaeridia minutissima* and *Bambuites erichsenii* zones are useful tools for a subdivision of the Sete Lagoas Formation in two chronostratigraphic interval, respectively lower/mid Ediacaran and upper Ediacaran. Despite the hiatus or the stratigraphic

condensed deposition between basal cap carbonate and the rest of the Sete Lagoas Formation, the assemblage distribution throughout the studied sections denote a continuous deposition along the fossiliferous levels, which comprises the deposition after the cap carbonate. Both biostratigraphic zones are independent of chemostratigraphy, chronostratigraphy, and lithostratigraphy studies but can be correlated to refine their significance. So, it is possible to note for *Leiosphaeridia minutissima* Zone a variation of negative to moderately positive $\delta^{13}C$ signature. For the *Bambuites erichsenii* Zone, it is possible to highlight the variation of lower positive values of $\delta^{13}C$ signature in the base of the zone with a remarkable shift in the upper portion, achieving ~ +12‰.

Based on the predominance of small leiospheres in the Sete Lagoas Formation and the previous radiometric data, with the maximum age constraint of ~ 557 Ma provided by detrital zircons from this unit, so, the *Bambuites erichsenii* Zone is positioned in the upper Ediacaran. For the *Leiosphaeridia minutissima* Zone, it is possible to suggest a lower/mid Ediacaran interval based on U-Pb age constraint of 615.4 ± 5.9 Ma for the cap carbonate. Besides this U-Pb data, the Pb-Pb dating of ~740 Ma for the same interval is tempting to consider even older than Ediacaran. Considering this, it is strongly recommended to expand geochronological analyses in the studied sections in order to date these lithostratigraphic intervals and refine their chronostratigraphic significance.

8. PALEOENVIRONMENTAL AND PALEOGEOGRAPHIC APPROACH

All nine identified organic-walled species are related to marine paleoenvironment of the Sete Lagoas Formation. Seven out of nine are possibly marine planktic: *Leiosphaeridia ternata, Leiosphaeridia crassa, Leiosphaeridia jacutica, Leiosphaeridia minutissima, Leiosphaeridia tenuissima, Bambuites erichsenii*, and *Germinosphaera bispinosa*. Five *Leiosphaeridia* species

recovered herein and *Bambuites erichsenii* are tentatively considered protists. *Ghoshia januarensis* and *Siphonophycus robustum* are probably photosynthetic benthic species assigned to cyanobacteria. *Germinosphaera bispinosa* lacks biological affinity. The occurrences of stromatolites identified as *Gymnosolen* sp. corroborate the interpretation of an internal carbonate ramp paleoenvironment influenced by wave/tide.

The paleogeographic evolution from Ediacaran to Cambrian periods has been improved due to the growing number of stratigraphic, geochronological, paleontological, and paleomagnetic investigations. The São Francisco paleogeographic location is usually analyzed based on examination of the joint paleomagnetic results with the Congo craton due to the inferred common history between these cratons throughout the Proterozoic (Tohver et al., 2006; Caxito et al., 2021; Trindade et al., 2021).

Tohver et al. (2006) conducted an evaluation of the Rodinia and Gondwana paleogeographic inferences based on previously published data. This review was focused on the paleomagnetic record of Africa and South America for the 1200–500 Ma interval. The São Francisco craton data analyzed by Tohver et al. (2006) comprised paleomagnetic, rock magnetic, and Pb isotopic data from previous studies (D'Agrella-Filho et al., 2000; Trindade et al., 2004).

For the 600–525 Ma interval, it was possible to track the cratons until the construction of western Gondwana. Tohver et al. (2006) suggested a two-stage collisional event. The first phase took place sometime around 550–580 Ma when Kalahari, São Francisco–Congo, and Arabian–Nubian cratons appear to have converged and collided, whereas the Amazonia–West Africa convergence with paleomagnetic poles from the other cratons is observed only at ca. 520 Ma (Tohver et al., 2006) (Fig. 21).

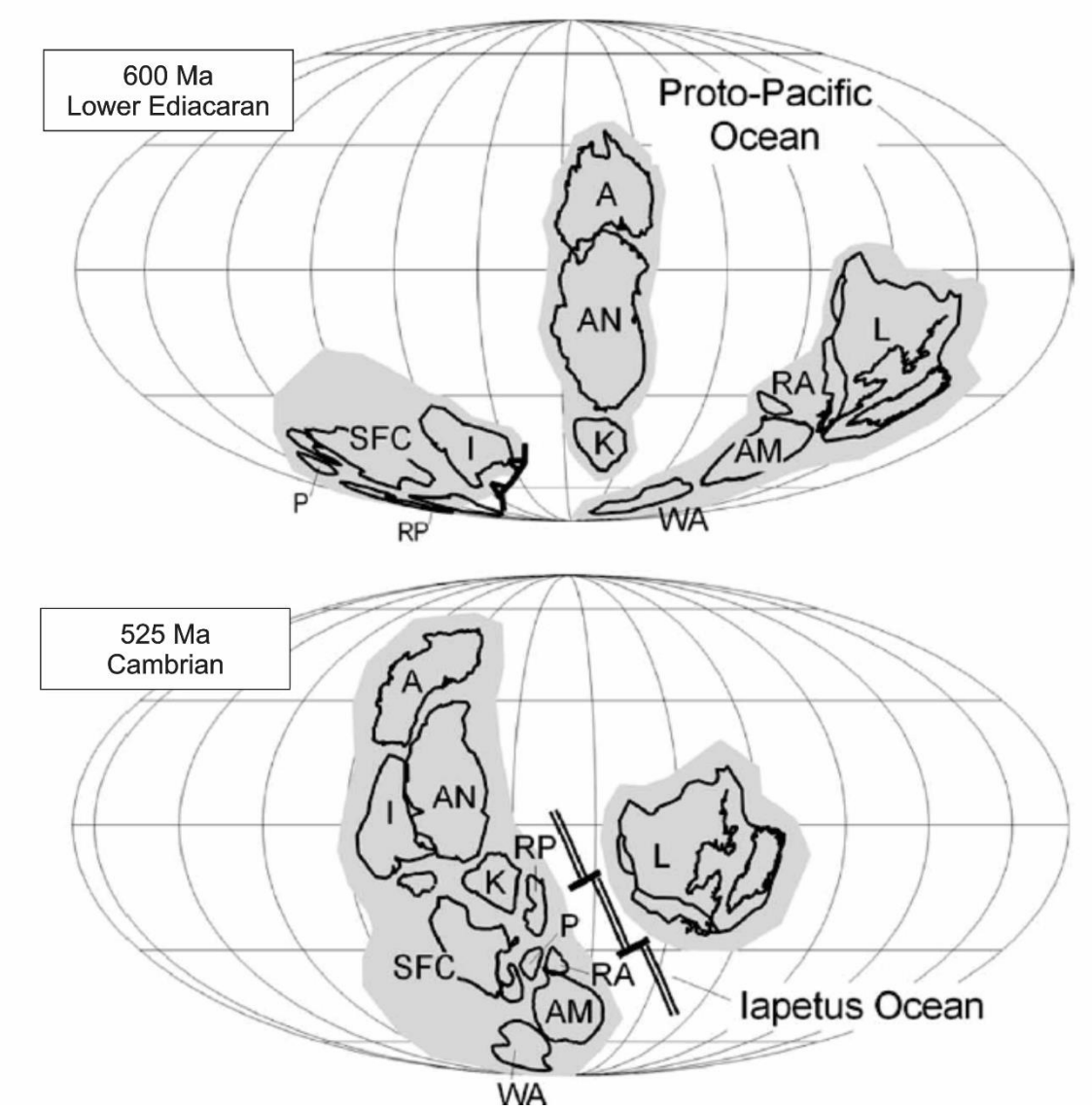

Figure 21: Paleogeographic reconstructions based on the paleomagnetic data reviewed by Thover et al. (2006): break-up along the western margin of Laurentia by 600 Ma and construction of West Gondwana (extracted from Tohver et al., 2006).

Moreover, Caxito et al. (2021) bring new radiometric U–Pb data from carbonate dating with elemental and isotope constraints to integrate orogenic evolution in western Gondwana. Caxito et al. (op. cit.) showed that the deposition of the Bambuí Group coincides with the closure of the Goiás-Pharusian (630–600 Ma) and Adamastor (585–530 Ma) oceans, followed by the collision of the Amazon craton with the closure of the Clymene ocean (540–500 Ma), eventually restricting

the São Francisco basin from open ocean connection (Fig. 22). On the other hand, Trindade et al. (2021) do not exclude the possibility of an early (650–600 Ma) collision of the Amazon craton due to the scarcity of paleomagnetic poles for these intervals. Further studies encompassing paleomagnetism, geochronological and paleontological analyses are needed to better understand the geodynamic scenarios of the western Gondwana amalgamation and when the collisional phases occurred.

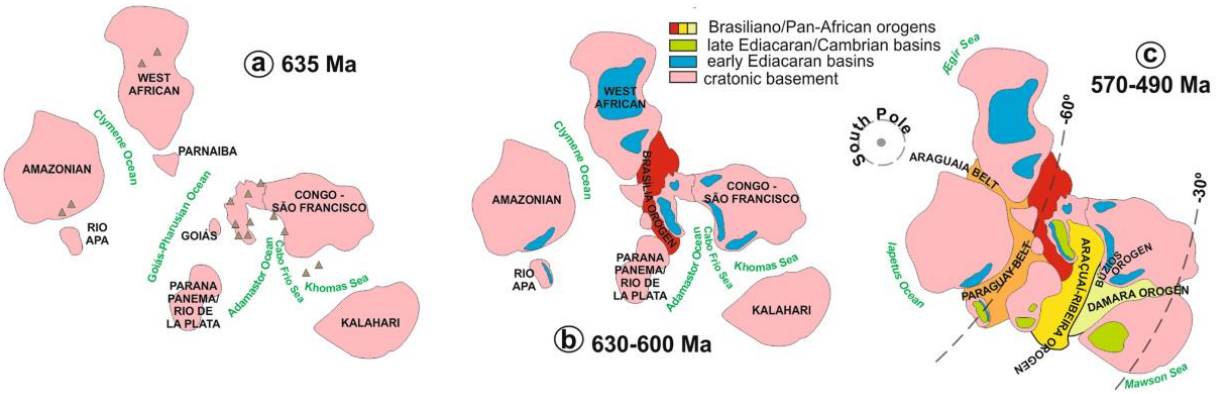

Figure 22: Integrated evolution from Ediacaran to Cambrian orogens and basins in western Gondwana by Caxito et al. (2021). Obs.: **a)** early Ediacaran; **b)** early-mid Ediacaran; **c)** late Ediacaran-Cambrian.

Occurrences of *Cloudina lucianoi, Cloudina carinata, Cloudina riemkeae, Gordia marina, Corumbella werneri*, and *Namacalathus hermanastes* were plotted in the paleogeographic map of the Proto-Gondwana in ~550 Ma (Warren et al., 2017; Adôrno, 2019). It is important to highlight that the update on the paleogeographic map presented is related to the use of taxonomy at the species level. This approach on paleobiogeographic distribution in which the occurrences of those invertebrate species show a cosmopolitan distribution encompassing several oceans and interior seas surrounding low latitude paleocontinents (Fig. 23.1).

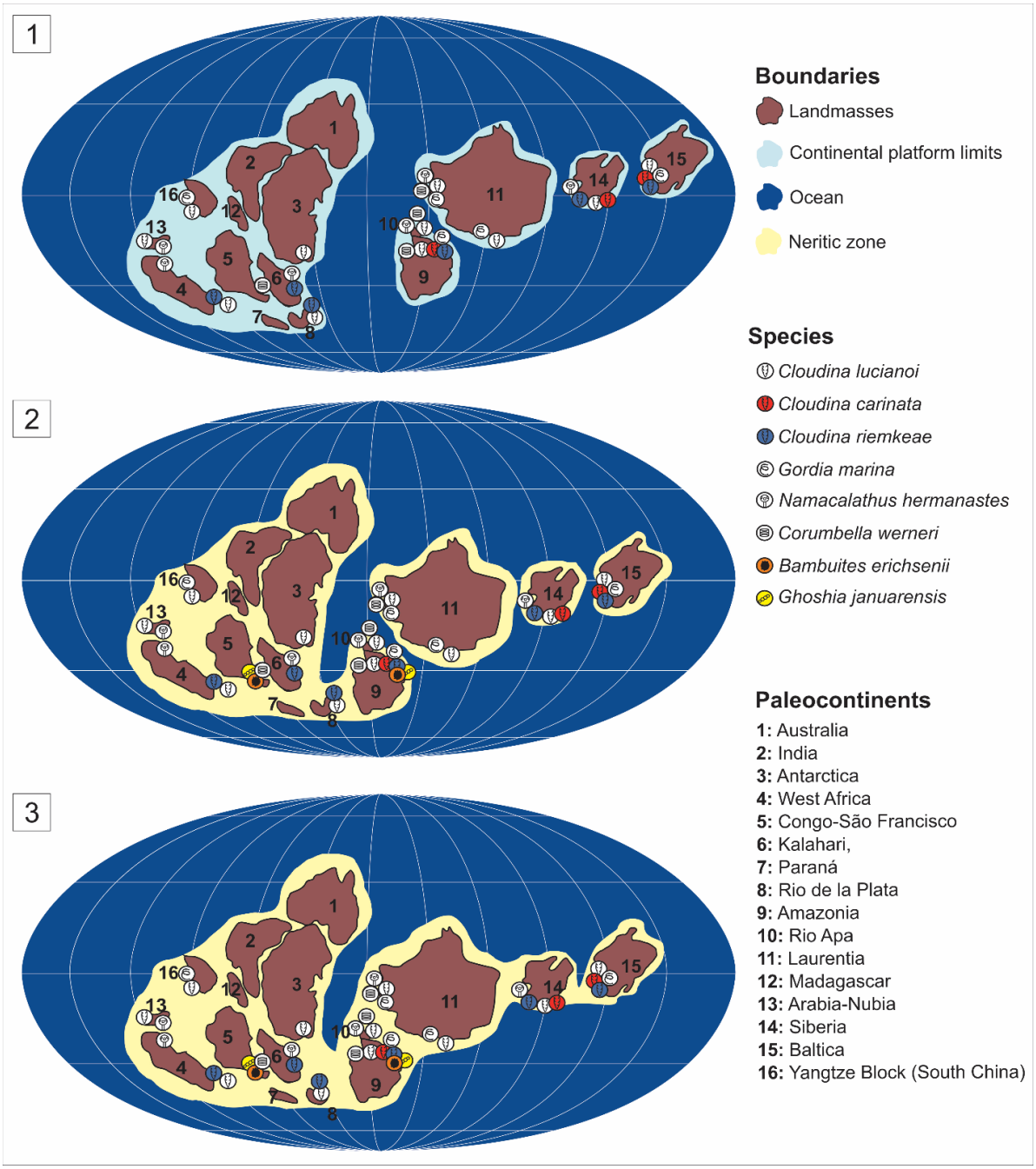

Figure 23: Different paleogeographic reconstructions of Gondwana ca. 550 Ma highlighting the *Cloudina lucianoi*, *Cloudina carinata*, *Cloudina riemkeae*, *Gordia marina*, *Corumbella werneri*, *Namacalathus hermanastes*, *Ghoshia januarensis*, and *Bambuites erichsenii* occurrences. (Modified from Warren et al., 2017 and Adôrno, 2019).

In addition to these occurrences in the Tamengo Formation, Corumbá Group, Ediacaran, Brazil, it was also reported occurrences of *Ghoshia januarensis* and *Bambuites erichsenii* (Fig. 23.2–23.3). Considering the distribution of all species throughout the western Gondwana and other paleocontinents, it seems that the landmasses were closer (Fig. 23.2–23.3) than previously approached by Warren et al. (2017) and Adôrno (2019) (Fig. 23.1). Therefore, it is presented two possible scenarios for the 550 Ma chronostratigraphic interval: 1: partial neritic connection, and 2: full neritic connection.

The scenario of partial neritic connection comprises the Amazonia, Rio de la Plata, Kalahari, Congo-São-Francisco, Arabia-Nubia, West-Africa, South China, and Antarctica connected by neritic zones, while Baltica, Siberia, and Laurentia would be apart of the western Gondwana (Fig. 23.2). The full neritic connection scenario would comprise Baltica, Siberia, Laurentia, Amazonia, Rio de la Plata, Kalahari, Congo-São-Francisco, Arabia-Nubia, West-Africa, South China, and Antarctica connected by neritic zones (Fig. 23.3).

The organic-walled microfossil data from Sete Lagoas retrieved from the present study allows the interpretation of the connection of Amazonia with the other cratons that formed the western Gondwana in 550 Ma in both scenarios. The full neritic connection is corroborated when considering the invertebrate species recorded from this chronostratigraphic interval.

On the other hand, the partial neritic connection is corroborated when restricting organic-walled microfossils data and previous plate tectonic models for the western Gondwana and for Laurentia, Baltica, and Siberia. In this scenario, the invertebrate species dispersion was possible probably by oceanic currents that transported for long distances planktonic larvae of the early life stage of these species (Warren et al., 2017). So, the partial connection would be the

paleogeographic inference corroborated by the herein presented data on organic-walled microfossils.

9. CONCLUSIONS

The present thesis embraces the first formal description of the lectostratotype section of the Sete Lagoas Formation, the proposal of two hypostratotype sections, and the description of an additional section with important fossil content. The studied sections are located in the Minas Gerais State, and in the Federal District, southeast Brazil: 1. Lectostratotype section, Sete Lagoas County; 2. Hypostratotype section from the PRF, Sete Lagoas County; 3. Hypostratotype section from the Barreiro community, Januária County; 4. Fercal section, Brasília. These descriptions contribute to the characterization of the Sete Lagoas Formation, as well as defining a reference section for future studies on the characterization of this lithostratigraphic unit and its correlation with other coeval units from Gondwana.

Nine marine species of organic-walled microfossils occur in the four studied sections: *Germinosphaera bispinosa* Mikhailova, 1986, *Leiosphaeridia crassa* (Naumova, 1949), *Leiosphaeridia jacutica* (Timofeev, 1966), *Leiosphaeridia minutissima* (Naumova, 1949), *Leiosphaeridia tenuissima* Eisenack, 1958, *Leiosphaeridia ternata* (Timofeev, 1966), *Bambuites erichsenii* Sommer, 1971, and *Siphonophycus robustum* (Schopf, 1968), *Ghoshia januarensis* new species. Seven species are inferred to be marine planktonic, while *Ghoshia januarensis* and *Siphonophycus robustum* are inferred to be marine benthic. Stratigraphic logging and stratigraphic distribution of studied species indicate that the Sete Lagoas Formation was deposited in a shelf environment.

Two biostratigraphic units are currently recognized in the Sete Lagoas Formation, approaching all four studied sections: *Leiosphaeridia minutissima* Zone, a lowest-occurrence interval zone, and *Bambuites erichsenii* Zone, a range zone. The *Bambuites erichsenii* Zone is positioned in the upper Ediacaran. The *Leiosphaeridia minutissima* Zone is suggested to be placed in the lower/mid Ediacaran interval. The connection by a neritic zone of Amazonia with other cratons that form western Gondwana, including the São Francisco craton, in 550 Ma is corroborated, while Laurentia, Baltica, and Siberia were separate paleocontinents. In future research perspectives, integrating studies herein conducted with new proxies to calibrate the biostratigraphic dating herein with a geochronological approach would certainly improve the chronostratigraphic inferences and paleogeographic evolution analyses of western Gondwana.

10. REFERENCES

Adôrno, R.R., 2019, Taxonomy, paleoecology and chronosbiostratigraphy across the Ediacaran-Cambrian boundary: Tamengo and Guaicurus formations: University of Brasília 213p.

Adôrno, R.R., Do Carmo, D.A., Germs, G.J.B., Walde, D.H.G., Denezine, M., Boggiani, P.C., Sousa e Silva, S.C., Moraes, R., Caminha, S.A., Suarez, P.A.Z., Rodrigues, C. V., Caixeta, G.M., Pinho, D., Schneider, G., and Muyamba, R., 2017, Cloudina lucianoi (Beurlen & Sommer, 1957), Tamengo Formation, Ediacaran, Brazil: Taxonomy analysis of stratigraphic distribution and biostratigraphy: Precambrian Research, v. 301, p. 19–35.

Adôrno, R.R., Walde, D.H.G., Erdtmann, B., Denezine, M., Cortijo, I., Do Carmo, D.A., Giorgioni, M., Ramos, M.E.A.F., and Fazio, G., 2019, First occurrence of Cloudina carinata Cortijo et al., 2010 in South America, Tamengo Formation, Corumbá Group, upper Ediacaran of Midwestern: Estudios Geologicos, v. 75.

Agić, H., Moczydłowska, M., and Yin, L., 2017, Diversity of organic-walled microfossils from the early Mesoproterozoic Ruyang Group, North China Craton – A window into the early eukaryote evolution: Precambrian Research, v. 297, p. 101–130.

Alvarenga, C.J.S., Santos, R. V., Vieira, L.C., Lima, B.A.F., and Mancini, L.H., 2014, Meso-Neoproterozoic isotope stratigraphy on carbonates platforms in the Brasília belt of Brazil: Precambrian Research, v. 251, p. 164–180.

Alvarenga, C.J.S., Oliveira, G.D., Vieira, L.C., Santos, R. V., Baptista, M.C., and Dantas, E.L., 2019, Carbonate chemostratigraphy of the Vazante Group, Brazil: A probable Tonian age: Precambrian Research, v. 331, p. 105378.

Alvarenga, C.J.S., Dardenne, M.A., Vieira, L.C., Martinho, C.T., Guimarães, E.M., Santos, R. V., and Santana, R.O., 2012, Estratigrafia da borda ocidental da Bacia do São Francisco: Boletim

de Geociências Da PETROBRAS, v. 20, p. 145–164.
Anderson, R.P., McMahon, S., Macdonald, F.A., Jones, D.S., and Briggs, D.E.G., 2019, Palaeobiology of latest Ediacaran phosphorites from the upper Khesen Formation, Khuvsgul Group, northern Mongolia: Journal of Systematic Palaeontology, v. 17, p. 501–532.
Arrouy, M.J., Gaucher, C., Poiré, D.G., Xiao, S., Peral, L.E.G., Warren, L. V., Bykova, N., and Quaglio, F., 2019, A new record of late Ediacaran acritarchs from La Providencia Group (Tandilia System, Argentina) and its biostratigraphical significance: Journal of South American Earth Sciences, v. 93, p. 283–293.
Arvestål, E.H.M., and Willman, S., 2020, Organic-walled microfossils in the Ediacaran of Estonia: Biodiversity on the East European Platform: Precambrian Research, v. 341, p. 1–27.
Babinski, M., Vieira, L.C., and Trindade, R.I.F., 2007, Direct dating of the Sete Lagoas cap carbonate (Bambuí Group, Brazil) and implications for the Neoproterozoic glacial events: Terra Nova, v. 19, p. 401–406.
Babu, R., Singh, V.K., and Mehrotra, N.C., 2014, Neoproterozoic Age Based on Microbiotas from the Raipur Group of Baradwar Sub-basin, Chhattisgarh: Journal Geological Society of India, v. 84, p. 442–448.
Baludikay, B.K., Storme, J.Y., François, C., Baudet, D., and Javaux, E.J., 2016, A diverse and exquisitely preserved organic-walled microfossil assemblage from the Meso-Neoproterozoic Mbuji-Mayi Supergroup (Democratic Republic of Congo) and implications for Proterozoic biostratigraphy: Precambrian Research, v. 281, p. 166–184.
Baptista, M.C., 2020, Fósseis do Grupo Bambuí (Ediacarano) no norte de Minas Gerais e suas implicações bioestratigráficas e geocronológicas: University of Brasília 154p.
Beghin, J., Storme, J.Y., Blanpied, C., Gueneli, N., Brocks, J.J., Poulton, S.W., and Javaux, E.J., 2017, Microfossils from the late Mesoproterozoic – early Neoproterozoic Atar/El Mreïti Group, Taoudeni Basin, Mauritania, northwestern Africa: Precambrian Research, v. 291, p. 63–82.
Beurlen, K., and Sommer, F.W., 1957, Observações estratigráficas e paleontológicas sobre o calcário Corumbá: Boletim Da Divisão de Geologia e Mineralogia, v. 168, p. 1–35.
Blanco, G., and Gaucher, C., 2005, Estratigrafia, paleontologia y edad de la Formacion Las Ventanas (Neoproterozoico, Uruguay): Latin American Journal of Sedimentology and Basin Analysis, v. 12, p. 109–124.
Bobrovskiy, I., Hope, J.M., Ivantsov, A., Nettersheim, B.J., Hallmann, C., and Brocks, J.J., 2018, Dickinsonia: One of the earliest animals: Science, v. 1249, p. 1246–1249.
Buatois, L.A., and Mángano, M.G., 2011, Ichnology: Organism-Substrate Interactions in Space and Time: Cambridge University Press, 370 p.
Buick, R., 2010, Ancient acritarchs: Nature, v. 463, p. 885–886.
Butterfield, N.J., and Chandler, F.W., 1992, Palaeoenvironmental distribution of Proterozoic microfossils, with an example from the Agu Bay Formation, Baffin Island: Palaeontology, v. 35, p. 943–957.
Butterfield, N.J., Knoll, A.H., and Swett, K., 1994, Paleobiology of the Neoproterozoic Svanbergfjellet Formation, Spitsbergen: Fossil and Strata, v. 34, p. 1–84.
Caetano-Filho, S., Sansjofre, P., Ader, M., Paula-Santos, G.M., Guacaneme, C., Babinski, M., Bedoya-Rueda, C., Kuchenbecker, M., Reis, H.L.S., and Trindade, R.I.F., 2021, A large epeiric methanogenic Bambuí sea in the core of Gondwana supercontinent? Geoscience Frontiers, v. 12, p. 203–218.
Campos, J.E.G., and Dardenne, M.A., 1994, A Glaciação Neopaleozóica na porção meridional da

bacia Sanfranciscana: Revista Brasileira de Geociências, v. 24, p. 65–76.
Campos, J.E.G., and Do Carmo, D.A., 2005, Bacia Sanfranciscana: Phoenix, v. 73, p. 1–5.
Carvalho, M.G., 2018, Geologia e quimioestratigrafia dos grupos Bambuí e Paranoá no Distrito Federal: University of Brasília 101p.
Carvalho, M.G., and Alvarenga, C.J.S., 2018, Estratigrafia da transição entre os grupos Bambuí e Paranoá no Distrito Federal: Geologia USP - Serie Cientifica, v. 18, p. 193–208.
Caxito, F.A., Lana, C., Frei, R., Uhlein, G.J., Sial, A.N., Dantas, E.L., Pinto, A.G., Campos, F.C., Galvão, P., Warren, L. V., Okubo, J., and Ganade, C.E., 2021, Goldilocks at the dawn of complex life : mountains might have damaged Ediacaran – Cambrian ecosystems and prompted an early Cambrian greenhouse world: Scientific Reports, p. 1–15.
Caxito, F.A., Halverson, G.P., Uhlein, A., Stevenson, R., Gonçalves Dias, T., and Uhlein, G.J., 2012, Marinoan glaciation in east central Brazil: Precambrian Research, v. 200–203, p. 38–58.
Chiglino, L., Gaucher, C., Sial, A.N., and Ferreira, V.P., 2015, Acritarchs of the Ediacaran Frecheirinha Formation , Ubajara Group , Northeastern Brazil: Anais Da Academia Brasileira de Ciências, v. 87, p. 635–649.
Cingolani, C.A., Rauscher, R., and Bonhomme, M., 1991, Grupo La Tinta (Precaámbrico y Paleozoico inferior) provinciade BuenosAires, Repu´ blica Argentina. Nuevos datos geocronoloógicos y micropaleontológicos en las sedimentitas de Villa Cacique, partido de Juarez.: Revista Técnica de YPFB, v. 12, p. 177–191.
Cotter, K.L., 1997, Neoproterozoic microfossils from the Officer basin, western Australia: Alcheringa, v. 21, p. 247–270.
Couëffé, R., and Vecolii, M., 2011, New sedimentological and biostratigraphic data in the Kwahu Group (Meso- to Neo-Proterozoic), southern margin of the Volta Basin, Ghana: Stratigraphic constraints and implications on regional lithostratigraphic correlations: Precambrian Research, v. 189, p. 155–175.
Couto, J.G.P., Cordani, U.G., Kawashita, K., Iyer, S.S., and Moraes, N.M.P., 1981, Considerações sobre a idade do Grupo Bambuí com base em análises isotópicas de Sr e Pb: Revista Brasileira de Geociências, v. 11, p. 5–16.
Croft, W.N., and George, E.A., 1959, Blue-green algae from the Middle Devonian of Rhynie, Aberdeenshire: Bulletin of the British Museum, v. 3, p. 341–353.
D'Agrella-Filho, M.S., Babinski, M., Trindade, R.I.F., Van Schmus, W.R., and Ernesto, M., 2000, Simultaneous remagnetization and U-Pb isotope resetting in Neoproterozoic carbonates of the Sao Francisco craton, Brazil: Precambrian Research, v. 99, p. 179–196.
Damassa, S.P., and Knoll, A.H., 1986, Micropalaeontology of the Late Proterozoic Arcoona Quartzite Member of the Tent Hill Formation, Stuart Shelf, South Australia: Alcheringa, v. 10, p. 417–430.
Dardenne, M.A., 1978, Síntese sobre a estratigrafia do Grupo Bambuí no Brasil Central: XXX Congresso Brasileiro de Geologia, p. 597–610.
DaSilva, L.G., Pufahl, P.K., James, N.P., Guimaraes, E.M., and Reis, C., 2022, Sequence stratigraphy and paleoenvironmental significance of the Neoproterozoic Bambui Group, Central Brazil: Precambrian Research, v. 379, p. 106710.
Denezine, M., Adôrno, R.R., Do Carmo, D.A., Guimarães, E.M., Walde, D.H.G., Alvarenga, C.J.S., Germs, G., Antonietto, L.S., Gianfranco, C.G.V.R., and Nunes Junior, O.O., 2022, Methodological development of a combined preparation for micropaleontological and sedimentological studies of samples from the Proterozoic record: Frontiers in Earth Science,

v. 10, p. 810406.
Dong, L., Xiao, S., Shen, B., Zhou, C., Li, G., and Yao, J., 2009, Basal Cambrian microfossils from the Yangtze Gorges area (South China) and the Aksu area (Tarim block, northwestern China): Journal of Paleontology, v. 83, p. 30–44.
Downie, C., and Sarjeant, W.A.S., 1963, On the interpretation and status of some hystrichosphere genera: Palaeontology, v. 6, p. 83–96.
Downie, C., Evitt, W.R., and Sarjeant, W.A.S., 1963, Dinoflagellates, hystrichospheres and the classification of the acritarchs: Geological Sciences, v. 7, p. 1–16.
Eisenack, A., 1958a, Microfossilien aus dem Ordovizium des Baltikums, 1, Markasitschicht, Dictyonema-Scheifer, Glaukonitsand, Glaukonitkalk: Senckenbergian Lethaea, v. 39, p. 389–404.
Eisenack, A., 1958b, Tasmanites Newton 1875 und Leiosphaeridia n. gen. Als Gattungen der Hystrichosphaeridea: Palaeontographica, v. 110, p. 1–19.
Elenkin, A.A., 1949, Monographie algarum Cyanophycearum aquidulcium et terrestrium infinibus URSS inventarum: Special Part 2. Izd. Akademia Nauk SSSR, p. 985–1908.
Evitt, W.R., 1963, A discussion and proposals concerning fossil dinoflagellates, hystrichospheres, and acritarchs: Geology, v. 49, p. 158–164.
Fairchild, T.R., and Dardenne, M.A., 1978, First report of well-preserved Precambrian microfossils in Brazil (Paraopeba Formation, Bambuí Group, near Brasília): Boletim IG, v. 9, p. 62–68.
Fairchild, T.R., and Schorscher, H.D., 1985, Ocorrência de microfósseis e estromatólitos no Grupo Bambuí, Proterozoico (?) Médio-Superior, na região de Piumhí-Pimenta, SW de Minas Gerais, Brasil: Paleobotânica Latinoamericana, v. 7, p. 14.
Fairchild, T.R., Sanchez, E.A.M., Pacheco, M.L.A.F., and Leme, J.M., 2012, Evolution of Precambrian life in the Brazilian geological record: International Journal of Astrobiology, v. 11, p. 309–323.
Fairchild, T.R., Schopf, J.W., Shen-Miller, J., Guimarães, E.M., Edwards, M.D., Lagstein, A., Li, X., Pabst, M., and Melo Filho, L.S., 1996, Recent discoveries of Proterozoic microfossils in south-central Brazil: Precambrian Research, v. 80, p. 125–152.
Fantinel, L.M., Kuchenbecker, M., Alvarenga, C.J.S., Guimarães, E.M., Fairchild, T.R., Rohn, R., Sanchez, E.A.M., and Dardenne, M.A., 2015, Microbialitos da Formação Sete Lagoas (Grupo Bambuí), Neoproterozoico, estados de Minas Gerais e Goiás, *in* Fairchild, T.R., Rohn, R., and Dias-Brito, D., eds., Microbialitos do Brasil do Pré-Cambriano ao recente, 1st ed.: Rio Claro, IGCE/UNESP, p. 392.
Fatka, O., Steiner, M., Weber, B., and Zhu, M., 2012, The Precambrian-Cambrian biosphere (r)evolution : Insights from the Chinese Yangtze Platform: Bulletin of Geosciences, v. 87, p. 67–70.
Fensome, R.A., Williams, G.L., Bars, M.S., Freeman, J.M., and Hill, J.M., 1990, Acritarchs and Fossil Prasinophytes: An Index to Genera, Species and Intraspecific Taxa: American Association of Stratigraphic Palynologist Foundation Contributions, 771 p.
Gaucher, C., 2000, Sedimentology, Palaeontology and Stratigraphy of the Arroyo Del Soldado Group (Vendian to Cambrian, Uruguay): Würzburg, Beringeria, 120 p.
Gaucher, C., and Germs, G.J.B., 2003, Preliminary Biostratigraphic Correlation of the Arroyo Del Soldado Group (Vendian to Cambrian, Uruguay) with the Cango Caves and Nama Groups (South Africa and Namibia): Revista de La Sociedad Uruguaya de Geología, v. 1, p. 141–160.

Gaucher, C., and Germs, G.J.B., 2006, Recent advances in South African Neoproterozoic-Early Palaeozoic biostratigraphy: correlation of the Cango Caves and Gamtoos Groups and acritarchs of the Sardinia Bay Formation, Saldania Belt: South African Journal of Geology, v. 109, p. 193–214.

Gaucher, C., and Germs, G.J.B., 2007, First report of organic-walled microfossils from the Otavi and Mulden groups (Neoproterozoic, Namibia): III Symposium on Neoproterozoic-Early Palaeozoic Events in Southwestern Gondwana, p. 13–17.

Gaucher, C., and Sprechmann, P., 2009, Neoproterozoic Acritarch Evolution: Elsevier, 319–326 p.

Gaucher, C., Chiglino, L., and Peçoits, E., 2004, Southernmost Exposures of the Arroyo del Soldado Group (Vendian to Cambrian, Uruguay): Palaeogeographic Implications for the Amalgamation of W-Gondwana: Gondwana Research, v. 7, p. 701–714.

Gaucher, C., Frimmel, H.E., and Germs, G.J.B., 2005a, Organic-walled microfossils and biostratigraphy of the upper Port Nolloth Group (Namibia): implications for latest Neoproterozoic glaciations: Geological Magazine, v. 142, p. 539–559.

Gaucher, C., Poire, D.G., Peral, L.G., and Chiglino, L., 2005b, Litoestratigrafia, Bioestratigrafia y Correlaciones De Las Sucesiones Sedimentarias Del Neoproterozoico-Cambrico Del Craton Del Rio De La Plata (Uruguay y Argentina): Latin American Journal of Sedimentology and Basin Analysis, v. 12, p. 145–160.

Gaucher, C., Boggiani, P.C., Sprechmann, P., Sial, A.N., and Fairchild, T.R., 2003, Integrated correlation of the Vendian to Cambrian Arroyo del Soldado and Corumbá Groups (Uruguay and Brazil): Palaeogeographic, palaeoclimatic and palaeobiologic implications: Precambrian Research, v. 120, p. 241–278.

Gaucher, C., Chiglino, L., Blanco, G., Poiré, D., and Germs, G.J.B., 2008a, Acritarchs of Las Ventanas Formation (Ediacaran, Uruguay): Implications for the timing of coeval rifting and glacial events in western Gondwana: Gondwana Research, v. 13, p. 488–501.

Gaucher, C., Finney, S.C., Poiré, D.G., Valencia, V.A., Grove, M., Blanco, G., Pamoukaghlián, K., and Peral, L.G., 2008b, Detrital zircon ages of Neoproterozoic sedimentary successions in Uruguay and Argentina: Insights into the geological evolution of the Río de la Plata Craton: Precambrian Research, v. 167, p. 150–170.

Geitler, L., 1925, Synoptische Darstellung der Cyanophyceen in morphologischer und systematishcer Hinsicht: Beihefte Zum Botanischen Centralblatt, v. 2, p. 163–324.

Germs, G.J.B., 1972, New shelly fossils from Nama Group, South West Africa: American Journal of Science, v. 272, p. 752–761.

Germs, G.J.B., Knoll, A.H., and Vidal, G., 1986, Latest Proterozoic microfossils from the Nama Group, Namibia (South West Africa): Precambrian Research, v. 32, p. 45–62.

Golovenok, V.K., and Belova., M.Y., 1993, The microfossils in the cherts from the Riphean deposits of the Turukhansk Uplift: Stratigraphy and Geological Correlation, v. 1, p. 51–61.

Golub, I.N., 1979, A new group of problematic microfossils from Vendian deposits of the Orshan depression (Russian Platform), *in* Sokolov, B.S., ed., Paleontology of Precambrian and Early Cambrian: Leningrad, Nauka, p. 147–155.

Grey, K., 2005, Ediacaran Palynology of Australia: Canberra, Memoir 31 of the Association of Australasian Palaeontologists, 439 p.

Grotzinger, J.P., Watters, W.A., and Knoll, A.H., 2000, Calcified metazoans in thrombolite-stromatolite reefs of the terminal Proterozoic Nama Group, Namibia: Paleobiology, v. 26, p. 334–359.

Guadagnin, F., Chemale, F., Magalhães, A.J.C., Santana, A., Dussin, I., and Takehara, L., 2015, Age constraints on crystal-tuff from the Espinhaço Supergroup - Insight into the Paleoproterozoic to Mesoproterozoic intracratonic basin cycles of the Congo-São Francisco Craton: Gondwana Research, v. 27, p. 363–376.

Hahn, G., Hahn, R., Leonardos, O.H., Pflug, H.D., and Walde, D.H.G., 1982, Körperlich erhaltene Scyphozoen-Reste aus dem Jungpräkambrium Brasiliens: Geologica et Palaeontologica, v. 16, p. 1–18.

Hall, J., 1847, Paleontology of New York, 1st ed.: Albany, C. van Benthuysen, 338 p.

Han, C.-M., Chen, L., Li, G.J., Pang, K., Wang, W., Zhou, G.Z., Yang, L., Lyu, W.G., Wang, K., Zhong, Z.H., Wu, C.X., and Yang, F.J., 2021, First record of organic-walled microfossils from the Tonian Shiwangzhuang Formation of the Tumen Group in western Shandong, North China: Palaeoworld, v. 30, p. 208–219.

Hannah, M.J., Wilson, G.S., and Wrenn, J., 2000, Oligocene and Miocene marine palynomorphs from CRP-2/2A, Victoria Land Basin, Antarctica: Terra Antartica, v. 7, p. 503–511.

Harris, C.R., Millman, K.J., van der Walt, S.J., Gommers, R., Virtanen, P., Cournapeau, D., Wieser, E., Taylor, J., Berg, S., Smith, N.J., Kern, R., Picus, M., Hoyer, S., van Kerkwijk, M.H., Brett, M., Haldane, A., del Río, J.F., Wiebe, M., Peterson, P., Gérard-Marchant, P., Sheppard, K., Reddy, T., Weckesser, W., Abbasi, H., Gohlke, C., and Oliphant, T.E., 2020, Array programming with NumPy: Nature, v. 585, p. 357–362.

Hassemer, G., Prado, J., and Baldini, R.M., 2020, Diagnoses and descriptions in Plant Taxonomy: Are we making proper use of them? Taxon, v. 69, p. 1–4.

Hermann, T.N., 1974, Nakhodki massovykh skopleniy trikhomov v rifee: B. V., p. 6–10.

Hidalgo, R., 2007, Vida após as glaciações neoproterozóicas: um estudo microfossilífero de capas carbonáticas dos crátons do São Francisco e Amazônico: University of São Paulo 200p.

Hofmann, H.J., 1976, Precambrian microflora, Belcher Island, Canada: Significance and systematics: Journal of Paleontology, v. 50, p. 1040–1073.

Hofmann, H.J., and Jackson, G.D., 1991, Shelf-facies microfossils from the Uluksan Group (Proterozoic Bylot Supergroup), Baffin Island, Canada: Journal of Paleontology, v. 65, p. 361–382.

Hofmann, H.J., and Jackson, G.D., 1994, Shale-Facies Microfossils from the Proterozoic Bylot Supergroup, Baffin Island, Canada: The Paleontological Society, v. 37, p. 1–39.

Horodyski, R.J., 1980, Middle Proterozoic shale-facies microbiota from the lower Belt Supergroup, Little Belt Mountains, Montana: Journal of Paleontology, v. 54, p. 649–663.

Hua, H., Chen, Z., Yuan, X., Zhang, L., and Xiao, S., 2005, Skeletogenesis and asexual reproduction in the earliest biomineralizing animal Cloudina: Geology, v. 33, p. 277–280.

Huntley, J.W., Xiao, S., and Kowalewski, M., 2006, 1.3 billion years of acritarch history: An empirical morphospace approach: Precambrian Research, v. 144, p. 52–68.

Jankauskas, T. V., Mikhailova, N.S., and German, T.N., 1989, Mikrofossilii Dokembriya SSSR (Precambrian Microfossils of the USSR): Leningrad, Nauka, 191 p.

Javaux, E.J., 2007, The early eukaryotic fossil record, *in* G Jékely, ed., Advances in Experimental Medicine and Biology, v. 607., 1st ed.: New York, Springer, p. 1–19.

Javaux, E.J., and Marshal, C.P., 2006, A new approach in deciphering early protist paleobiology and evolution: Combined microscopy and microchemistry of single Proterozoic acritarchs: Review of Palaeobotany and Palynology, v. 139, p. 1–15.

Javaux, E.J., and Knoll, A.H., 2017, Micropaleontology of the lower Mesoproterozoic Roper Group, Australia, and implications for early eukaryotic evolution: Journal of Paleontology, v.

91, p. 199–229.
Javaux, E.J., and Lepot, K., 2018, The Paleoproterozoic fossil record: Implications for the evolution of the biosphere during Earth's middle-age: Earth-Science Reviews, v. 176, p. 68–86.
Javaux, E.J., Knoll, A.H., and Walter, M.R., 2004, TEM evidence for eukaryotic diversity in mid-Proterozoic oceans: Geobiology, v. 2, p. 121–132.
Kirchner, O., 1900, Shizophyceae, *in* Engler, A. and Prantl, K., eds., Die Natürlichen Pflanzenfamilien: Leipzig, I Teil, Abteilung Ia, p. 115–121.
Knoll, A.H., 1982, Microfossils from the Late Precambrian Draken Conglomerate, Ny Friesland, Svalbard: Journal of Paleontology, v. 56, p. 755–790.
Knoll, A.H., 1994, Proterozoic and early Cambrian protists: Evidence for accelerating evolutionary tempo: Proceedings of the National Academy of Sciences of the United States of America, v. 91, p. 6743–6750.
Knoll, A.H., and Golubic, S., 1979, Anatomy and taphonomy of a Precambrian algal stromatolite: Precambrian Research, v. 10, p. 115–151.
Knoll, A.H., and Walter, M.R., 1992, Latest Proterozoic stratigraphy and Earth history: Nature, v. 356, p. 673–678.
Knoll, A.H., Swett, K., and Mark, J., 1991, Paleobiology of a Neoproterozoic tidal flat/lagoonal complex: the Draken Conglomerate Formation, Spitsbergen: Journal of Paleontology, v. 65, p. 531–570.
Knoll, A.H., Wörndle, S., and Kah, L.C., 2013, Covariance of microfossil assemblages and microbialite textures across an upper Mesoproterozoic carbonate platform: Palaios, v. 28, p. 453–470.
Knoll, A.H., Germs, G.J.B., Tankard, A., and Welsink, H., 2020, Tonian microfossils from subsurface shales in Botswana: Precambrian Research, v. 345, p. 1–8.
Kouketsu, Y., Mizukami, T., Mori, H., Endo, S., Aoya, M., Hara, H., Nakamura, D., and Wallis, S., 2014, A new approach to develop the Raman carbonaceous material geothermometer for low-grade metamorphism using peak width: Island Arc, v. 23, p. 33–50.
Kumar, A., and Venkatachala, B.S., 1998, Proterozoic chert microbiota from the Riasi Inlier of the Vaishnodevi Limestone in the Himalayan Foot-hills, Jammu, India: Indian Journal of Petroleum Geology, v. 7, p. 51–70.
Kumar, S., and Srivastava, P., 1995, Microfossils from the Kheinjua Formation, Mesoproterozoic Semri Group, Newari area, central India: Precambrian Research, v. 74, p. 91–117.
Kumar, S., and Pandey, S.K., 2008, Discovery of organic-walled microbiota from the black-bedded chert, Balwan Limestone, the Bhander Group, Lakheri area, Rajasthan: Current Science, v. 94, p. 797–800.
Lamb, D.M., Awramik, S.M., Chapman, D.J., and Zhu, S., 2009, Evidence for eukaryotic diversification in the ~1800 million-year-old Changzhougou Formation, North China: Precambrian Research, v. 173, p. 93–104.
Lei, Y., Shen, J., Algeo, T.J., Servais, T., Feng, Q., and Yu, J., 2019, Phytoplankton (acritarch) community changes during the Permian-Triassic transition in South China: Palaeogeography, Palaeoclimatology, Palaeoecology, v. 519, p. 84–94.
Li, G., Pang, K., Chen, L., Zhou, G., Han, C., Yang, L., Wang, W., Yang, F., and Yin, L., 2019, Organic-walled microfossils from the Tonian Tongjiazhuang Formation of the Tumen Group in western Shandong, North China Craton and their biostratigraphic significance: Gondwana Research, v. 76, p. 260–289.

Lindholm, R.C., 1987, Trace fossils, *in* Allen and Unwin, eds., A practical approach to sedimentology, 1st ed.: London, Springer, p. 276.

Liu, P., and Moczydłowska, M., 2019, Ediacaran microfossils from the Doushantuo Formation chert nodules in the Yangtze Gorges area, South China, and new biozones: Fossils and Strata, v. 65, p. 1–172.

Liu, P., Xiao, S., Yin, C., Chen, S., Zhou, C., and Li, M., 2014, Ediacaran acanthomorphic acritarchs and other microfossil from chert nodules of the Upper Doushantuo Formation in the Yangtze Gorges area, South China: Paleontology Memoir, v. 72, p. 1–139.

Lopes, J.N., 1995, Faciologia e gênese dos carbonatos do Grupo Bambuí na região de Arcos, Estado de Minas Gerais: University of São Paulo 166p.

Loron, C., and Moczydłowska, M., 2017, Tonian (Neoproterozoic) eukaryotic and prokaryotic organic-walled microfossils from the upper Visingsö Group, Sweden: Palynology, v. 42, p. 220–254.

Loron, C.C., Rainbird, R.H., Turner, E.C., Greenman, J.W., and Javaux, E.J., 2019, Organic-walled microfossils from the late Mesoproterozoic to early Neoproterozoic lower Shaler Supergroup (Arctic Canada): Diversity and biostratigraphic significance: Precambrian Research, v. 321, p. 349–374.

Loron, C.C., Halverson, G.P., Rainbird, R.H., Skulski, T., Turner, E.C., and Javaux, E.J., 2021, Shale-hosted biota from the Dismal Lakes Group in Arctic Canada supports an early Mesoproterozoic diversi fi cation of eukaryotes: v. 95, p. 1113–1137.

Lottaroli, F., Craig, J., and Thusu, B., 2014, Neoproterozoic-Early Cambrian (Infracambrian) hydrocarbon prospectivity of North Africa: a synthesis: Geological Society, London, Special Publications, v. 326, p. 137–156.

Maithy, P.K., 1975, Micro-organisms from the Bushimay System (late Precambrian) of Kanshi, Zaire: The Palaeoobotanist, v. 22, p. 33–149.

Maithy, P.K., and Shukla, M.J., 1977, Microbiota from the Suket Shales, Ramapura, Vindhyan System (Late Pre-Cambrian), Madhya Pradesh: Palaeobotanist, v. 23, p. 176–188.

Mandal, J., Maithy, P.K., Barman, G., and Verma, K.K., 1984, Microbiota from the Kushalgarh Formation, Delhi, India: Palaeobotanist, v. 32, p. 1–19.

Marchese, H.G., 1974, Estromatolitos “Gymnosolenidos” en el lado oriental de Minas Gerais, Brasil: Revista Brasileira de Geociências, v. 4, p. 172–190.

Marshall, C.P., Javaux, E.J., Knoll, A.H., and Walter, M.R., 2005, Combined micro-Fourier transform infrared (FTIR) spectroscopy and micro-Raman spectroscopy of Proterozoic acritarchs: A new approach to Palaeobiology: Precambrian Research, v. 138, p. 208–224.

Mazoni, A.F., 2021, Raman Online. Available at https://github.com/alyssonmazoni/raman_online.

Mendelson, C. V., and Schopf, J.W., 1982, Proterozoic microfossils from the Sukhaya Tunguska, Shorikha, and Yudoma formations of the Siberian platform, USSR: Journal of Palaeontological Society of India, v. 56, p. 42–83.

Miao, L., Moczydłowska, M., and Zhu, M., 2021, A diverse organic-walled microfossil assemblage from the Mesoproterozoic Xiamaling Formation, North China: Precambrian Research, v. 360, p. 1–21.

Miao, L., Moczydłowska, M., Zhu, S., and Zhu, M., 2019, New record of organic-walled, morphologically distinct microfossils from the late Paleoproterozoic Changcheng Group in the Yanshan Range, North China: Precambrian Research, v. 321, p. 172–198.

Mikhailova, N.S., 1986, Novye nakhodki mikrofitofossilij iz otlozhenij verkhnego rifeya Krasnoyarskogo kraya: B.S. Sokolov (Ed.), Aktual ’nye Voprosy Sovremennoj, Naukova

Dumka, p. 31–37.
Moczydłowska, M., 2008a, New records of late Ediacaran microbiota from Poland: Precambrian Research, v. 167, p. 71–92.
Moczydłowska, M., 2008b, The Ediacaran microbiota and the survival of Snowball Earth conditions: Precambrian Research, v. 167, p. 71–92.
Moreira, D.S., Uhlein, A., Dussin, I.A., Uhlein, G.J., and Pimentel Misuzaki, A.M., 2020a, A Cambrian age for the upper Bambuí Group, Brazil, supported by the first U-Pb dating of volcaniclastic bed: Journal of South American Earth Sciences, v. 99, p. 102503.
Moreira, D.S., Uhlein, A., Dussin, I.A., Uhlein, G.J., and Misuzaki, A.M.P., 2020b, A Cambrian age for the upper Bambuí Group, Brazil, supported by the first U-Pb dating of volcaniclastic bed: Journal of South American Earth Sciences, v. 99, p. 1–15.
Murphy, M.A., and Salvador, A., 1999, International Stratigraphic Guide — An abridged version: Episodes, v. 22, p. 255–271.
Nagovitsin, K.E., and Kochnev, B.B., 2015, Microfossils and biofacies of the Vendian fossil biota in the southern Siberian Platform: Russian Geology and Geophysics, v. 56, p. 584–593.
Naumova, S.N., 1949, Spores of the Lower Cambrian: Izvestiya Akademii Nauk SSSR, v. 4, p. 49–56.
Naumova, S.N., 1950, Pollen of angiosperm type in deposits of the Lower Carboniferous: Izvestiya Akademii Nauk SSSR, v. 3, p. 103–113.
Nemerov, V.K., Stanevich, A.M., Razvozzhaeva, E.A., Budyak, A.E., and Kornilova, T.A., 2010, Biogenic sedimentation factors of mineralization in the Neoproterozoic strata of the Baikal – Patom region: Russian Geology and Geophysics, v. 51, p. 572–586.
Nobre, J., and Coimbra, A.M., 2000, Microfitólitos associados a construções estromatolíticas do Grupo Bambuí, Proterozóico superior, na região de Arcos - MG: Revista Brasileira de Geociências, v. 30, p. 589–592.
North American Commission on Stratigraphic Nomenclature, 2005, North American Stratigraphic Code: American Association of Petroleum Geologists Bulletin, v. 89, p. 1547–1591.
Nyberg, A. V., and Schopf., J.W., 1984, Microfossils in stromatolitic cherts from the upper Proterozoic Min'yar Formation, southern Ural Mountains, USSR: Journal of Paleontology, v. 58, p. 738–772.
Oehler, J.H., 1977, Microflora of the H.Y.C. Pyritic Shale Member of the Barney Creek Formation (McArthur Group), middle Proterozoic of northern Australia: Alcheringa, v. 1, p. 315–349.
Okubo, J., Kaufman, A.J., Warren, L. V., Evans, M.N., Marroquín, S., Varni, M.A., Misi, A., Bahniuk, A.M., and Xiao, S., 2022, The sulfur isotopic consequence of seawater sulfate distillation preserved in the Neoproterozoic Sete Lagoas post-glacial carbonate, eastern Brazil: Journal of the Geological Society, v. 179, p. jgs2021-091.
Oliveira, R.G., Martins, M., Queiroga, G., Silva de Souza, M.E., Lana, C., Alkmim, A.R., da Silva, M.A.L., Bueno, C., and Linhares, D., 2021, Sedimentary provenance and role of tectonic inheritance on the control of the Macaúbas group, eastern margin of São Francisco Craton (SE Brazil): Journal of South American Earth Sciences, v. 109.
Ouyang, Q., Zhou, C., Xiao, S., Guan, C., Chen, Z., Yuan, X., and Sun, Y., 2021, Distribution of Ediacaran acanthomorphic acritarchs in the lower Doushantuo Formation of the Yangtze Gorges area, South China: Evolutionary and stratigraphic implications: Precambrian Research, v. 353, p. 1–47.
Ouyang, S., Yin, L., and Zaiping, L., 1974, Sinian and Cambrian spores and acritarchs, *in* Press, S., ed., Handbook of the Stratigraphy and Paleontology of South Western China: Beijing,

Science Publishing House, p. 72–80, 114-123,.
Palacios, T., 1989, Microfósiles de Pared Orgánica Del Proterozoico Superior (Región Central de La Península Ibérica): Memorias del Museo Paleontológico de la Universidad de Zaragoza, 1–91 p.
Pandey, S.K., and Kumar, S., 2013, Organic walled microbiota from the silicified algal clasts, Bhander limestone, Satna area, Madhya Pradesh: Journal of the Geological Society of India, v. 82, p. 499–508.
Pang, K., Tang, Q., Wu, C., Li, G., Chen, L., Wan, B., Yuan, X., Bodnar, R.J., and Xiao, S., 2020, Raman spectroscopy and structural heterogeneity of carbonaceous material in Proterozoic organic-walled microfossils in the North China Craton: Precambrian Research, v. 346, p. 1–15.
Paula-Santos, G.M., Babinski, M., Kuchenbecker, M., Caetano-Filho, S., Trindade, R.I.F., and Pedrosa-Soares, A.C., 2015, New evidence of an Ediacaran age for the Bambuí Group in southern São Francisco craton (eastern Brazil) from zircon U-Pb data and isotope chemostratigraphy: Gondwana Research, v. 28, p. 702–720.
Perrella Júnior, P., Uhlein, A., Uhlein, G.J., Sial, A.N., Pedrosa-Soares, A.C., and Lima, O.N.B., 2017, Facies analysis, sequence stratigraphy and chemostratigraphy of the Sete Lagoas Formation (Bambuí Group), northern Minas Gerais State, Brazil: evidence of a cap carbonate deposited on the Januária basement high: Brazilian Journal of Geology, v. 47, p. 59–77.
Peterson, K.J., and Butterfield, N.J., 2005, Origin of the Eumetazoa: Testing ecological predictions of molecular clocks against the Proterozoic fossil record: Proceedings of the National Academy of Sciences of the United States of America, v. 102, p. 9547–9552.
Pimentel, M.M., and Fuck, R.A., 1992, Neoproterozoic crustal accretion in central: Geology, v. 20, p. 375–379.
Pimentel, M.M., Fuck, R.A., and Botelho, N.F., 1999, Granites and the geodynamic history of the Neoproterozoic Brasilia belt, Central Brazil: A review: Lithos, v. 46, p. 463–483.
Pimentel, M.M., Rodrigues, J.B., DellaGiustina, M.E.S., Junges, S., Matteini, M., and Armstrong, R., 2011, The tectonic evolution of the Neoproterozoic Brasília Belt, central Brazil, based on SHRIMP and LA-ICPMS U-Pb sedimentary provenance data: A review: Journal of South American Earth Sciences, v. 31, p. 345–357.
Porter, S.M., and Riedman, L.A., 2016, Systematics of organic-walled microfossils from the ca. 780 – 740 Ma Chuar Group, Grand Canyon, Arizona: Journal of Paleontology, v. 90, p. 815–853.
Prasad, B., Uniyal, S.N., and Asher, R., 2005, Organic-walled microfossils from the Proterozoic Vindhyan Supergroup of Son Valley, Madhya Pradesh, India: Palaeobotanist, v. 54, p. 13–60.
Prasad, B., Asher, R., and Borgohai, B., 2010, Late Neoproterozoic (Ediacaran)-Early Paleozoic (Cambrian) Acritarchs from the Marwar Supergroup, Bikaner-Nagaur Basin, Rajasthan: Journal Geological Society of India, v. 75, p. 415–431.
Pykhova, N.G., 1973, Dokembriskie akritarhi Moskovskogo graben I Yuzhnogo: Obshchestva Ispitateli Prirody Otdel Geologicheskii Novaya, v. 48, p. 91–107.
Qu, Y., Engdahl, A., Zhu, S., Vajda, V., and McLoughlin, N., 2015, Ultrastructural heterogeneity of carbonaceous material in ancient cherts: investigating biosignature origin and preservation: Astrobiology, v. 15, p. 825–842.
Ragozina, A.L., Weis, A.F., and Afonin, S.A., 2003, Colonial cyanobacteria of the genus ostiana (microcystis) from the upper vendian of Arkhangelsk region: Instruments, Methods, and

Missions for Astrobiology VI, v. 4939, p. 53.
Reis, H.L.S., and Alkmim, F.F., 2015, Anatomy of a basin-controlled foreland fold-thrust belt curve: The Três Marias salient, São Francisco basin, Brazil: Marine and Petroleum Geology, v. 66, p. 711–731.
Reis, H.L.S., and Suss, J.F., 2016, Mixed carbonate-siliciclastic sedimentation in forebulge grabens: An example from the Ediacaran Bambuí Group, São Francisco Basin, Brazil: Sedimentary Geology, v. 339, p. 83–103.
Riedman, L.A., Porter, S.M., and Calver, C.R., 2018, Vase-shaped microfossil biostratigraphy with new data from Tasmania, Svalbard, Greenland, Sweden and the Yukon: Precambrian Research, v. 319, p. 19–36.
Rodrigues, J.B., 2008, Proveniência de sedimentos dos grupos Canastra, Ibiá, Vazante e Bambuí - Um estudo de zircões detríticos e idades modelos Sm-Nd: Universidade de Brasília 128p.
Le Rosq, C.R., 2021, [rampy]. Available at https://github.com/charlesll/rampy.
Samuelsson, J., and Butterfield, N.J., 2001, Neoproterozoic fossils from the Franklin Mountains, northwestern Canada: stratigraphic and palaeobiological implications: Precambrian Research, v. 107, p. 235–251.
Sanchez, E.A.M., 2014, Microbialitos e microfósseis da Formação Sete Lagoas, Neoproterozoico, Brasil: implicações geomicrobiológicas em um contexto de mudanças climáticas e evolutivas: University of São Paulo 298p.
Sanchez, E.A.M., and Fairchild, T.R., 2018, Reavaliação De Fósseis Do Grupo Bambuí: Implicações Paleobiológicas Para O Neoproterozoico Tardio Do Brasil: Geonomos, v. 25, p. 1–11.
Sanchez, E.A.M., Uhlein, A., and Fairchild, T.R., 2021, Treptichnus pedum in the Três Marias Formation, south-central Brazil, and its implications for the Ediacaran-Cambrian transition in South America: Journal of South American Earth Sciences, v. 105, p. 1–9.
Sanchez, E.A.M., Vieira, T.A., Reis, H.L.S., and Kuchenbecker, M., 2018, Fossil microbialites of the Jaíba Formation, Bambuí Group, Minas Gerais, Brazil: Revista Brasileira de Paleontologia, v. 21, p. 175–186.
Santos, D.M., Sanchez, E.A.M., and Santucci, R.M., 2018, Morphological and petrographic analysis of newly identified stromatolitic occurrences in the Lagoa do Jacaré Formation, BambuÍ Group, State of Minas Gerais, Brazil: Revista Brasileira de Paleontologia, v. 21, p. 195–207.
Schopf, J.W., 1968, Microflora of the Bitter Springs Formation, Late Precambrian, Central Australia: Journal of Paleontology, v. 42, p. 651–688.
Schopf, J.W., Sergeev, V.N., and Kudryavtsev, A.B., 2015, A new approach to ancient microorganisms: Taxonomy, paleoecology, and biostratigraphy of the Lower Cambrian Berkuta and Chulaktau microbiotas of South Kazakhstan: Journal of Paleontology, v. 89, p. 695–729.
Sergeev, V.N., 1984, Microfossils in the silicified columnar stromatolites from the Upper Riphean deposits of the Turukhansk Uplift: Doklady AN SSSR, v. 278, p. 436–440.
Sergeev, V.N., 1992, Silicified Microfossils from the Precambrian and Cambrian Deposits of the Southern Ural Mountains and Middle Asia: Moscow, Nauka, 134 p.
Sergeev, V.N., 1994, Microfossils in cherts from the Middle Riphean (Mesoproterozoic) Avzyan Formation, southern Ural Mountains, Russian Federation: Precambrian Research, v. 65, p. 231–254.
Sergeev, V.N., 2001, Paleobiology of the Neoproterozoic (Upper Riphean) Shorikha and Burovaya

Silicified Microbiotas, Turukhansk Uplift, Siberia: Journal of Paleontology, v. 75, p. 427–448.

Sergeev, V.N., 2006, Precambrian Microfossils in Cherts: Their Paleobiology, Classification, and Biostratigraphic Usefulness: Moscow, Geos, 280 p.

Sergeev, V.N., and Lee, S.-J., 2001, Microfossils from cherts of the Middle Riphean Svetlyi Formation, the Uchur-Maya Region of Siberia and their stratigraphic significance: Stratigraphy and Geological Correlation, v. 9, p. 1–10.

Sergeev, V.N., and Lee, S.-J., 2004, New data on silicified microfossils from the Satka Formation of the Lowe Riphean Stratotype, the Urals: Stratigraphy and Geological Correlation, v. 12, p. 1–21.

Sergeev, V.N., and Seong-Joo, L., 2006, Real Eukaryotes and Precipitates First Found in the Middle Riphean Stratotype, Southern Urals: Stratigraphy and Geological Correlation, v. 14, p. 1–18.

Sergeev, V.N., and Schopf, J.W., 2010, Taxonomy, paleoecology and biostratigraphy of the Late Neoproterozoic Chichkan Microbiota of South Kazakhstan: the marine biosphere on the eve of metazoan radiation: Journal of Paleontology, v. 84, p. 363–401.

Sergeev, V.N., Knoll, A.H., and Petrov, P.Y., 1997, Paleobiology of the Mesoproterozoic-Neoproterozoic transition: The Sukhaya Tunguska Formation, Turukhansk Uplift, Siberia: Precambrian Research, v. 85, p. 201–239.

Sergeev, V.N., Sharma, M., and Shukla, Y., 2008, Mesoproterozoic silicified microbiotas of Russia and India—Characteristics and Contrasts: The Palaeobotanist, v. 57, p. 323–358.

Sergeev, V.N., Sharma, M., and Shukla, Y., 2012, Proterozoic fossil cyanobacteria: The Paleobotanist, v. 61, p. 189–358.

Sergeev, V.N., Vorob'eva, N.G., and Petrov, P.Y., 2017a, The biostratigraphic conundrum of Siberia: Do true Tonian–Cryogenian microfossils occur in Mesoproterozoic rocks? Precambrian Research, v. 299, p. 282–302.

Sergeev, V.N., Knoll, A.H., Kolosova, S.P., and Kolosov., P.N., 1994, Microfossils in cherts from the Mesoproterozoic Debengda Formation, Olenek Uplift, Northeastern Siberia: Stratigraphy and Geological Correlation, v. 2, p. 23–38.

Sergeev, V.N., Knoll, A.H., Vorob'eva, N.G., and Sergeeva, N.D., 2016, Microfossils from the lower Mesoproterozoic Kaltasy Formation, East European Platform: Precambrian Research, v. 278, p. 87–107.

Sergeev, V.N., Vorob'eva, N.G., Petrov, P.Y., and Semikhatov, M.A., 2017b, Taxonomic composition and biostratigraphic value of the Early Riphean organic-walled microfossil association from the Ust'-Il'ya Formation of the Anabar Uplift, Northern Siberia: Stratigraphy and Geological Correlation, v. 25, p. 241–255.

Shang, X., Liu, P., and Moczydłowska, M., 2019, Acritarchs from the Doushantuo Formation at Liujing section in Songlin area of Guizhou Province, South China: Implications for early–middle Ediacaran biostratigraphy: Precambrian Research, v. 334, p. 1–34.

Sharma, M., and Sergeev, V.N., 2004, Genesis of carbonate precipitate patterns and associated microfossils in Mesoproterozoic formations of India and Russia — a comparative study: Precambrian Research, v. 134, p. 317–347.

Shepeleva, E.D., 1963, Spores from the Lower Devonian Beds of the Podol Ian Dniester River area: Material on Regional Stratigraphy of the USSR, p. 98–101.

Shi, M., Feng, Q., Khan, M.Z., and Zhu, S., 2017a, An eukaryote-bearing microbiota from the early Mesoproterozoic Gaoyuzhuang Formation, Tianjin, China and its significance:

Precambrian Research, v. 303, p. 709–726.
Shi, M., Feng, Q., Khan, M.Z., Awramik, S.M., and Zhu, S., 2017b, Silicified microbiota from the Paleoproterozoic Dahongyu Formation, Tianjin, China: Journal of Paleontology, v. 91, p. 369–392.
Shukla, Y., Sharma, M., and Sergeev, V.N., 2020, Organic walled microfossils from the Neoproterozoic Owk Shale, Kurnool Group, South India: Palaeoworld, v. 29, p. 490–511.
Simonetti, C., 1994, Paleobiologia de sedimentos meso e neoproterozóicos da porção meridional do cráton do São Francisco: Universidade de São Paulo 137p.
Simonetti, C., and Fairchild, T.R., 1989, Paleobiologia de uma nova microflórula silicificada do Grupo Bambuí (Proterozoico Superior), da região de Unaí, MG: Boletim IG, v. 7, p. 1–25.
Simonetti, C., and Fairchild, T.R., 2000, Proterozoic microfossils from subsurface siliciclastic rocks of the São Francisco Craton, south-central Brazil: Precambrian Research, v. 103, p. 1–29.
Singh, V.K., and Sharma, M., 2016, Mesoproterozoic organic-walled microfossils from the Chaporadih Formation, Chandarpur Group, Chhattisgarh Supergroup, Odisha, India: Journal of Palaeontological Society of India, v. 61, p. 75–84.
Sommer, F.W., 1971, Microfósseis do Calcário Bambuí, de Pedro Leopoldo, Estado de Minas Gerais: Anais Da Academia Brasileira de Ciências, v. 61, p. 75–84.
Sousa Júnior, G.R., Nogueira, A.C.R., Santos Neto, E. V., Moura, C.A.V., Araújo, B.Q., and Reis, F. de A.M., 2016, Organic matter in the Neoproterozoic cap carbonate from the Amazonian Craton, Brazil: Journal of South American Earth Sciences, v. 72, p. 7–24.
Stanevich, A.M., Maksimova, E.N., Kornilova, T.A., Gladkochub, D.P., Mazukabzov, A.M., and Donskaya, T. V., 2009, Microfossils from the Arymas and Debengda formations, the Riphean of the Olenek Uplift: Age and presumable nature: Stratigraphy and Geological Correlation, v. 17, p. 20–35.
Stanier, R.Y., Sistrom, W.R., Hansen, T.A., Whitton, B.A., Castenholz, R.W., Pfennig, N., Gorlenko, V.N., Kondratieva, E.N., Eimhjellen, K.E., Whittenbury, R., Gherna, R.L., and Trüper., H.G., 1978, Proposal to place nomenclature of the Cyanobacteria (blue-green algae) under the rules of the International Code of Nomenclature of bacteria: International Journal of Systematic Bacteriology, v. 28, p. 335–336.
Steinmann, G., 1911, Uber Gymnosolen ramsayi, eine coelenterate von der Halbinsel Kanin: Bulletin of the Geographical Society of Finland, v. 31, p. 18–23.
Strother, P.K., and Wellman, C.H., 2016, Palaeoecology of a billion-year-old non-marine cyanobacterium from the Torridon Group and Nonesuch Formation: Palaeontology, v. 59, p. 89–108.
Strother, P.K., Battison, L., Brasier, M.D., and Wellman, C.H., 2011, Earth's earliest non-marine eukaryotes: Nature, v. 473, p. 505–509.
Suslova, E.A., Parfenova, T.M., Saraev, S. V., and Nagovitsyn, K.E., 2017, Organic geochemistry of rocks of the Mesoproterozoic Malgin Formation and their depositional environments (southeastern Siberian Platform): Russian Geology and Geophysics, v. 58, p. 516–528.
Tang, Q., Hu, J., Xie, G., Yuan, X., Wan, B., Zhou, C., Dong, X., Cao, G., Lieberman, B.S., Leys, S.P., and Xiao, S., 2019, A problematic animal fossil from the early Cambrian Hetang Formation, South China - A reply: Journal of Paleontology, v. 93, p. 1279–1282.
Tang, Q., Pang, K., Yuan, X., Wan, B., and Xiao, S., 2015, Organic-walled microfossils from the Tonian Gouhou Formation, Huaibei region, North China Craton, and their biostratigraphic implications: Precambrian Research, v. 266, p. 296–318.

Tang, Q., Hughes, N.C., McKenzie, N.R., Myrow, P.M., and Xiao, S., 2017, Late Mesoproterozoic – early Neoproterozoic organic-walled microfossils from the Madhubani Group of the Ganga Valley, northern India: Palaeontology, v. 60, p. 869–891.

Tang, Q., Pang, K., Xiao, S., Yuan, X., Ou, Z., and Wan, B., 2013, Organic-walled microfossils from the early Neoproterozoic Liulaobei Formation in the Huainan region of North China and their biostratigraphic significance: Precambrian Research, v. 236, p. 157–181.

Tang, Q., Pang, K., Li, G., Chen, L., Yuan, X., Sharma, M., and Xiao, S., 2021, The Proterozoic macrofossil Tawuia as a coenocytic eukaryote and a possible macroalga: Palaeogeography, Palaeoclimatology, Palaeoecology, v. 576, p. 1–15.

Thuret, G., 1875, Essai de classification des nostocines: Annales Des Sciences Naturelles; Botanique, v. 6, p. 372–382.

Timofeev, B. V., 1966, Micropaleophytological Investigation into Ancient Formations: Moscow-Leningrad, Nauka, 238 p.

Timofeev, B. V., Hermann, T.N., and Mikhailova, N.S., 1976, Microphytofossils of the Precambrian, Cambrian and Ordovician: Leningrad, Nauka, 106 p.

Tiwari, M., and Pant, C.C., 2004, Organic-walled microfossils from the Neoproterozoic black phosphatic stringers in the Gangolihat Dolomite, Lesser Himalaya, India: Current Science, v. 87, p. 1733–1738.

Tiwari, M., and Pant, I., 2009, Journal of Asian Earth Sciences Microfossils from the Neoproterozoic Gangolihat Formation, Kumaun Lesser Himalaya: Their stratigraphic and evolutionary significance: Journal of Asian Earth Sciences, v. 35, p. 137–149.

Tobias, T.C., 2014, Micropaleontologia da Formação Tamengo, Eco Parque Cacimba da Saúde, Ediacarano, Grupo Corumbá, Estado de Mato Grosso do Sul, Brasil: University of Brasília 78p.

Tohver, E., D'Agrella-Filho, M.S., and Trindade, R.I.F., 2006, Paleomagnetic record of Africa and South America for the 1200-500 Ma interval, and evaluation of Rodinia and Gondwana assemblies: Precambrian Research, v. 147, p. 193–222.

Trindade, R.I.F., D'Agrella-Filho, M.S., Antonio, P.Y.J., and Teixeira, W., 2021, The Precambrian Drift History and Paleogeography of Congo−São Francisco Craton: INC, 445–464 p.

Trindade, R.I.F., D'Agrella-Filho, M.S., Babinski, M., Font, E., and Brito Neves, B.B., 2004, Paleomagnetism and geochronology of the Bebedouro cap carbonate: Evidence for continental-scale Cambrian remagnetization in the São Francisco craton, Brazil: Precambrian Research, v. 128, p. 83–103.

Turland, N.J., Wiersema, J.H., Barrie, F.R., Greuter, W., Hawksworth, D.L., Herendeen, P.S., Knapp, S., Kusber, W.-H., Li, D.-Z., Marhold, K., May, T.W., McNeill, J., Monro, A.M., Prado, J., Price, M.J., and Smith, G.F., 2018, International Code of Nomenclature for Algae, Fungi, and Plants (Shenzhen Code) Adopted by the Nineteenth International Botanical Congress Shenzhen, China, July 2017: Regnum Vegetabile 159, Glashütten: Koeltz Botanical Books, .

Turnau, E., and Racki, G., 1999, Givetian palynostratigraphy and palynofacies: new data from the Bodzentyn Syncline (Holy Cross Mountains, central Poland): Review of Paleobotany and Palynology, v. 106, p. 237–271.

Uhlein, G.J., Uhlein, A., Pereira, E., Caxito, F.A., Okubo, J., Warren, L. V., and Sial, A.N., 2019, Ediacaran paleoenvironmental changes recorded in the mixed carbonate-siliciclastic Bambuí Basin, Brazil: Palaeogeography, Palaeoclimatology, Palaeoecology, v. 517, p. 39–51.

Vidal, G., and Moczydłowska-Vidal, M., 1997, Biodiversity, speciation, and extinction trends of

Proterozoic and Cambrian phytoplankton: Paleobiology, v. 23, p. 230–246.
Vieira, L.C., Trindade, R.I.F., Nogueira, A.C.R., and Ader, M., 2007, Identification of a Sturtian cap carbonate in the Neoproterozoic Sete Lagoas carbonate platform, Bambuí Group, Brazil: Comptes Rendus - Geoscience, v. 339, p. 240–258.
Vieira, L.C., Nédélec, A., Fabre, S., Trindade, R.I.F., and De Almeida, R.P., 2015, Aragonite crystal fans in Neoproterozoic cap carbonates: A case study from Brazil and implications for the post-snowball earth coastal environment: Journal of Sedimentary Research, v. 85, p. 285–300.
Virtanen, P., Gommers, R., Oliphant, T.E., Haberland, M., Reddy, T., Cournapeau, D., Burovski, E., Peterson, P., Weckesser, W., Bright, J., van der Walt, S.J., Brett, M., Wilson, J., Millman, K.J., Mayorov, N., Nelson, A.R.J., Jones, E., Kern, R., Larson, E., Carey, C.J., Polat, İ., Feng, Y., Moore, E.W., VanderPlas, J., Laxalde, D., Perktold, J., Cimrman, R., Henriksen, I., Quintero, E.A., Harris, C.R., Archibald, A.M., Ribeiro, A.H., Pedregosa, F., van Mulbregt, P., Vijaykumar, A., Bardelli, A. Pietro, Rothberg, A., Hilboll, A., Kloeckner, A., Scopatz, A., Lee, A., Rokem, A., Woods, C.N., Fulton, C., Masson, C., Häggström, C., Fitzgerald, C., Nicholson, D.A., Hagen, D.R., Pasechnik, D. V., Olivetti, E., Martin, E., Wieser, E., Silva, F., Lenders, F., Wilhelm, F., Young, G., Price, G.A., Ingold, G.L., Allen, G.E., Lee, G.R., Audren, H., Probst, I., Dietrich, J.P., Silterra, J., Webber, J.T., Slavič, J., Nothman, J., Buchner, J., Kulick, J., Schönberger, J.L., de Miranda Cardoso, J.V., Reimer, J., Harrington, J., Rodríguez, J.L.C., Nunez-Iglesias, J., Kuczynski, J., Tritz, K., Thoma, M., Newville, M., Kümmerer, M., Bolingbroke, M., Tartre, M., Pak, M., Smith, N.J., Nowaczyk, N., Shebanov, N., Pavlyk, O., Brodtkorb, P.A., Lee, P., McGibbon, R.T., Feldbauer, R., Lewis, S., Tygier, S., Sievert, S., Vigna, S., Peterson, S., More, S., Pudlik, T., Oshima, T., Pingel, T.J., Robitaille, T.P., Spura, T., Jones, T.R., Cera, T., Leslie, T., Zito, T., Krauss, T., Upadhyay, U., Halchenko, Y.O., and Vázquez-Baeza, Y., 2020, SciPy 1.0: fundamental algorithms for scientific computing in Python: Nature Methods, v. 17, p. 261–272.
Vorob'eva, N.G., and Petrov, P.Y., 2014, The Genus Vendomyces Burzin and Facies – Ecological Specificity of the Staraya Rechka Microbiota of the Late Vendian of the Anabar Uplift of Siberia and Its Stratigraphic Analogues: Paleontological Journal, v. 48, p. 655–666.
Vorob'eva, N.G., Sergeev, V.N., and Knoll, A.H., 2009, Neoproterozoic microfossils from the northeastern margin of the East European Platform: Journal of Paleontology, v. 83, p. 161–196.
Vorob'eva, N.G., Sergeev, V.N., and Petrov, P.Y., 2015, Kotuikan Formation assemblage: A diverse organic-walled microbiota in the Mesoproterozoic Anabar succession, northern Siberia: Precambrian Research, v. 256, p. 201–222.
Walcott, C.D., 1899, Pre-Cambrian fossiliferous formations: Geological Society of America, v. 10, p. 199–244.
Walde, D.H.G., Do Carmo, D.A., Guimarães, E.M., Vieira, L.C., Erdtmann, B., Sanchez, E.A.M., Adôrno, R.R., and Tobias, T.C., 2015, New aspects of Neoproterozoic-Cambrian transition in the Corumbá region (state of Mato Grosso do Sul, Brazil): Annales de Paléontologie, v. 101, p. 213–224.
Wan, B., Tang, Q., Pang, K., Wang, X., Bao, Z., Meng, F., Zhou, C., Yuan, X., Hua, H., and Xiao, S., 2019, Repositioning the Great Unconformity at the southeastern margin of the North China Craton: Precambrian Research, v. 324, p. 1–17.
Warren, L. V., Quaglio, F., Riccomini, C., Simões, M.G., Poiré, D.G., Strikis, N.M., Anelli, L.E., and Strikis, P.C., 2014, The puzzle assembled: Ediacaran guide fossil Cloudina reveals an old

proto-Gondwana seaway: Geology, v. 42, p. 391–394.
Warren, L. V., Quaglio, F., Simões, M.G., Gaucher, C., Riccomini, C., Poiré, D.G., Tavares, B., Boggiani, P.C., and Sial, A.N., 2017, Cloudina-Corumbella-Namacalathus association from the Itapucumi Group, Paraguay: increasing ecosystem complexity and tiering at the end of the Ediacaran: Precambrian Research,.
Woese, C., and Fox, G., 1977, No Phylogenetic structure of the prokaryotic domain: Proceedings, National Academy of Sciences, U.S.A., v. 74, p. 5088–5090.
Xiao, S., and Knoll, A.H., 2000, Phosphatized animal embryos from the Neoproterozoic Doushantuo Formation at Weng'an, Guizhou, South China: Journal of Paleontology, v. 74, p. 767–788.
Xiao, S., Chen, Z., Zhou, C., and Yuan, X., 2019, Surfing in and on microbial mats: Oxygen-related behavior of a terminal Ediacaran bilaterian animal: Geology, v. 47, p. 1054–1058.
Xing, Y.S., and Liu, K.C., 1972, On Sinian micropalaeoflora in Yenliao Region of China and its geological significance: Publication of the Institute of Geology and Mineral Resources, Chinese Academy of Sciences, p. 1–12.
Yan, Y., and Liu, Z., 1993, Significance of eucaryotic organisms in the microfossil flora of Changcheng System: Acta Micropalaeontologica Sinica, v. 10, p. 167–180.
Yin, L., and Guan, B., 1999, Organic-walled microfossils of Neoproterozoic Dongjia Formation, Lushan County, Henan Province, North China: Precambrian Research, v. 94, p. 121–137.
Yin, L., and Yuan, X., 2007, Radiation of Meso-Neoproterozoic and early Cambrian protists inferred from the microfossil record of China: Palaeogeography, Palaeoclimatology, Palaeoecology, v. 254, p. 350–361.
Yin, L., Yang, R., Peng, J., and Kong, F., 2009, New data regarding acritarch biostratigraphy from the Early-Middle Cambrian Kaili Formation in Chuandong, Guizhou Province, China: Progress in Natural Science, v. 19, p. 107–114.
Yin, L.M., Singh, B.P., Bhargava, O.N., Zhao, Y.L., Negi, R.S., Meng, F.W., and Sharma, C.A., 2018, Palynomorphs from the Cambrian Series 3, Parahio valley (Spiti), Northwest Himalaya: Palaeoworld, v. 27, p. 30–41.
Zaine, M.F., 1991, Análise dos fósseis de parte da Faixa Paraguai (MS, MT) e seu contexto temporal e paleoambiental: Universidade de São Paulo 215p.
Zalán, P. V., and Silva, P.C.R., 2007, Bacia do São Francisco: Boletim de Geociencias Da Petrobras, v. 15, p. 561–571.
Zang, W., 1995, Early Neoproterozoic sequence stratigraphy and acritarch biostratigraphy, eastern Officer Basin, South Australia: Precambrian Research, v. 74, p. 119–175.
Zang, W., and Walter, M.R., 1992, Late Proterozoic and Early Cambrian microfossils and biostratigraphy, northern Anhui and Jiangsu, central-eastern China: Precambrian Research, v. 57, p. 243–323.
Zhang, Y., Yin, L., Xiao, S., and Knoll, A.H., 1998, Permineralized fossils from the terminal Proterozoic Doushantuo Formation, South China: Paleontological Society Memoir, v. 72, p. 1–52.
Zhou, C., Xie, G., McFadden, K., Xiao, S., and Yuan, X., 2007, The diversification and extinction of Doushantuo-Pertatataka acritarchs in South China: causes and biostratigraphic significance: Geological Journal, v. 42, p. 229–262.

APPENDIX 1

frontiers in Earth Science

METHODS
published: 30 March 2022
doi: 10.3389/feart.2022.810406

Methodological Development of a Combined Preparation for Micropaleontological and Sedimentological Studies of Samples From the Proterozoic Record

Matheus Denezine [1], Rodrigo Rodrigues Adôrno [1,2], Dermeval Aparecido Do Carmo [1], Edi Mendes Guimarães [1], Detlef Hans Gert Walde [1], Carlos José Souza De Alvarenga [1], Gerard Germs [3], Lucas Silveira Antonietto [1], Christian Gianfranco Valdivia Rodríguez [4] and Osvaldo De Oliveira Nunes Junior [1]*

[1]Institute of Geosciences, University of Brasília, Brasília, Brazil, [2]Geological Survey of Brazil, Brasília, Brazil, [3]Department of Geology, University of the Free State, Bloemfontein, South Africa, [4]Institute of Chemistry, University of Brasília, Brasília, Brazil

OPEN ACCESS

Edited by:
Juliana Leme,
University of São Paulo, Brazil

Reviewed by:
Luana Morais,
University of São Paulo, Brazil
Clive Francis Burrett,
Mahasarakham University, Thailand

***Correspondence:**
Matheus Denezine
matheusdenezine@gmail.com

Specialty section:
This article was submitted to Paleontology, a section of the journal Frontiers in Earth Science

Received: 06 November 2021
Accepted: 18 January 2022
Published: 30 March 2022

Citation:
Denezine M, Adôrno RR, Do Carmo DA, Guimarães EM, Walde DHG, De Alvarenga CJS, Germs G, Antonietto LS, Valdivia Rodriguez CG and Nunes Junior ODO (2022) Methodological Development of a Combined Preparation for Micropaleontological and Sedimentological Studies of Samples From the Proterozoic Record. Front. Earth Sci. 10:810406. doi: 10.3389/feart.2022.810406

The recovery of microfossils from Proterozoic rocks is commonly challenging because of metamorphism. In this study, an application of different methods usually applied on Phanerozoic rocks to test efficiency on recovering microfossil from Proterozoic units is presented. Chemical, physical, and biological factors can influence the recovery of microfossils, thereby becoming a barrier for biostratigraphic and paleoecological studies. Furthermore, low-cost projects with a reduced amount of sample collected, such as drill core sampling, need to optimize the preparation time and sample needed for different analyses. To overcome this challenge, the classical procedure of mineralized microfossil preparation, the palynological technique, and the study of clay mineralogy with the analyses of diagenetic alteration and the search for possible microfossils in thin sections were combined. Three Proterozoic lithostratigraphic units were selected to develop an integrated procedure for preparing samples for micropaleontologic and sedimentologic studies: the Paranoá Group, Mesoproterozoic, and the Bambuí Group, Ediacarian-Cambrian, Brazil, and Nama Group, Ediacaran-Cambrian, Namibia. Recovering individual microfossils from the Paranoá and Bambuí groups has been a challenge for paleontologists. Therefore, most micropaleontological studies have been done as a part of microbiofacies analyses in thin sections. All sediment fractions were studied in trial for the examination (and picking) of mineralized microfossils, even the finest ones. The microfossil picking was conducted using a stereomicroscope. Three species were recovered following this procedure: *Vetronostocale* aff *V. amoenum* Schopf and Blacic, 1971, *Myxococcoides* sp., and *Melanocyrillium* sp. Analyses in whole rock samples of residues from water (H_2O) and hydrogen peroxide 30% (H_2O_2) procedures showed similar results when the clay fraction studied was obtained as part of micropaleontological preparation compared with the results from the standard clay mineral preparation method. The clay fraction diffractograms showed that the micropaleontological preparation with H_2O and H_2O_2 caused an increase in the intensity of the quartz reflections compared with

untreated samples. Moreover, detailed protocols for organic-walled microfossil preparation and low concentrated acetic and formic acids attacks for mineralized microfossil extraction were presented.

Keywords: micropaleontological preparation, sedimentalogical preparation, proterozoic microfossils, clay minerals, curatorship protocol

INTRODUCTION

The diversity and preservation of fossil specimens from the Precambrian have been considered rare compared with those recovered from the Phanerozoic (Knoll, 1985; Schopf, 1995). Among other causes, such as taphonomic alterations, which greatly influence the fossil record, the preparation methodology also plays an essential role in recovering. Therefore, this barrier in the study of the Precambrian strata requires methodological considerations because, depending on the method applied, the fossil record may be lost. The present study proposes a protocol to increase microfossil recovery based on a combined methodology focused on micropaleontological and sedimentological analysis integration (Alves, 1987; Campos, 2012; Horne and Siveter, 2016; Leite et al., 2018). Samples from Paranoá and Bambuí groups, Brazil, and Nama Group, Namibia, were analyzed to assess all methods presented in this study.

Because of distinctive micropaleontological recoveries procedures on samples from Phanerozoic to other strata, it is necessary to formalize preparation methodologies for recovery of organic-walled and mineralized microfossils from Precambrian lithostratigraphic units. With mineralized micropaleontological analyses, the residues from the same preparation can be used for clay mineral analyses. This combination accelerates the whole research besides reducing the costs of preparation procedures. The application of this protocol could improve the recovery of microfossils from Precambrian units and, consequently, improve biostratigraphic studies besides combining analyses for micropaleontology and sedimentology for integration and reduction of costs. In the present case, at least three laboratories are working together, Laboratory of Mineralized Microfossils, Laboratory of Organic-walled Microfossils, and Laboratory of X-ray Diffraction, so curatorial procedures must be shared and followed to promote efficiency on data acquisition and analysis integration.

Moreover, it also detailed the curatorship procedures, identification, allocation by collection category, packaging, and housing samples under the policy of the Museum of Geosciences, University of Brasilia. In addition to the management methodology, rules for the transit of samples between laboratories are also described.

GEOLOGICAL SETTINGS

Two localities in Minas Gerais State, Brazil, were studied: the Buritis Municipality, which is part of the Brasília belt within the Tocantins province, and the Januária Municipality, which is located in a nondeformed domain of the São Francisco craton (**Figure 1**). A thick interval of Meso-Neoproterozoic sedimentary rocks was deposited along the west portion of the San Francisco craton. These rocks were separated into three stratigraphic units, from bottom to top: Paranoá Group, Jequitaí Formation, and Bambuí Group.

The deposition of terrigenous and chemical sedimentary rocks belonging to the Paranoá Group dates from the Mesoproterozoic when the separation of the Rodinia supercontinent generated a passive rift-margin basin, West of the São Francisco craton (Alvarenga et al., 2014). Faria (1995) studied the stratigraphy of the Paranoá Group in the type locality of Alto Paraíso de Goiás and São João D'Aliança municipalities, Goiás State, Brazil; however, the study did not formalize the units according to any stratigraphic code. Thereafter, Campos et al. (2013) formalized 11 stratigraphic units within the Paranoá Group according to the Brazilian Code of Stratigraphic Nomenclature in order to adjust the informal units proposed by Faria (1995). The Paranoá Group consists of, in ascending stratigraphic order, the Ribeirão São Miguel, Córrego Cordovil, Serra da Boa Vista, Serra Almécegas, Serra do Paranã, Ribeirão Piçarrão, Ribeirão do Torto, Serra da Meia Noite, Ribeirão Contagem, Córrego do Sansão, and Córrego do Barreiro formations (Campos et al., 2013) (**Figure 3**).

After the deposition of the Paranoá Group, because of climatic changes, the Jequitaí Formation was deposited under glacial conditions, and their records remain in erosional contact with the Paranoá Group (unconformity) (Uhlein et al., 1995; Caxito et al., 2012). Right above in conformable contact, the carbonated-terrigenous Bambuí Group was deposited in a foreland-type basin generated from the flexure caused by tectonics in the Brasília belt. The Bambuí Group consists of five lithostratigraphic units, from base to top, the Sete Lagoas, Serra de Santa Helena, Lagoa do Jacaré, Serra da Saudade, and Três Marias formations (Dardenne, 1978) (**Figure 3**). Lately, the Bambuí Group has been attributed to the Ediacaran/Cambrian interval (Pimentel et al., 2011; Warren et al., 2014; Paula-Santos et al., 2015; Moreira et al., 2020; Sanchez et al., 2021).

The Nama Group, Namibia (**Figure 2**), represents the deposition in a shallow water foreland system; the deposition of the basal portion started around 550 Ma, followed by the deposition of siliciclastic Molasse sediments from the upper portion deposited in 540 Ma (Germs, 1983; Germs and Gresse, 1991). In the central and southern part of Namibia, the Nama Group rests discordantly on the crystalline basement. Its basal portion is represented by a succession of siliciclastic and carbonate rocks with occurrences of skeletal fossils of *Cloudina lucianoi* and other fossils with carbonate skeletons, as well as ichnofossils and palynomorphs in the Kuibis Formation (Germs, 1995; Gaucher et al., 2005). The upper portion of the Nama Group is represented by the Schwarzrand subgroup, which contains the ichnofossil *Phycodes pedum*, *Cloudina*, and palynomorphs (**Figure 3**) (Germs, 1983; Germs and Gresse, 1991; Gaucher et al., 2005).

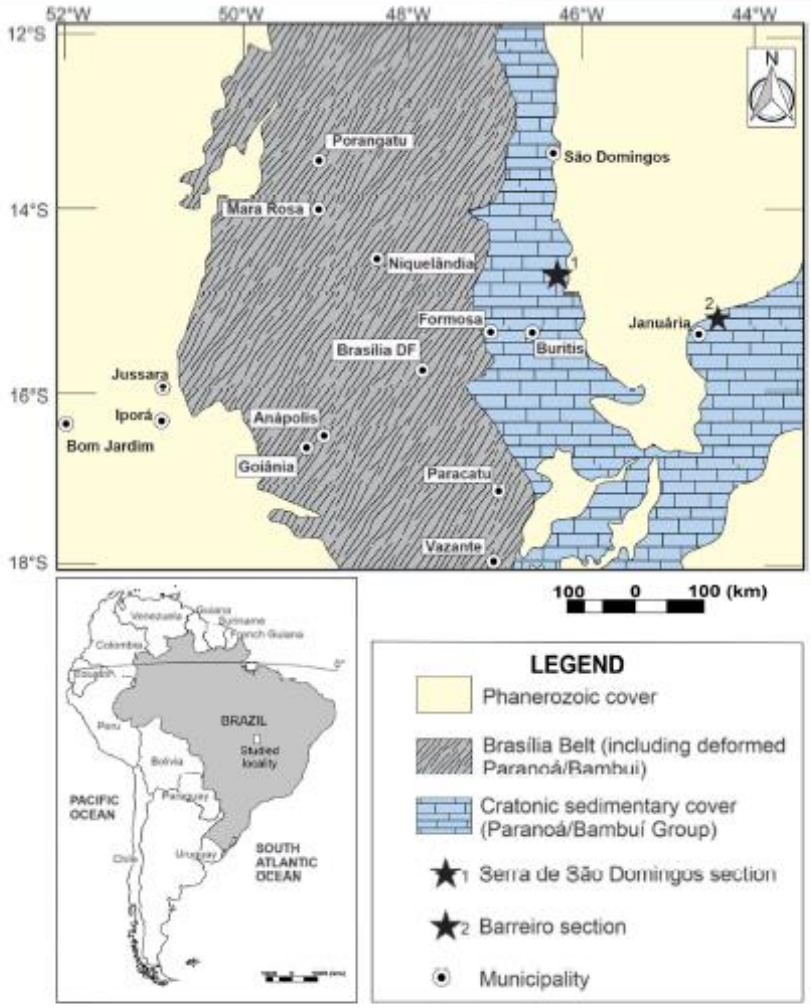

FIGURE 1 | Geological map of studied areas in Brazil. (1) Serra de São Domingos section, Buritis Municipality, Minas Gerais State; (2) Barreiro section, Januária Municipality, Minas Gerais State.

MATERIALS AND METHODS

The studied material is from three Precambrian units: Paranoá (Mesoproterozoic) and Bambuí (Ediacaran-Cambrian) groups, São Francisco craton, Brazil, and Nama Group (Ediacaran-Cambrian), Namibia. The samples from Brazil were collected in outcrops from Buritis and Januária municipalities, Minas Gerais State (**Table 1**). Detailed methodological processes for microfossiliferous recovery are discussed in *Preparation Methodologies*.

The same sample was analyzed throw different ways to obtain clay minerals information: (1) using the residues from water (H_2O) and hydrogen peroxide 30% (H_2O_2) micropaleontological preparations; (2) using the standard clay preparation, which initially included material disaggregation with a hammer and powdering in the Planetary Mill pulverisette by Fritsch for 5 min with 400 revolutions/min. X-ray powder diffraction was carried out on clay fractions. Clay fractions (<2 μm) were separated by centrifugation routine at LARIX described by Campos (2012) and modified from Alves (1987). The measurements were undertaken in oriented clay fractions in air-dried conditions. Analyses were performed in a RIGAKU Ultima IV diffractometer equipped with CuKα radiation, Ni filter, under 35 kV and 15 mA. The samples were scanned at 5°/min velocity, 0.05 stepping ranging from 2 to 40°2Θ for clay fraction. Mineral phases were identified using Jade XRD 9.0 (Materials Data) with PC-PDF (Powder Diffraction File—PDF for PC—ICDD). Major (M), minor (m), and trace (tr) components were established by comparing the reflection intensities in d: 4.26 Å for quartz, 10 Å for illite, and 7 Å for chlorite.

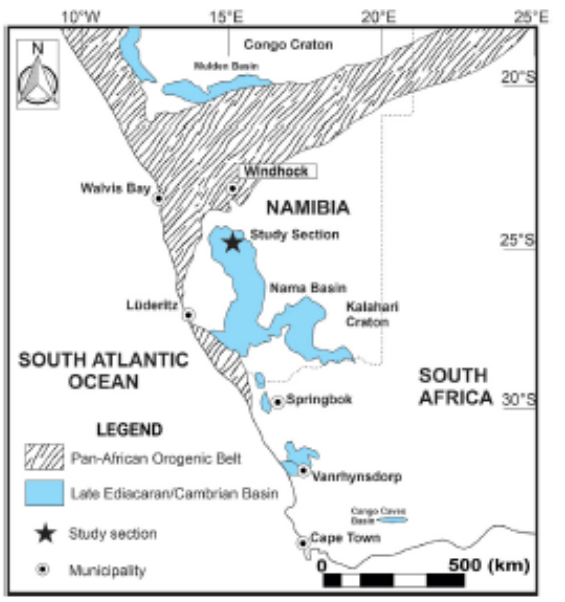

FIGURE 2 | Map of the Precambrian expositions in Namibia and the studied area positioning (after Gaucher et al., 2005).

CURATORSHIP PROTOCOL

Curatorship procedures must rule the studied material (rocks and fossils samples) management when multiple analysis is performed in different laboratories. This procedure aims to share information about samples, data acquisition, and analysis integration. In this study, the protocol used at the Micropaleontology Laboratory of the University of Brasilia (LabMicro), on curatorship of geological and paleontological samples that become housed at the Museum of Geosciences, was presented. The LabMicro is currently responsible for the Paleontological Collection of the Museum of Geosciences of the University of Brasilia (MGeo), which is subdivided into seven collections: (1) field collection, 2) residual samples, (3) recovered collection, (4) research collection, (5) special collection, (6) didactical collection, and (7) macrofossil collection (**Table 2**).

Sample curatorship starts during fieldwork. Field sampling is always accompanied by labeling to identify collected samples once they arrive at the laboratory. This is guaranteed by the mandatory completion of an individual sample tag containing data about their recollection site (**Figure 4**). The field collection comprises materials that have recently arrived at the LabMicro through fieldwork, independent of its immediate use (or not) as research, teaching, and/or training material. If they generate such interest, samples are due to be processed through laboratory work, which will result in both a residual sample and possible recovered fossil assemblage. The residual sample left from preparation is stored in the residual collection in field bags inside storage cabinets, whereas the recovered fossil assemblage is encased in micropaleontological slides to be held in specific fossil cabinets, consisting of the recovered collection. Research macrofossil and microfossil specimens, used to illustrate taxa in publications such as articles, theses, and reports, are isolated from others either in macrofossil cabinets or microslides that will be deposited at their specific fossil cabinets. In this case, the specimen is relocated into the research collection and recoded with a CP prefix.

Special collection covers fossil material of scientific interest donated or temporarily transferred to the MGeo by partner institutions such as universities, private companies, and other museums. The didactical collection is used in undergraduate and graduate courses given by the Institute of Geosciences, University of Brasília (IG); it comprises fossil material from other collections at the LabMicro and those collected by professors and students at the IG, as well as third-party direct donations. Finally, the macrofossil collection comprises macrofossil samples that require special conditions for safekeeping because of their size; therefore, they are stored in a cabinet of their own.

Samples arriving at the LabMicro initially get separated into three collections: field, macrofossils, or residual collections (the latter to be prepared for possible microfossil recovery). Once the fossil content is recovered from analyzed samples by picking, it is deposited either on multicelled micropaleontological slides (carbonate/siliceous fossils separated from rock through sieving) or glass microscope slides (organic-walled microfossils concentrated through organic preparation). The possible use of any microfossils on publications requires their relocation into single-celled micropaleontological slides to be stored in the research collection cabinet or the relocation of the entire glass microscope slide (with microfossils of scientific relevance properly marked) into the same space.

PREPARATION METHODOLOGIES

Once the initial steps of the curatorial procedure are completed, thin-section slides of the samples are produced for sedimentological/paleontological studies. Subsequently, a mechanical fragmentation of samples can be performed by using several possible methodologies, including soaking them in H_2O and/or chemical attack with H_2O_2, acetic acid 4%–10%, formic acid 10%, hydrochloric acid 36% (HCl), and hydrofluoric acid 40% (HF).

In the present work, both water and oxygen peroxide preparations were performed for mineralized microfossiliferous recovery. After washing both preparations on a sieve set (composed of 630-, 250-, 120-, 80-, and 50-μm mesh sieves plus a collecting bucket underneath), each fraction was analyzed on a stereoscopic microscope to pick for mineralized fossil remains.

Combined Preparation for Mineralized Microfossils and Clay Minerals (H_2O or H_2O_2)

The preparation presented herein aims to recover mineralized fossiliferous remains from disaggregating 30 g of sedimentary

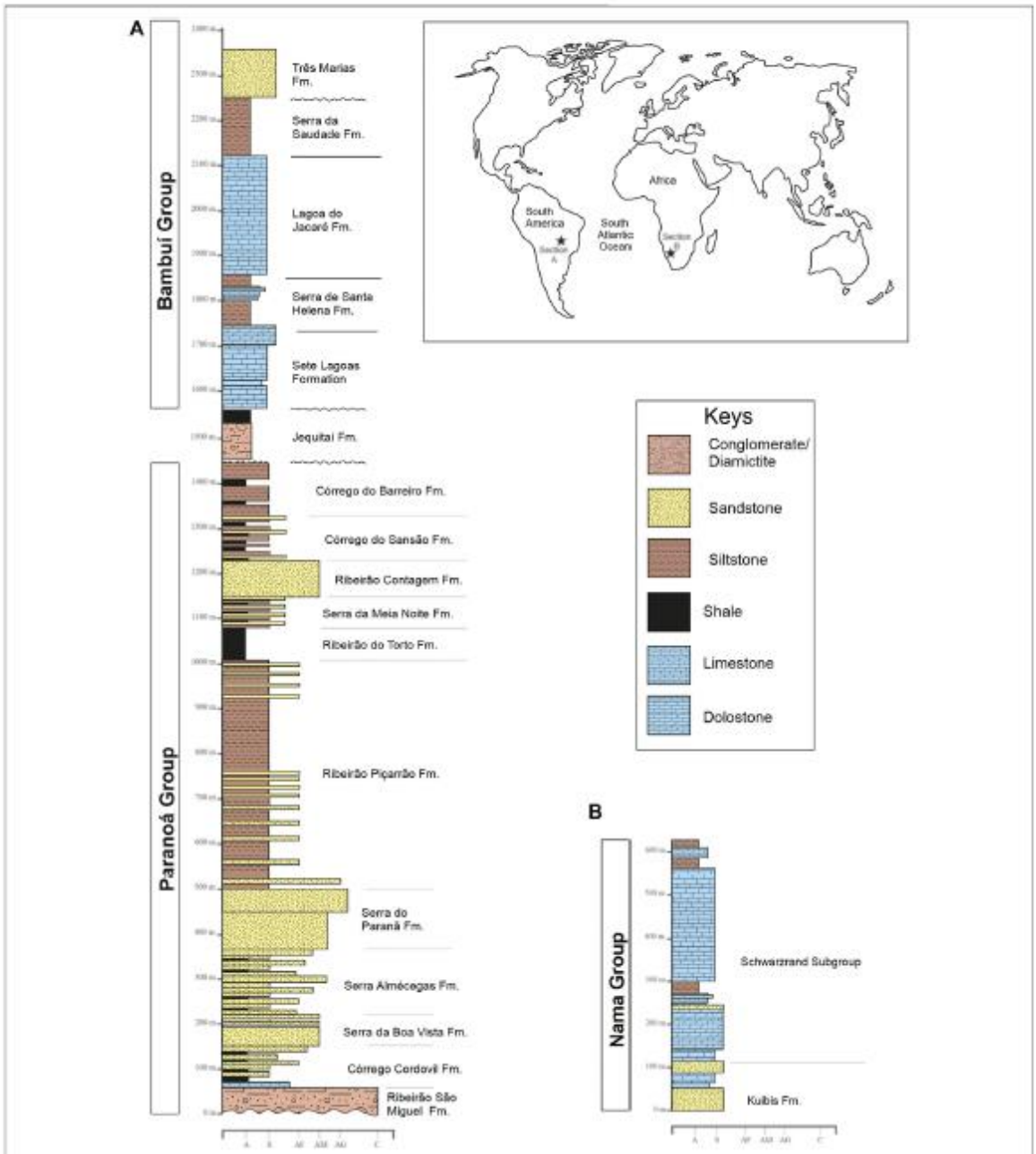

FIGURE 3 | (A) Regional stratigraphy of the Paranoá and Bambuí groups, adapted from Campos et al. (2013); **(B)** Nama Group (after Gaucher et al., 2005).

rock samples. This method is commonly used with Quaternary and Cretaceous units (Horne and Siveter, 2016; Leite et al., 2018; Machado et al., 2020). Two distinct sieving procedures were conducted on the same sample for mineralized microfossil recovery and clay mineral analyses: (1) treatment with water before sieving and (2) attack with hydrogen peroxide before sieving. Both methods aim to disaggregate the rock sample. After sieving both products from the water treatment and

TABLE 1 | Samples from Ediacaran units analyzed for specific preparations.

Sample	Fossils recovered	Lithotype	Stratigraphic unit	Locality	Applied methods
MP1203	CP965; CP966; CP967; CP968; CP969	Siltstone	Paranoá Group	Serra de São Domingos section, Buritis, Brazil	H_2O and H_2O_2 analyses
MP1221	CP970	Siltstone	Bambuí Group, Sete Lagoas Formation	Rio de São Domingos section, Buritis, Brazil	H_2O, H_2O_2, and clay mineral analyses
MP1226	—	Siltstone	Bambuí Group, Serra de Santa Helena Formation	Rio de São Domingos section, Buritis, Brazil	H_2O, H_2O_2, and clay mineral analyses
MP1231	CP971; CP972; CP 973	Siltstone	Bambuí Group, Serra de Santa Helena Formation	Rio de São Domingos section, Buritis, Brazil	H_2O, H_2O_2, and clay mineral analyses
MP2289	CP974	Limestone	Nama Group, Kubis Subgroup	Namibia	Low concentrated acetic acid
MP2995	CP961	Limestone	Bambuí Group, Sete Lagoas Formation	Barreiro section, Januária, Brazil	H_2O, H_2O_2, HCl, and HF attacks
MP3013	CP914	Limestone	Bambuí Group, Sete Lagoas Formation	Barreiro section, Januária, Brazil	H_2O, H_2O_2, HCl, and HF attacks
MP3034	CP963	Limestone	Bambuí Group, Sete Lagoas Formation	Barreiro section, Januária, Brazil	H_2O, H_2O_2, HCl, and HF attacks
MP3710	CP916	Limestone	Bambuí Group, Sete Lagoas Formation	Barreiro section, Januária, Brazil	H_2O, H_2O_2, HCl, and HF attacks
MP3714	CP917	Limestone	Bambuí Group, Sete Lagoas Formation	Barreiro section, Januária, Brazil	H_2O, H_2O_2, HCl, and HF attacks

TABLE 2 | Collections into the paleontological collection of the Museum of Geosciences, University of Brasília.

Collection	Code	Material
Field collection	Code gave during fieldwork	Rock sample
Residual collection	MP	Residual rock and organic fractions
Recovered collection	MP (same as the residual collection)	Microfossils recovered but not illustrated in publications
Research collection	CP	Microfossils illustrated in publications
Special collection	Coded according to their previous repository	Microfossils donated and loaned from another institution
Didactical collection	CD	Rock, microfossils, and macrofossils for didactical purposes
Macrofossil collection	MAF	Macrofossils

SAMPLE FORM - IG/UnB

SAMPLE P_____Am_____

P = GPS point (arabic); Am = sampling sequence by point

Special Collection nº UnB-GEO-E_____

City_____

Objective of the fieldwork _____

Participantes _____

Sampling date ____/____/_____

Group/Formation/Member/Suite/Complex_____

_____

Geographic location _____

Lithotype_____

Column level _____

GPS point _____ Zone _____ Datum _____ Altitude _____

Coord UTM _____ mL _____ mN,

Obs: _____ MP: _____

FIGURE 4 | Sample datasheet used to identify samples during the Laboratory of Micropaleontology fieldwork, University of Brasília, Brazil. The datasheet contains all information needed for further curatorship.

hydrogen peroxide attack, the sedimentary fractions were dried in a laboratory drying oven, and then analyses were performed under a stereoscope microscope to pick microfossils.

After mechanical disaggregation, a single sample followed two preparation routes: (1) left in beaker for 48 h with H_2O and (2) left in beaker for 48 h with H_2O_2 30% (PV). After these procedures, the samples were washed in a battery of sieves (630, 250, 160, 80, and 50 μm) (**Figure 5**). The fraction smaller than 50 μm were kept in an appropriate container. All fractions were dried in a laboratory drying oven at 60°C and then examined under a stereoscope microscope to pick microfossils. This drying temperature prevents unwanted fragmentation of microfossils. The finest fraction (>50 μm) from both preparations was also analyzed through X-ray diffraction for clay minerals studies.

Mineralized Microfossiliferous Recovery (Acetic and Formic Acid Attacks)

The traditional study of *Cloudina* species and other tubular carbonate fossils hosted in limestone is performed preferably in two-dimensional (2D) views. This analysis uses polish or thin sections due to the ease of this methodology and quick

2815

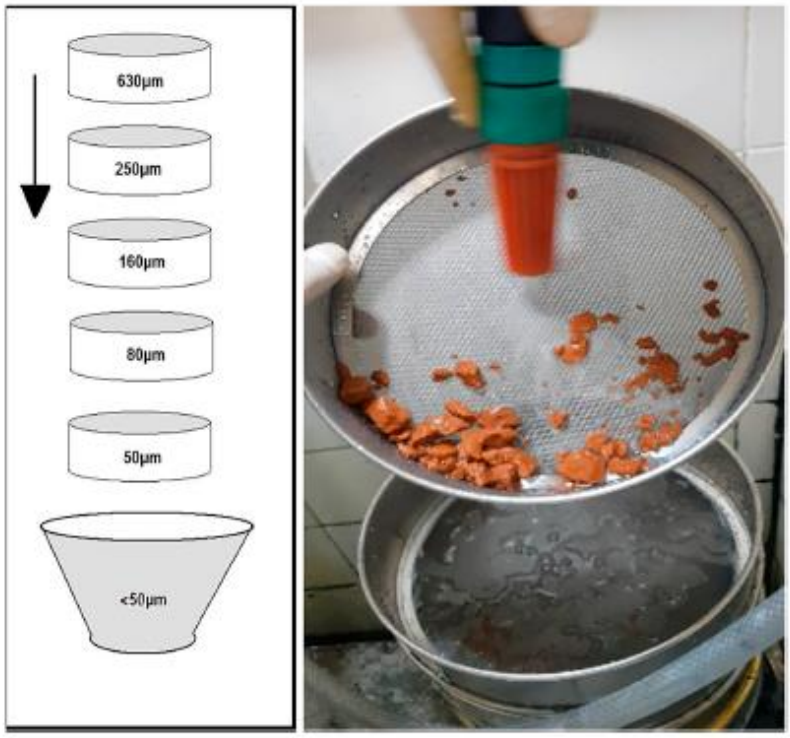

FIGURE 5 | Battery of sieves (630, 250, 160, 80, and 50 μm) and final recipient to store sediments smaller than 50 μm.

preparation, although studying fossils in 2D views make the 3D morphology reconstruction more complex and less accurate. In some cases, phosphatization processes offer an opportunity to know more about its morphology. The fossil can be easily isolated from the rock matrix by acid attack without destroying the specimen (Hua et al., 2003). In contrast, when the composition of the fossil and that of the matrix are both carbonates, it becomes a challenge to separate the specimen from the rock. This work shows a new methodology of fossil extraction using a low concentrated acetic acid such as vinegar (~4% acetic acid).

The preparation returned a positive result because acetic acid (4%) attacks the carbonate matrix preferentially, to the detriment of the carapace. Its slightly larger magnesium content is dissolved more slowly than the carbonate matrix. The dissolved fraction of the sample can be separated to analyze the palynological content (**Figure 6**).

The methodology consists of selecting a fossiliferous sample and introducing acetic acid solution 4% concentration. As the shell composition varies slightly from the matrix's, it allows the acid to act differently, releasing the specimens following the reaction: $CaCO_{3(s)} + 2CH_3COOH_{(aq)} \rightarrow Ca(CH_3\text{-}COO)_{2(aq)} + H_2O_{(l)} + CO_{2(g)}$. A similar, but slower, process occurs in the outcrops of these carbonate fossiliferous rocks, where the carbonic acid (H_2CO_3) of the rain erodes the matrix resulting in the eventual exposition of the skeleton. The reaction can be controlled daily by observing the acid's reaction on the fossiliferous sample. The entire preparation cycle takes approximately 15–20 days. The acid must be replaced every 3 days. At the end of the preparation, the sample must be gently and thoroughly washed with running water for approximately 5 min.

After the preparation mentioned previously, the fragments retained in sieves with mesh equal to or greater than 160 μm undergo a new preparation, this time using weak acids, such as acetic acid, to attack limestone, and formic acid, to attack dolomites, both at 10% concentration, with the aim of disaggregating the sample. For each sample to be prepared, it is recommended to use 1 L of 10% diluted acid solution for 200 g of sample. The sample is then placed in a hood, where it will remain until the chemical reaction is complete.

Periodically, after every 24 h of acid attack, it is recommended to change this acidic solution, as it loses its reaction power as the limestone is attacked. The solution that would initially be discarded during the exchange process, as it is a methodological evaluation, is separated for testing in micropaleontology. These tests are carried out with an emphasis on permineralized palynomorphs and for those

2816

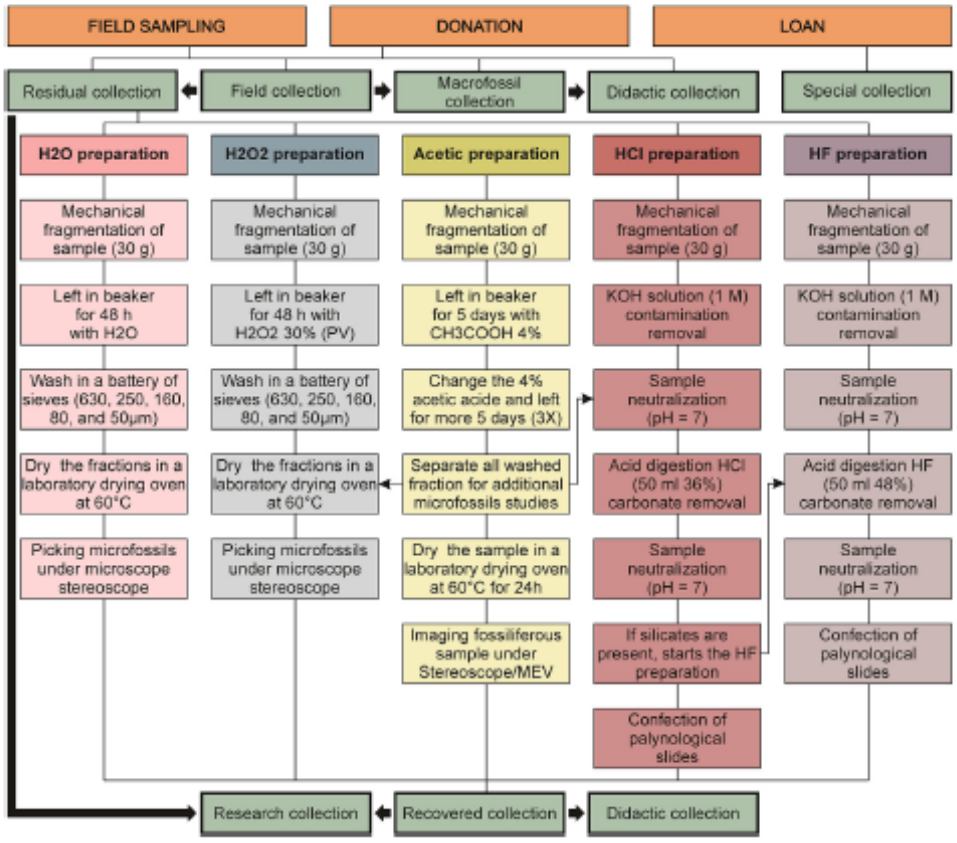

FIGURE 6 | Flowchart of curatorship management and sample preparations of the Laboratory of Micropaleontology, University of Brasília. The great black arrows indicate the possibilities of relocation of samples.

microfossils that may be sorted with the aid of a stereoscopic microscope (any particle in suspension).

When weak acids are used, the preparation can take up to 2 months to be completed, but instead, the risk of destruction of mineralized microfossils is reduced. After being disaggregated, the material is washed in a battery of sieves. The fraction retained in each sieve is dried in an oven at 60°C and then examined under a stereoscopic microscope.

Organic-Walled Microfossils Preparation (Hydrochloric and Hydrofluoric Acid Attacks)

Approximately 30 g of sample is used for preparation to recover organic microfossils. Here, the mineral components of the rock are dissolved using two acids: HCl and HF (**Figure 6**). First, fragmented samples are put in a 400-mL beaker, adding 50 mL of HCl at 36% concentration during 24 h to dissolve carbonates. The next step is to bring the sample solution to a neutral pH value, using distilled water in periodic washings. The neutralization procedure involves the addition of distilled water to beaker capacity, waiting for the decantation of the organic extract, carefully removing the acid solution; the process is repeated until neutral pH is reached. Then 50 mL of HF at 40% concentration is added to dissolve silicates for 48 h. Then, the washing procedure is repeated. All recovered organic residues are placed in polypropylene tubes and distilled water at pH 7 to further conserve these residues.

After the acid attack process, the final remains are named palynological extract. This material is kept in water solution and, sometimes, when following the classic procedure, needs to be sieved before preparing palynological slides. In synthesis, this traditional procedure uses aleatory organic remains distributed in this solution to prepare palynological slides. Nevertheless, an approach to this classic procedure on picking palynological remains under a stereoscope microscope is presented. Using a very liner brush (000), it is possible to select specimens to prepare palynological slides with this procedure. There are two ways of making palynological slides: (1) palynological slides created after picking microfossils under a stereoscope microscope; (2)

2817
2818

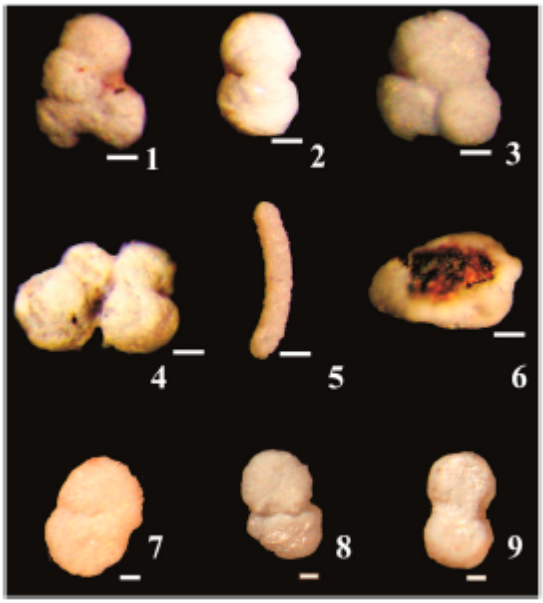

FIGURE 7 | Recovered specimens from the Proterozoic units of the São Francisco craton, São Domingos River section (samples from the Sete Lagoas, MP1221, and Serra de Santa Helena, MP1231, formations) and from São Domingos Hill section (sample from the Paranoá Group, MP1203), Municipality of Buritis, Minas Gerais State, Brazil. **(1–5)** Specimens from the Paranoá Group; **(6)** Specimens from the Sete Lagoas Formation, Bambuí Group; **(7–9)** Specimens from the Serra de Santa Helena, Bambuí Group. **(1–4, 7–9)** *Myxococcoides* sp., respectively, CP965, CP966, CP967, CP968, CP971, CP972, CP 973; **(5)** *Vetronostocale* aff. *V. amoenum* Schopf and Blacic, 1971, CP969; **(6)** *Melanocyrillium* sp., CP970. Scale bar: 10 μm.

palynological slides without preanalyses under stereoscope microscope, which involves placing a few drops of the recovered organic residue and distilled water on a glass cover. Both types of slides are prepared after putting on a heating plate at 30°C. After the water had evaporated, a few drops of Entelan® resin were added to the coverslip to be completely sealed after contact with the blade. The resin used has the function of drying together with the material mounted on the blade and preventing oxidation of the organic matter and its degradation.

RESULTS AND REMARKS

The results presented comprehend micropaleontological, mineralized, organic-walled microfossils, and sedimentological data, specifically clay mineral analyses. The oxidation attack was conducted to promote the complete or partial disaggregation of sedimentary rock. When sedimentary rock is composed of organic matrix, the H_2O_2 reacts with it and may result in a full or partial disaggregation. In this case, it is possible to recover microfossils in the H_2O_2 preparation, even in samples with oxidation considered ineffective (MP1226) and low efficiency (MP1203, MP1221, and MP1231). After the chemical reaction, the sedimentary material was sieved and by picking finest fractions. The coccoidal structures, as well as tubular and vase-shaped structures, recovered (**Figure 7**) were recognized as fossil content due to their similar morphological and size features assigned to well-described species and genus commonly found in Precambrian units. Besides that, they are very distinct from other grain particles analyzed from the same sample. The species recovered from the Paranoá Group, Mesoproterozoic, from sample MP1203, comprehends *Myxococcoides* sp. (CP965, CP966, CP967, CP968) (**Figures 7.1–4**) and *Vetronostocale* aff. *V. amoenum* Schopf and Blacic, 1971 (CP969) (**Figure 7.5**). One species was recovered in the Sete Lagoas Formation, Bambuí Group, from sample MP1221: *Melanocyrillium* sp. (CP970) (**Figure 7.6**), and one species was recovered from the Serra de Santa Helena Formation, Bambuí Group, from sample MP1231: *Myxococcoides* sp. (CP971, CP972, CP973) (**Figures 7.7–9**).

The limestone samples of Sete Lagoas Formation, Januária Municipality, did not show a considerable disaggregation effectiveness. The H_2O_2 disaggregation method shows more effectiveness on siliciclastic rocks when compared with carbonate rocks. This could be due to the difference in permeability of those two lithotypes. The more permeable the rock, the easier the H_2O_2 reacts with the organic matter content. In this context, metamorphism can also affect the H_2O_2 disaggregation process as, depending on the metamorphic grade, it could change the rock permeability because of rock compaction.

The finest fraction (>50 μm) sieved from samples MP1226, MP1221, and MP1231 from three distinct micropaleontological preparations procedures were analyzed: (1) treatment with tap water before sieving, (2) treatment with deionized water before sieving, and (3) hydrogen peroxide attack before sieving. Analyses in whole rock from all three procedures showed similar results when the clay fraction studied was obtained as part of micropaleontological preparation compared with the results from the standard clay mineral preparation method. The total similarities between diffractograms could be verified when both oxidized (H_2O_2) and nonoxidized (tap water and deionized water) preparations of the same sample (**Table 3**) are compared. The mineral composition of the whole rock sample, determined by X-ray diffraction, shows that all samples have quartz as their major constituent, besides the sample MP1221, which also has calcite as the major component. Illite and albite are minor constituents of all samples.

The standard clay mineral preparation results present changes in reflection intensities compared with the whole rock: the phyllosilicates have higher reflection intensity, which becomes major constituents, whereas the quartz reflection intensity decreases, which becomes a minor constituent. When the standard clay mineral preparation results are analyzed, the clay fraction shows the same composition as the whole rock, but (except for calcite in MP1221) the reflection intensities are opposite to those of the whole rock. Chlorite and illite are major constituents in the clay fraction, whereas quartz and albite are minor constituents (**Figure 8**). The diffractograms of samples MP1226 and MP1221 show a low and ill-defined band at the d~28 position that expands slightly under treatment with

2819
2820

TABLE 3 | Mineral composition of siltstones in whole rock and clay fraction, indicating the major constituents (M), minor (m), and trace (tr).

Sample	Preparation		Identified minerals	Whole rock	Clay fraction
MP1226	Standard clay mineral preparation		Clinochlore (chlorite)	m or tr	M
			Illite (muscovite)	m or tr	M
			Quartz	M	M
			Albite (feldspar)	m	M
	Micropaleontological residues	H_2O	Clinochlore (chlorite)	m	m
			Illite (muscovite)	m	m
			Quartz	M	M
			Albite (feldspar)	m	m
		H_2O_2	Clinochlore (chlorite)	m	m or tr
			Illite (muscovite)	m	m
			Quartz	M	M
			Albite (feldspar)	m	m
MP 1221	Standard clay mineral preparation		Clinochlore (chlorite)	m	M
			Illite (muscovite)	m	M
			Quartz	M	m
			Albite (feldspar)	M	m
			Calcite	M	M
	Micropaleontological residues	H_2O	Clinochlore (chlorite)	m	M
			Illite (muscovite)	m	M
			Quartz	M	M
			Albite (feldspar)	m	m
			Calcite	M	M
		H_2O_2	Clinochlore (chlorite)	m	m or tr
			Illite (muscovite)	m	m
			Quartz	M	M
			Albite (feldspar)	m	m
			Calcite	M	M
MP 1231	Standard clay mineral preparation		Clinochlore (chlorite)	M	M
			Illite (muscovite)	M	M
			Quartz	M	m or tr
			Albite (feldspar)	m	m or tr
	Micropaleontological residues	H_2O	Clinochlore (chlorite)	M	M
			Illite (muscovite)	m	m
			Quartz	M	M
			Albite (feldspar)	m	M
		H_2O_2	Clinochlore (chlorite)	M	M
			Illite (muscovite)	m	m
			Quartz	M	M
			Albite (feldspar)	m	M

glycerol, indicating the presence of interstratified clay mineral, possibly illite/vermiculite. Clay residues obtained from samples treated with H_2O and H_2O_2 during the micropaleontological preparation do not maintain this trend. The clay fraction maintains the same intensities as the total sample: quartz remains a major constituent, whereas phyllosilicates are presented as minor or trace constituents (**Figure 9**). This effect can be explained as the effect of disaggregation, dispersion, or release of quartz particles during micropaleontological treatment.

The procedure of analyzing the same sample residue for both micropaleontological and sedimentological approaches as a combined preparation reduces time of maceration and costs, besides being sure that both analyses comprehend the same depositional interval. This association leads to a more precise paleoenvironmental interpretation. In addition, it can save samples when a small amount is available for multiple analyses.

The acetic acid preparation was conducted on a sample from the Nama Group, Namibia; it showed efficient extraction of carbonate *C. lucianoi* skeleton within a carbonate matrix. This extraction technique allowed 3D imaging of the carbonate skeleton (**Figure 10**). This preparation shows similar results compared with phosphatized skeleton preparations from Dengying Formation in China (Hua et al., 2005). Researchers might use this easy, accessible, and environmentally friendly method to conduct 3D studies on carbonate skeleton fossils within limestone rocks. This

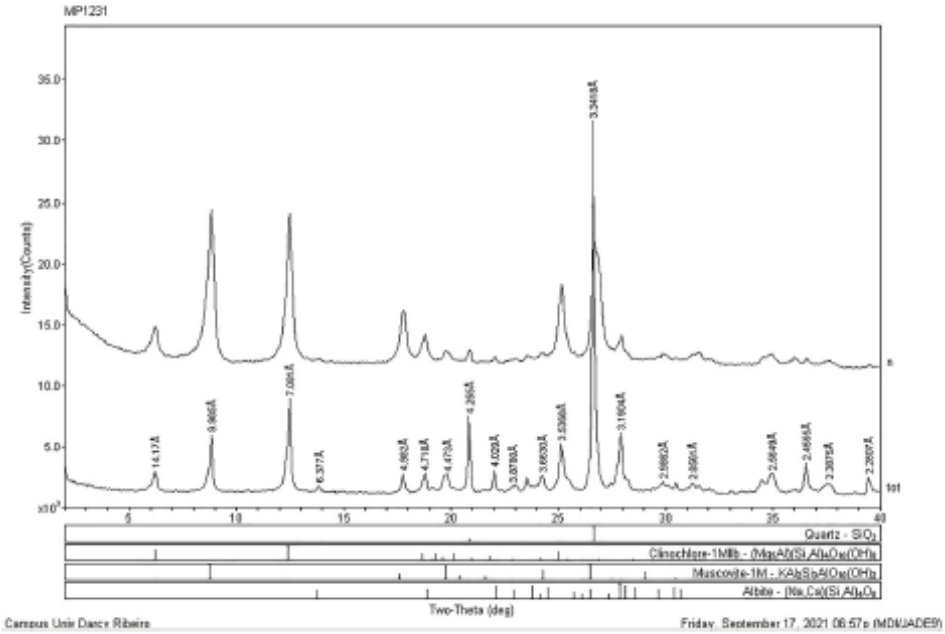

FIGURE 8 | Diffractograms of sample MP1231 from Bambuí Group, Municipality of Buritis, Minas Gerais State, Brazil. Whole rock (tot) and clay fraction (n); note the variation in reflection intensities.

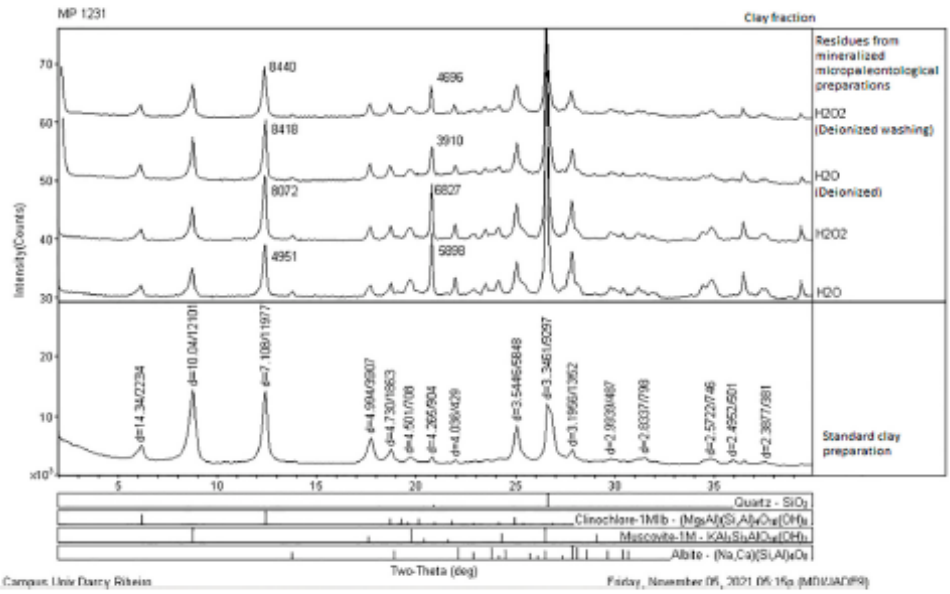

FIGURE 9 | Diffractogram of the sample MP1231 from Bambuí Group, Municipality of Buritis, Minas Gerais State, Brazil. Clay fraction (n); note the variation in reflection intensities between the diffractogram of untreated sample (base) and treated samples; note that all treatments have the same effect on the clay fraction.

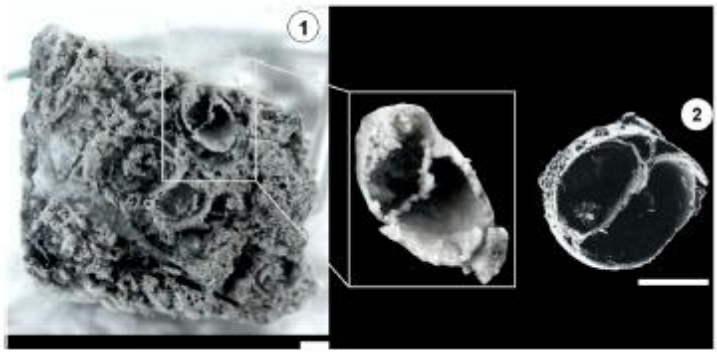

FIGURE 10 | Comparison between results of different preparations. **(1)** *Cloudina lucianoi* (Beurlen and Sommer, 1957), CP974. Sample MP2289, carbonate from the type-section of *Cloudina riemkeae* Germs, 1972, Nomtsas Formation, Namibia, (UTM Coord. 33 k 0667883 7358829); **(2)** Phosphatized skeleton of *Cloudina lucianoi* from Dengying Formation, China (Hua et al., 2005). Scale bars: 400 μm.

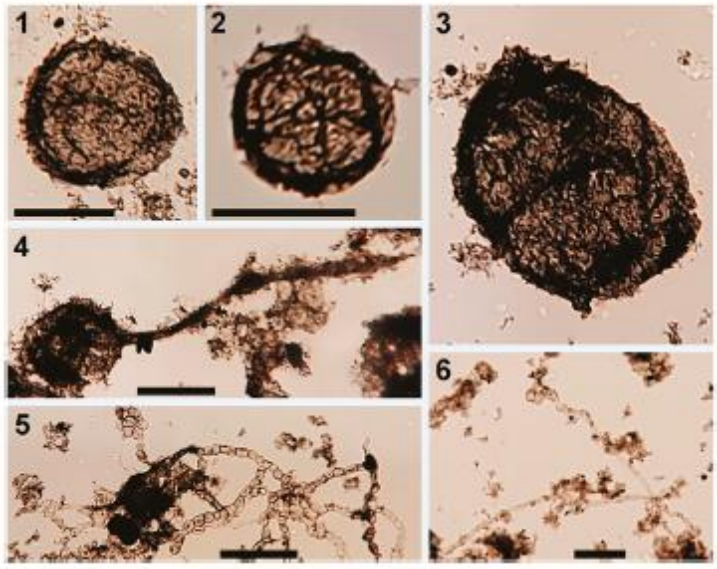

FIGURE 11 | Organic-walled microfossils recovered from Sete Lagoas Formation, Bambuí Group, Januária Municipality. **(1–2)** *Leiosphaeridia minutissima* (Naumova, 1949)—CP963; **(3)** *Leiosphaeridia tenuissima* Eisenack, 1958—CP914; **(4)** *Germinosphaera bispinosa* Mikhailova, 1986 - CP917; **(5)** *Ghoshia* sp.—CP916; **(6)** *Siphonophycus robustum* (Schopf, 1968)—CP961. Scale bars: 25 μm.

extraction is possible when the skeleton composition is slightly or entirely different compared with the host carbonate matrix, such as the case of (1) the slightly richer magnesium *C. lucianoi* skeleton from Namibia and (2) the complete different composition of the phosphatized *C. lucianoi* skeleton from Dengying Formation, China (Hua et al., 2005).

The organic-walled microfossil preparation of limestones from Sete Lagoas Formation, Bambuí Group, Januária Municipality, Minas Gerais State, Brazil (**Table 1**), which followed the protocol presented in this work, led to the recovery of exquisitely specimens of organic-walled microfossils. The recovered assemblage comprises *Leiosphaeridia minutissima* (Naumova, 1949), CP963 (**Figures 11.1, 2**) and *Leiosphaeridia tenuissima* Eisenack, 1958, CP914 (**Figure 11.3**), one acritarch: *Germinosphaera bispinosa* Mikhailova, 1986, CP917 (**Figure 11.4**), and two cyanobacteria species: *Ghoshia* sp., CP916 (**Figure 11.5**), and *Siphonophycus robustum* (Schopf, 1968), CP961 (**Figure 11.6**).

CONCLUSION

(1) Efficiency of mineralized microfossiliferous disaggregation using H_2O_2: differences in disaggregation efficiency were observed, varying from ineffective (MP1226) to low efficiency (MP1203, MP1221, and MP1231). The lithotype, the amount of organic matter within the matrix, and the metamorphic grade can influence the disaggregation efficacy. The H_2O_2 disaggregation method shows more effectiveness on siliciclastic rocks when compared with carbonate rocks. This could be due to the difference in permeability of those two lithotypes. The more permeable the rock, the easier the H_2O_2 reacts with the organic matter content. In this context, metamorphism can also affect the H_2O_2 disaggregation process as, depending on the metamorphic grade, it could change the rock permeability due to rock compaction.

(2) Mineralized microfossils recovered using the H_2O_2 preparation: three permineralized species were recovered: *Vetronostocale* aff *V. amoenum* Schopf and Blacic, 1971 (from Paranoá Group), *Myxococcoides* sp. (from Paranoá Group and Lagoa do Jacaré Formation, Bambuí Group), and *Melanocyrillium* sp. (from Sete Lagoas Formation, Bambuí Group).

(3) Organic-walled microfossils recovered from Sete Lagoas Formation, Bambuí Group, using HCl and HF preparation: *L. minutissima* (Naumova, 1949), *L. tenuissima* Eisenack, 1958, *G. bispinosa* Mikhailova, 1986, *Ghoshia* sp., *S. robustum* (Schopf, 1968). The organic residue can integrate organic carbon isotopic studies.

(4) Mineralized microfossils recovered using acetic acid preparation: *C. lucianoi* (Beurlen and Sommer, 1957).

(5) Integration of clay mineral and micropaleontology preparations methods: the whole rock diffractograms of siltstones without treatments (standard preparation for clay mineral analyses) or treated in micropaleontological preparation with H_2O (tap water or deionized water) and H_2O_2 did not show differences and allow the determination of mineral composition.

(6) Clay fraction diffractograms of residues from micropaleontological preparation: The clay fraction diffractograms showed that the micropaleontological preparation caused an increase in the intensity of the quartz reflections compared with untreated samples. Samples obtained after micropaleontological treatment may not be suitable for assessing the intensity of diagenesis using the Kübler Index, but they are useful for identifying the mineral assemblage.

(7) 3D extraction of a skeletal fossil can be possible even when the skeleton is carbonate in a carbonate matrix using weak acetic acid dissolution. This extraction is possible when the skeleton composition is slightly or entirely different from the host carbonate matrix. The organic material released by this preparation can be integrated into palynology studies.

DATA AVAILABILITY STATEMENT

The original contributions presented in the study are included in the article/Supplementary Material, further inquiries can be directed to the corresponding author.

AUTHOR CONTRIBUTIONS

MD—Fieldwork, data collection and interpretation, drawing of the figures and writing of the manuscript. RA—Fieldwork, data collection and interpretation, drawing of the figures and writing of the manuscript. DC—Ph.D. supervisor of MD, fieldwork, data interpretation and writing of the manuscript. EG—Data interpretation, drawing of the figures and writing of the manuscript. DW—Fieldwork and review of the paleontological and stratigraphic aspects of the manuscript. CA—Fieldwork and review of the stratigraphic aspects of the manuscript. GG—Fieldwork, data collection. LA—Curator of the Paleontology Collection of the Museum of Geosciences, University of Brasília, review the curatorship protocol and the mineralized microfossiliferous preparation protocol. CV—Data interpretation and review of the manuscript. OJ—Data collection and interpretation of the mineralized microfossils.

FUNDING

This study was financed in part by the Coordination for the Improvement of Higher Education Personnel—Brazil (CAPES)—Finance Code 001. Part of the studied samples was obtained from the Ediacariano Project, funded by the National Agency for Petroleum, Gas, and Biofuels (ANP) and the Brazilian Petroleum Corporation (PETROBRAS).

ACKNOWLEDGMENTS

We want to thank all institutions that participated in the development of this research: the National Council for Scientific and Technological Development (CNPq), the Coordination for the Improvement of Higher Education Personnel (CAPES), CAPES/IODP—Brazil Program via project 88887.091704/2014-01, the Brazilian Petroleum Corporation (PETROBRAS), the National Agency for Petroleum, Gas, and Biofuels (ANP) and the University of Brasília (UnB). We thank FINATEC for assistance in administrative affairs supporting scientific projects in Brasília. We would like to specially thank Dr. Norma Maria da Costa Cruz for approaching and sharing the palynological preparation method with students. We thank the two reviewers whose comments and suggestions helped improve and clarify this manuscript.

REFERENCES

Alvarenga, C. J. S., Santos, R. V., Vieira, L. C., Lima, B. A. F., and Mancini, L. H. (2014). Meso-Neoproterozoic Isotope Stratigraphy on Carbonates Platforms in the Brasília Belt of Brazil. *Precambrian Res.* 251, 164–180. doi:10.1016/j.precamres.2014.06.011

Alves, D. B. (1987). Desenvolvimento da metodologia de preparação de amostras para análise difratométrica de argilominerais no Centro de Pesquisas da Petrobrás. *Bol. Geociências da Petrobras* 1, 157–175.

Beurlen, K., and Sommer, F. W. (1957). *Observações estratigráficas e paleontológicas sobre o calcário Corumbá*. Rio de Janeiro: Departamento Nacional de Produção Mineral, Divisão de Geologia e Mineralogia, Boletim, Vol. 168, 1–35.

Campos, J. E. G., Dardenne, M. A., Freitas-Silva, F. H., and Martins-Ferreira, M. A. C. (2013). Geologia Do Grupo Paranoá na porção externa da Faixa Brasília. *Braz. J. Geol.* 43, 461–476. doi:10.5327/Z2317-48892013000300004

Campos, L. F. B. (2012). *Diagênese das sequências Proterozóicas com base na caracterização de argilominerais – topo do Grupo Paranoá e base do Grupo Bambuí – Norte do Distrito Federal* Masters Dissertation. Brasília: Institute of Geosciences, University of Brasília, 145.

Caxito, F. d. A., Halverson, G. P., Uhlein, A., Stevenson, R., Gonçalves Dias, T., and Uhlein, G. J. (2012). Marinoan Glaciation in East central Brazil. *Precambrian Res.* 200-203, 38–58. doi:10.1016/j.precamres.2012.01.005

Dardenne, M. A. (1978). "Síntese sobre a estratigrafia Do Grupo Bambuí no Brasil Central," in *XXX Congresso Brasileiro de Geologia* (Recife: Trabalho completo), 597–610.

Eisenack, A. (1958). Microfossilien aus dem Ordovizium des Baltikums, 1, Markasitschicht, Dictyonema-Scheifer, Glaukonitsand, Glaukonitkalk. *Senckenbergian Lethaea* 39, 389–404.

Faria, A. (1995). *Estratigrafia e sistemas deposicionais do Grupo Paranoá nas áreas de Cristalina. Distrito Federal e São João D'aliança-Alto Paraíso de Goiás*. Doctoral Thesis. Brasília: Institute of Geosciences, University of Brasília, 199.

Gaucher, C., Frimmel, H. E., and Germs, G. J. B. (2005). Organic-walled Microfossils and Biostratigraphy of the Upper Port Nolloth Group (Namibia): Implications for Latest Neoproterozoic Glaciations. *Geol. Mag.* 142, 539–559. doi:10.1017/S0016756805001123

Germs, G. J. B., and Gresse, P. G. (1991). The Foreland basin of the Damara and Gariep Orogens in Namaqualand and Southern Namibia: Stratigraphic Correlations and basin Dynamics. *South Afr. J. Geol.* 94, 159–169.

Germs, G. J. B. (1983). "Implications of a Sedimentary Facies and Depositional Environmental Analysis of the Nama Group in South West Africa/Namibia," in *Evolution of the Damara Orogen of South Africa/Namibia*. Editor R. M. Miller (South Africa: Geological Society of South Africa), 89–114.

Germs, G. J. B. (1972). New Shelly Fossils from Nama Group, South West Africa. *Am. J. Sci.* 272, 752–761. doi:10.2475/ajs.272.8.752

Germs, G. (1995). The Neoproterozoic of Southwestern Africa, with Emphasis on Platform Stratigraphy and Paleontology. *Precambrian Res.* 73, 137–151. doi:10.1016/0301-9268(94)00075-3

Horne, D. J., and Siveter, D. J. (2016). Collecting and Processing Fossil Ostracods. *J. Crustac. Biol.* 36, 841–848. doi:10.1163/1937240X-00002487

Hua, H., Chen, Z., Yuan, X., Zhang, L., and Xiao, S. (2005). Skeletogenesis and Asexual Reproduction in the Earliest Biomineralizing Animal Cloudina. *Geol* 33, 277–280. doi:10.1130/G21198.1

Hua, H., Pratt, B. R., and Zhang, L.-Y. (2003). Borings in Cloudina Shells: Complex Predator-Prey Dynamics in the Terminal Neoproterozoic. *Palaios* 18, 454–459. doi:10.1669/0883-1351(2003)018<0454:biscpr>2.0.co;2

Knoll, A. H. (1985). Patterns of Evolution in the Archean and Proterozoic Eons. *Paleobiology* 11, 53–64. doi:10.1017/s0094837300011398

Leite, A. M., Do Carmo, D. A., Ress, C. B., Pessoa, M., Caixeta, G. M., Denezine, M., et al. (2018). Taxonomy of Limnic Ostracoda (Crustacea) from the Quiricó Formation, Lower Cretaceous, São Francisco basin, Minas Gerais State, Southeast Brazil. *J. Paleontol.* 92, 661–680. doi:10.1017/jpa.2018.1

Machado, C. P., Coimbra, J. C., and Bergue, C. T. (2020). Provinciality of Ostracoda (Crustacea) in the Northeastern and Eastern Brazilian Shelves Based on Neontological and Paleontological Analyses. *Rev. Bras. Paleontol.* 23, 3–31. doi:10.4072/rbp.2020.1.01

Milchailova, N. S. (1986). "Novye Nakhodki Mikrofitofossilij Iz Orlozhenij Verkhnego Rifeya Krasnoyarskogo Kraya," in *Aktual 'nye Voprosy Sovremennoj, Naukowa Dumka*. Editor B. S. Sokolov (Kiev: Nauka), 31–37.

Moreira, D. S., Uhlein, A., Dussin, I. A., Uhlein, G. J., and Pimentel Misuzaki, A. M. (2020). A Cambrian Age for the Upper Bambuí Group, Brazil, Supported by the First U-Pb Dating of Volcaniclastic Bed. *J. South Am. Earth Sci.* 99, 102503–102515. doi:10.1016/j.jsames.2020.102503

Naumova, S. N. (1949). Spores of the Lower Cambrian. *Izv. Akad. Nauk SSSR* 4, 49–56.

Paula-Santos, G. M., Babinski, M., Kuchenbecker, M., Caetano-Filho, S., Trindade, R. I., and Pedrosa-Soares, A. C. (2015). New Evidence of an Ediacaran Age for the Bambuí Group in Southern São Francisco Craton (Eastern Brazil) from Zircon U-Pb Data and Isotope Chemostratigraphy. *Gondwana Res.* 28, 702–720. doi:10.1016/j.gr.2014.07.012

Pimentel, M. M., Rodrigues, J. B., DellaGiustina, M. E. S., Junges, S., Matteini, M., and Armstrong, R. (2011). The Tectonic Evolution of the Neoproterozoic Brasília Belt, central Brazil, Based on SHRIMP and LA-ICPMS U-Pb Sedimentary Provenance Data: A Review. *J. South Am. Earth Sci.* 31, 345–357. doi:10.1016/j.jsames.2011.02.011

Sanchez, E. A. M., Uhlein, A., and Fairchild, T. R. (2021). Treptichnus Pedum in the Três Marias Formation, South-central Brazil, and its Implications for the Ediacaran-Cambrian Transition in South America. *J. South Am. Earth Sci.* 105, 102983–102989. doi:10.1016/j.jsames.2020.102983

Schopf, J. W., and Blacic, J. M. (1971). New Microorganisms from the Bitter Springs Formation (Late Precambrian) of the north-central Amadeus Basin, Australia. *J. Paleontol.* 45, 105–114.

Schopf, J. W. (1995). "Disparate Rates, Differing Fates: Tempo and Mode of Evolution Changed from the Precambrian to the Phanerozoic," in *Tempo and Mode in Evolution*. Editors W. M. Fitch and F. J. Ayala (Washington, D.C.: National Academy of Sciences), 41–62. Available at: https://www.ncbi.nlm.nih.gov/books/NBK232208/

Schopf, J. W. (1968). Microflora of the Bitter Springs Formation, Late Precambrian, Central Australia. *J. Paleontol.* 42, 651–688.

Uhlein, A., Trompette, R., and Egydio-Silva, M. (1995). Rifteamentos Superpostos E Tectônica De Inversão Na Borda Sudeste Do Cráton Do São Francisco. *Revista Geonomos* 3, 99–107. doi:10.18285/geonomos.v3i1.219

Warren, L. V., Quaglio, F., Riccomini, C., Simões, M. G., Poiré, D. G., Strikis, N. M., et al. (2014). The Puzzle Assembled: Ediacaran Guide Fossil Cloudina Reveals an Old Proto-Gondwana Seaway. *Geology* 42, 391–394. doi:10.1130/G35304.1

Conflict of Interest: The authors declare that the research was conducted in the absence of any commercial or financial relationships that could be construed as a potential conflict of interest.

Publisher's Note: All claims expressed in this article are solely those of the authors and do not necessarily represent those of their affiliated organizations, or those of the publisher, the editors and the reviewers. Any product that may be evaluated in this article, or claim that may be made by its manufacturer, is not guaranteed or endorsed by the publisher.

Copyright © 2022 Denezine, Adôrno, Do Carmo, Guimarães, Walde, De Alvarenga, Germs, Antonietto, Valdivia Rodriguez and Nunes Junior. This is an open-access article distributed under the terms of the Creative Commons Attribution License (CC BY). The use, distribution or reproduction in other forums is permitted, provided the original author(s) and the copyright owner(s) are credited and that the original publication in this journal is cited, in accordance with accepted academic practice. No use, distribution or reproduction is permitted which does not comply with these terms.

APPENDIX 2

Sample	Section	Level	*Bambuites erichsenii*	*Germinosphaera bispinosa*	*Ghoshia januarensis*	*Leiosphaeridia crassa*	*Leiosphaeridia jacutica*	*Leiosphaeridia minutissima*	*Leiosphaeridia tenuissima*	*Leiosphaeridia ternata*	*Siphonophycus robustum*
MP5131	Rei do Mato	0.3 m	-	-	-	-	-	7	2	-	-
MP5132	Rei do Mato	1 m	-	-	-	-	-	-	-	-	-
MP5133	Rei do Mato	2 m	-	-	-	-	-	-	-	-	-
MP5134	Rei do Mato	3 m	-	-	-	-	-	-	-	-	-
MP5135	Rei do Mato	4 m	-	-	-	-	-	-	-	-	-
MP5136	Rei do Mato	5 m	10	-	-	-	-	2	-	-	-
MP5137	Rei do Mato	6 m	-	-	-	-	-	-	-	-	-
MP5138	Rei do Mato	7 m	-	-	-	-	-	-	-	-	-
MP5139	Rei do Mato	8 m	-	-	-	-	-	3	-	-	-
MP5140	Rei do Mato	9.2 m	-	-	-	-	-	-	-	-	-
MP5141	Rei do Mato	10 m	-	-	-	-	-	-	-	-	-
MP5142	Rei do Mato	11 m	-	-	-	-	-	-	-	-	-
MP5143	Rei do Mato	12 m	-	-	-	-	-	-	-	-	-
MP5144	Rei do Mato	13 m	-	-	-	-	-	-	-	-	-
MP5145	Rei do Mato	14 m	-	-	-	-	-	-	-	-	-
MP5146	Rei do Mato	15 m	-	-	-	-	-	-	-	-	-
MP5147	Rei do Mato	16 m	-	-	-	-	-	-	-	-	-
MP5148	Rei do Mato	17 m	-	-	-	-	-	-	-	-	-
MP5149	Rei do Mato	18 m	-	-	-	-	-	-	-	-	-
MP5150	Rei do Mato	19.5 m	-	-	-	-	-	-	-	-	-
MP5151	Rei do Mato	21 m	-	-	-	-	-	-	-	-	-
MP5152	Rei do Mato	23 m	-	-	x	-	-	-	1	-	-
MP5153	Rei do Mato	25 m	-	-	-	-	-	-	-	-	-
MP5154	Rei do Mato	26 m	-	-	-	-	-	-	-	-	-
MP5155	Rei do Mato	28 m	-	-	-	-	-	-	-	-	-
MP5156	Rei do Mato	30 m	-	-	-	-	-	-	-	-	-
MP5157	Rei do Mato	32 m	-	-	-	-	-	-	-	-	-
MP5158	Rei do Mato	33 m	-	-	-	-	-	-	-	-	-
MP5159	Rei do Mato	34 m	-	-	x	16	-	15	-	-	x
MP5160	Rei do Mato	35 m	-	-	-	-	-	15	1	-	-
MP5161	Rei do Mato	36 m	-	-	-	-	-	-	-	-	-
MP5162	Rei do Mato	37 m	-	-	-	-	-	-	-	-	-
MP5163	Rei do Mato	38 m	-	-	-	-	-	-	-	-	-
MP5164	Rei do Mato	39 m	-	-	-	-	-	-	-	-	-

Sample	Section	Level	*Bambuites erichsenii*	*Germinosphaera bispinosa*	*Ghoshia januarensis*	*Leiosphaeridia crassa*	*Leiosphaeridia jacutica*	*Leiosphaeridia minutissima*	*Leiosphaeridia tenuissima*	*Leiosphaeridia ternata*	*Siphonophycus robustum*
MP5165	Rei do Mato	40 m	-	-	-	3	-	-	-	-	-
MP5166	Rei do Mato	41 m	-	-	-	-	-	-	-	-	-
MP5167	Rei do Mato	42 m	-	-	-	-	-	-	-	-	-
MP5168	Rei do Mato	43 m	-	-	-	-	-	-	-	-	-
MP5169	Rei do Mato	44 m	-	-	-	-	-	-	-	-	-
MP5170	Rei do Mato	45 m	-	-	-	-	-	-	-	-	-
MP5171	Rei do Mato	46 m	-	-	-	1	-	-	-	-	-
MP5172	Rei do Mato	46.7 m	-	-	-	-	-	-	-	-	-
MP5173	Rei do Mato	49 m	-	-	-	-	-	-	-	-	-
MP5174	Rei do Mato	50 m	-	-	-	-	-	-	-	-	-
MP5175	Rei do Mato	52 m	-	-	-	-	-	1	-		-
MP5176	Rei do Mato	53 m	-	-	-	-	-	-	-	1	-
MP5177	Rei do Mato	54 m	-	-	-	-	-	-	-	-	-
MP5178	Rei do Mato	55 m	-	-	-	-	-	1	-	2	-
MP5179	Rei do Mato	56 m	-	-	-	-	-	-	-	-	-
MP5180	Rei do Mato	57 m	-	-	-	-	-	3	1	-	-
MP5181	Rei do Mato	58 m	-	-	-	-	-	-	-	-	-
MP5182	Rei do Mato	59 m	-	-	-	-	-	5	-	-	-
MP5183	Rei do Mato	60 m	-	-	-	-	-	-	-	-	-
MP5184	Rei do Mato	61 m	-	-	-	1	-	2	-	-	-
MP5185	Rei do Mato	62 m	-	-	-	-	-	2	-	-	-
MP5186	Rei do Mato	63 m	-	-	-	-	-	-	-	-	-
MP5187	Rei do Mato	64 m	-	-	-	-	1	-	-	-	-
MP5188	Rei do Mato	65 m	-	-	-	-	-	-	-	-	-
MP5189	Rei do Mato	66 m	-	-	-	-	-	7	-	-	-
MP5190	Rei do Mato	67 m	-	-	-	-	-	-	-	-	-
MP5191	Rei do Mato	68 m	-	-	-	1	-	-	-	-	-
MP5192	Rei do Mato	69 m	1	-	-	3	1	4	-	-	-
MP5193	Rei do Mato	70 m	21	-	-	3	2		-	-	-
MP5194	Rei do Mato	71 m	9	-	-	16	-	1	1	-	-
MP5195	Rei do Mato	72 m	-	-	-	-	-	-	-	-	-
MP5196	Rei do Mato	73 m	-	-	x	1	-	3	-	-	-
MP5197	Rei do Mato	74 m	-	-	-	-	1	-	1	-	-
MP5198	Rei do Mato	75 m	-	-	-	-	-	-	-	-	-
MP5199	Rei do Mato	76 m	-	-	-	-	-	-	-	-	-
MP5200	Rei do Mato	77 m	-	-	-	-	-	1	-	-	-
MP5201	Rei do Mato	78 m	-	-	-	-	-	1	-	-	-
MP5202	Rei do Mato	79 m	-	-	-	-	-	-	-	-	-

Sample	Section	Level	*Bambuites erichsenii*	*Germinosphaera bispinosa*	*Ghoshia januarensis*	*Leiosphaeridia crassa*	*Leiosphaeridia jacutica*	*Leiosphaeridia minutissima*	*Leiosphaeridia tenuissima*	*Leiosphaeridia ternata*	*Siphonophycus robustum*
MP5203	Rei do Mato	80 m	-	-	-	-	-	-	-	-	-
MP5204	Rei do Mato	81 m	-	-	-	-	-	-	-	-	-
MP5205	Rei do Mato	82 m	-	-	-	-	-	1	-	-	-
MP5206	Rei do Mato	83 m	-	-	-	-	-	-	-	-	-
MP5207	Rei do Mato	84 m	-	1	-	-	-	4	2	-	-
MP5208	Rei do Mato	85 m	-	-	-	-	-	-	-	-	-
MP5209	Rei do Mato	86 m	-	-	-	-	-	-	-	-	-
MP5210	Rei do Mato	87 m	-	-	-	-	-	-	-	-	-
MP5211	Rei do Mato	89 m	-	-	-	-	-	-	-	-	-
MP5212	Rei do Mato	91 m	-	-	-	-	-	-	-	-	-
MP5213	Rei do Mato	93 m	-	-	-	-	-	-	-	-	-
MP5214	Rei do Mato	95 m	-	-	-	-	-	-	-	-	-
MP5215	Rei do Mato	97 m	-	-	-	-	-	-	-	-	-
MP5216	Rei do Mato	99 m	-	-	-	-	-	1	-	-	-
MP5217	Rei do Mato	101 m	-	-	-	-	-	-	-	-	-
MP5218	Rei do Mato	103 m	-	-	-	-	-	-	-	-	-
MP5219	Rei do Mato	105 m	-	-	-	-	-	-	-	-	-
MP5220	Rei do Mato	107 m	-	-	-	-	-	-	-	-	-
MP5221	Rei do Mato	109 m	-	-	-	-	-	8	1		
MP5222	Rei do Mato	111 m	-	-	-	-	-	-	-	-	-
MP5223	Rei do Mato	113 m	-	-	-	-	-	-	-	-	-
MP5224	Rei do Mato	114 m	-	-	-	-	-	-	-	-	-
MP5225	Rei do Mato	115 m	-	-	-	-	-	-	-	-	-
MP5226	Rei do Mato	116 m	-	-	-	-	-	-	-	-	-
MP5227	Rei do Mato	117 m	-	-	-	-	-	-	-	-	-
MP5228	Rei do Mato	118 m	-	-	-	-	-	-	-	-	-
MP5229	Rei do Mato	119 m	-	-	-	-	-	-	-	-	-
MP5230	Rei do Mato	120.1 m	-	-	-	-	-	-	-	-	-
MP5231	Rei do Mato	121 m	-	-	-	-	-	-	-	-	-
MP5232	Rei do Mato	122.3 m	-	-	-	-	-	-	-	-	-
MP5233	Rei do Mato	123 m	-	-	-	-	-	-	-	-	-
MP5234	Rei do Mato	124 m	-	-	x	-	-	-	-	-	-
MP5235	Rei do Mato	125 m	-	-	-	-	-	-	-	-	-
MP4219	PRF	0.05	-	-	-	-	-	-	-	-	-
MP4220	PRF	0.45	-	-	-	-	-	3	-	-	-
MP4221	PRF	0.6	-	-	-	-	-	1	-	-	-
MP4222	PRF	1.3	-	-	-	-	-	-	-	-	-
MP4223	PRF	1.6	-	-	-	-	-	-	-	-	-

Sample	Section	Level	*Bambuites erichsenii*	*Germinosphaera bispinosa*	*Ghoshia januarensis*	*Leiosphaeridia crassa*	*Leiosphaeridia jacutica*	*Leiosphaeridia minutissima*	*Leiosphaeridia tenuissima*	*Leiosphaeridia ternata*	*Siphonophycus robustum*
MP4224	PRF	2	-	-	-	-	-	-	-	-	-
MP4225	PRF	2,3	-	-	-	-	-	-	-	-	-
MP4226	PRF	3	-	-	-	-	-	-	-	-	-
MP4227	PRF	4 m	-	-	-	-	-	-	-	-	-
MP4228	PRF	5.8 m	-	-	-	-	-	-	-	-	-
MP4229	PRF	8.4 m	-	-	-	-	-	-	-	-	-
MP2977	Barreiro	0 m	-	-	-	-	-	5	-	-	-
MP2978	Barreiro	0.15 m	-	-	-	-	-	-	-	-	-
MP2979	Barreiro	0.3 m	-	-	-	-	-	2	-	-	-
MP2980	Barreiro	0.4 m	-	-	x	-	-	2	-	-	-
MP2982	Barreiro	0.53 m	-	-	-	-	-	-	-	-	-
MP2983	Barreiro	0.9 m	-	-	-	-	-	2	-	-	-
MP2984	Barreiro	1.3 m	-	-	-	-	-	-	-	-	-
MP2985	Barreiro	1.9 m	-	-	-	-	-	21	-	-	x
MP2986	Barreiro	2.15 m	-	-	-	-	-	2	-	-	-
MP2987	Barreiro	2.2 m	-	-	-	-	-	2	-	-	-
MP2988	Barreiro	2.25 m	-	-	-	-	-	31	-	-	-
MP2989	Barreiro	2.5 m	-	-	-	-	-	-	-	-	-
MP2990	Barreiro	2.8 m	-	-	-	-	1	-	-	-	-
MP2991	Barreiro	3.25 m	-	-	-	-	-	-	-	-	-
MP2992	Barreiro	3.4 m	-	-	-	-	-	6	-	-	-
MP2993	Barreiro	3.8 m	-	-	-	-	-	1	-	-	-
MP2994	Barreiro	4 m	-	-	-	-	-	4	2	-	-
MP2995	Barreiro	4.25 m	-	-	-	-	-	2	-	-	x
MP2996	Barreiro	5 m	-	-	-	-	-	-	-	-	-
MP3704	Barreiro	5.5 m	-	-	-	-	-	-	-	-	-
MP2997	Barreiro	5.7 m	-	-	-	-	-	-	-	-	-
MP2998	Barreiro	6.3 m	-	-	-	-	-	7	-	-	-
MP2999	Barreiro	6.35 m	-	-	-	-	-	3	-	-	-
MP3000	Barreiro	6.6 m	-	-	-	-	-	-	-	-	-
MP3705	Barreiro	6.8 m	-	-	-	-	-	20	-	-	-
MP3706	Barreiro	7.3 m	-	-	-	-	-	-	-	-	-
MP3001	Barreiro	7 m	-	-	-	-	-	-	-	-	-
MP3002	Barreiro	7.15 m	-	-	-	-	-	6	3	-	-
MP3003	Barreiro	7.7m	-	-	-	-	-	-	-	-	-
MP3004	Barreiro	8.05m	-	-	-	-	-	1	-	-	-
MP3005	Barreiro	8.1 m	-	-	-	-	-	3	-	-	-
MP3006	Barreiro	8.5 m	-	-	-	-	-	4	-	-	-

Sample	Section	Level	*Bambuites erichsenii*	*Germinosphaera bispinosa*	*Ghoshia januarensis*	*Leiosphaeridia crassa*	*Leiosphaeridia jacutica*	*Leiosphaeridia minutissima*	*Leiosphaeridia tenuissima*	*Leiosphaeridia ternata*	*Siphonophycus robustum*
MP3007	Barreiro	8.9 m	-	-	-	-	-	2	1	-	-
MP3008	Barreiro	9.5 m	-	-	-	-	-	-	-	-	-
MP3061	Barreiro	9.6 m	-	-	-	-	-	-	-	-	-
MP3009	Barreiro	9.82 m	-	-	-	-	-	-	-	-	-
MP3010	Barreiro	10.15 m	-	-	-	-	-	-	-	-	-
MP3011	Barreiro	10.9 m	-	-	-	-	-	12	-	-	-
MP3012	Barreiro	11.6 m	-	-	-	-	-	6	-	-	-
MP3013	Barreiro	12 m	-	-	x	-	-	13	1	-	-
MP3014	Barreiro	12.5 m	-	-	-	-	-	-	-	-	-
MP3015	Barreiro	12.8 m	-	-	x	-	-	4	-	-	-
MP3016	Barreiro	13 m	-	-	-	-	-	2	-	-	-
MP3017	Barreiro	13.9 m	-	-	-	-	-	-	-	-	-
MP3707	Barreiro	14.5 m	-	-	-	-	-	21	2	-	-
MP3708	Barreiro	15 m	-	-	-	-	-	12	-	-	x
MP3028	Barreiro	17.2 m	-	-	-	-	-	4	-	-	-
MP3029	Barreiro	17.5 m	-	-	-	-	-	-	-	-	-
MP3030	Barreiro	19 m	-	-	-	-	-	3	-	-	-
MP3031	Barreiro	19.9 m	-	-	-	-	-	6	-	-	-
MP3032	Barreiro	21 m	-	-	-	-	-	-	-	-	-
MP3033	Barreiro	22 m	-	-	-	-	-	5	-	-	-
MP3034	Barreiro	22.1 m	-	-	-	-	-	2	-	-	-
MP3035	Barreiro	22.15 m	-	-	-	-	-	1	-	-	-
MP3036	Barreiro	23.35 m	-	3	-	-	-	3		-	-
MP3037	Barreiro	25.6 m	-	-	-	-	-	-	-	-	-
MP3038	Barreiro	27.5 m	-	-	-	-	-	-	-	-	-
MP3039	Barreiro	28 m	-	-	-	-	-	-	-	-	-
MP3040	Barreiro	28.1 m	-	-	x	-	-	-	-	-	x
MP3709	Barreiro	24 m	-	-	-	-	-	1	1	-	x
MP3710	Barreiro	24.5 m	-	-	x	-	-	13	-	-	x
MP3711	Barreiro	24.7 m	-	-	-	-	-	-	-	-	-
MP3712	Barreiro	25.5 m	-	-	-	-	-	12	-	-	-
MP3713	Barreiro	26 m	-	-	-	-	-	2	-	-	-
MP3714	Barreiro	26.5 m	-	21	x	-	1	37	1	-	-
MP3715	Barreiro	27 m	-	-	-	-	-	3	-	-	-
MP3716	Barreiro	29 m	-	-	-	-	-	22	-	-	-
MP3717	Barreiro	30 m	-	-	-	-	-	-	-	-	-
MP3718	Barreiro	30.6 m	-	-	x	-	-	-	-	-	-
MP3719	Barreiro	31.5 m	-	-	-	6	2	2	2	-	-

Sample	Section	Level	*Bambuites erichsenii*	*Germinosphaera bispinosa*	*Ghoshia januarensis*	*Leiosphaeridia crassa*	*Leiosphaeridia jacutica*	*Leiosphaeridia minutissima*	*Leiosphaeridia tenuissima*	*Leiosphaeridia ternata*	*Siphonophycus robustum*
MP3720	Barreiro	36.4 m	-	-	-	8	-	33	1	-	-
MP3721	Barreiro	41.5 m	-	-	-	-	-	-	-	-	-
MP3722	Barreiro	46.5 m	-	-	-	-	-	-	-	-	-
MP3723	Barreiro	48 m	-	-	x	-	-	-	-	-	-
MP3724	Barreiro	57.5 m	-	-	x	-	-	-	-	-	-
MP3725	Barreiro	59.5 m	-	-	-	-	-	-	-	-	-
MP3726	Barreiro	61.5 m	-	-	-	-	-	-	-	-	-
MP3727	Barreiro	66.5 m	-	-	-	-	-	-	-	-	-
MP3728	Barreiro	69 m	-	-	-	-	-	-	-	-	-
MP4651	Fercal	260.1	-	-	-	-	-	-	-	-	-
MP4649	Fercal	258.1	-	-	-	-	-	-	-	-	-
MP4647	Fercal	255.1	-	-	-	-	-	-	-	-	-
MP4645	Fercal	253.1	-	-	-	-	-	-	-	-	-
MP4643	Fercal	251.1	-	-	-	-	-	-	-	-	-
MP4641	Fercal	249.1	-	-	-	-	-	-	-	-	-
MP4639	Fercal	247.1	-	-	-	-	-	-	-	-	-
MP4637	Fercal	245.1	3	-	-	-	-	-	-	-	-
MP4635	Fercal	242.1	-	-	-	-	-	14	-	-	
MP4634	Fercal	241.1	-	-	-	-	-	2	1	-	x
MP4632	Fercal	239.1	-	-	-	-	-	-	-	-	-
MP4630	Fercal	237.1	-	-	-	-	-	2	2	-	-
MP4627	Fercal	235.1	-	-	-	-	-	-	-	-	-
MP4624	Fercal	233.1	-	-	-	-	-	-	-	-	-
MP4620	Fercal	231.1	-	-	-	-	-	-	-	-	-
MP4617	Fercal	229.1	-	-	-	-	-	1	-	-	-
MP4613	Fercal	227.1	-	-	-	-	-	-	-	-	-
MP4609	Fercal	225.1	-	-	-	-	-	-	-	-	-
MP4605	Fercal	223.1	-	-	x	-	-	-	-	-	-
MP4601	Fercal	221.1	-	-	-	-	-	8	-	-	-
MP4495	Fercal	222.4	-	-	-	-	-	-	-	-	-
MP4496	Fercal	219.75	-	-	-	-	-	-	-	-	-
MP4501	Fercal	214.25	-	-	-	-	-	-	-	-	-
MP4503	Fercal	211.50	-	-	-	-	-	6	3	-	-
MP4506	Fercal	205.25	-	-	-	-	-	-	-	-	-
MP4507	Fercal	202.25	-	-	-	-	-	1	-	-	-
MP4509	Fercal	195	-	-	-	-	-	-	-	-	-
MP4510	Fercal	191.1	-	-	-	5	2	-	2	-	x
MP4512	Fercal	185.95	-	-	-	-	-	-	-	-	-

Sample	Section	Level	*Bambuites erichsenii*	*Germinosphaera bispinosa*	*Ghoshia januarensis*	*Leiosphaeridia crassa*	*Leiosphaeridia jacutica*	*Leiosphaeridia minutissima*	*Leiosphaeridia tenuissima*	*Leiosphaeridia ternata*	*Siphonophycus robustum*
MP4513	Fercal	183.2	-	-	-	-	-	-	-	-	-
MP4516	Fercal	179.6	-	-	-	-	-	-	-	-	-
MP4517	Fercal	175.8	-	-	-	-	-	-	-	-	-
MP4518	Fercal	166	-	-	x	-	-	-	-	-	-
MP4519	Fercal	162.8	-	-	-	-	-	1	-	-	-
MP4520	Fercal	159.8	-	-	-	-	-	1	-	-	-
MP4521	Fercal	156.8	-	-	-	-	-	3	-	-	-
MP4522	Fercal	153.8	-	-	-	-	-	-	-	-	-
MP4523	Fercal	150.9	-	-	-	-	-	-	-	-	-
MP4524	Fercal	146.9	-	-	-	-	-	-	-	-	-
MP4525	Fercal	144	-	-	-	-	-	-	-	-	-
MP4526	Fercal	141	-	-	-	-	-	5		-	-
MP4527	Fercal	137.85	1	-	-	-	-	-	2	-	-
MP4529	Fercal	131.85	2	-	x	-	-	-	-	-	-
MP4531	Fercal	128.85	-	-	-	-	-	-	-	-	-
MP4532	Fercal	125.85	-	-	-	-	1	-	-	-	
MP4533	Fercal	123	-	-	-	-	-	-	-	-	-
MP4535	Fercal	120.3	-	-	-	5		1	-	-	-
MP4537	Fercal	117.3	-	-	-	-	-	-	-	-	-
MP4538	Fercal	114.3	-	-	-	-	-	2	-	-	-
MP4540	Fercal	108.5	-	-	-	-	-	-	-	-	-
MP4541	Fercal	105.5	-	-	x	1		-	-	-	-
MP4543	Fercal	102.7	-	-	-	-	-	-	-	-	x
MP4545	Fercal	98.2	-	-	-	-	-	4	-	-	-
MP4547	Fercal	94.2	-	-	-	-	-	18	-	-	-
MP4549	Fercal	88.2	-	-	-	9	5	1	-	-	-
MP4551	Fercal	82	-	-	-	-	-	-	-	-	-
MP4552	Fercal	78.6	-	-	-	-	-	-	-	-	-
MP4554	Fercal	72.65	-	-	-	-	-	-	-	-	-
MP4556	Fercal	67.65	-	-	-	-	-	-	-	-	-
MP4557	Fercal	64.7	-	-	-	-	-	-	-	-	-
MP4558	Fercal	61.7	-	-	-	-	-		1	-	
4560	Fercal	54.9	-	-	-	-	-	-	-	-	-
4562	Fercal	48.85	-	-	-	-	-	-	-	-	-
4563	Fercal	44.85	-	-	-	-	-	-	-	-	-
4565	Fercal	40.7	-	-	-	-	-	2	-	-	-
4566	Fercal	36.6	-	-	-	2	-	7	-	-	-
4567	Fercal	32.8	-	-	-	-	-	22	4	-	-

Sample	Section	Level	*Bambuites erichsenii*	*Germinosphaera bispinosa*	*Ghoshia januarensis*	*Leiosphaeridia crassa*	*Leiosphaeridia jacutica*	*Leiosphaeridia minutissima*	*Leiosphaeridia tenuissima*	*Leiosphaeridia ternata*	*Siphonophycus robustum*
4569	Fercal	28.8	-	-	-	-	-	-	-	-	-
4573	Fercal	22.1	-	-	-	-	-	-	-	-	-

2831